CAPITAL UNIVERSITY OF SCIENCE AND TECHNOLOGY, ISLAMABAD

Study of RCS Simulation Tools and Functional Enhancement of Physical Optics Facet (POFACETS$^{©}$4.2) Software Package for RCS Computations

by

Muhammad Haris

A thesis submitted in partial fulfillment for the
degree of Master of Science

in the

Faculty of Engineering

Department of Electrical Engineering

2021

This thesis is dedicated to my Parents and Family, for their endless love, support, care and encouragement.

CERTIFICATE OF APPROVAL

Study of RCS Simulation Tools and Functional Enhancement of Physical Optics Facet (POFACETS©4.2) Software Package for RCS Computations

by

Muhammad Haris

Registration No: MEE173017

THESIS EXAMINING COMMITTEE

S. No.	Examiner	Name	Organization
(a)	External Examiner	Dr. Hamood-ur-Rehman	NUST, Islamabad
(b)	Internal Examiner	Dr. Imtiaz Ahmad Taj	CUST, Islamabad
(c)	Supervisor	Dr. Noor Muhammad Khan	CUST, Islamabad

Dr. Noor Muhammad Khan

Thesis Supervisor

September, 2021

Dr. Noor Muhammad Khan

Head

Dept. of Electrical Engineering

September, 2021

Dr. Imtiaz Ahmad Taj

Dean

Faculty of Engineering

September, 2021

Author's Declaration

I, **Muhammad Haris** hereby state that my MS thesis titled "**Study of RCS Simulation Tools and Functional Enhancement of Physical Optics Facet (POFACETS$^©$4.2) Software Package for RCS Computations**" is my own work and has not been submitted previously by me for taking any degree from Capital University of Science and Technology, Islamabad or anywhere else in the country/abroad.

At any time if my statement is found to be incorrect even after my graduation, the University has the right to withdraw my MS Degree.

(Muhammad Haris)

Registration No: MEE173017

Plagiarism Undertaking

I solemnly declare that research work presented in this thesis titled "*Study of RCS Simulation Tools and Functional Enhancement of Physical Optics Facet (POFACE-TS© 4.2) Software Package for RCS Computations*" is solely my research work with no significant contribution from any other person. Small contribution/help wherever taken has been dully acknowledged and that complete thesis has been written by me.

I understand the zero tolerance policy of the HEC and Capital University of Science and Technology towards plagiarism. Therefore, I as an author of the above titled thesis declare that no portion of my thesis has been plagiarized and any material used as reference is properly referred/cited.

I undertake that if I am found guilty of any formal plagiarism in the above titled thesis even after award of MS Degree, the University reserves the right to withdraw/revoke my MS degree and that HEC and the University have the right to publish my name on the HEC/University website on which names of students are placed who submitted plagiarized work.

(Muhammad Haris)

Registration No: MEE173017

Acknowledgement

First and foremost I would like to thank Allah almighty, who gave me the courage and support to continue my graduate studies with the research work. The determination granted by Allah helped me to tolerate the hard time to produce this thesis.

I cannot forget the ideal man of the world and most respectable personality for whom Allah created the whole universe, Prophet Mohammed (Peace Be Upon Him).

I would like to thank to my supervisor, Prof. Dr. Noor Muhammad Khan, with whom it has been an honor to work. He allowed me tremendous freedom in choosing my area of research and gave me outstanding guidance all along the way. His "outside of the box" thinking has taught me to do the same and for that I am grateful to him.

I am highly grateful to my loving parents and family who kept me motivated, guided and focused throughout my Master. Their help in various regards contributed in keeping my moral high. I extend my heartiest thanks to my colleagues in Communication research group, especially Dr. Mirza Muhammad Yasir Masood, Mr. Nadir Mehmood, Mr. Fawad Ahmad, Mr. Fazal Noor, Mr. Muhammad Nasir Khan, Mr. Qaiser khan, Mr. Syed Wahid Shah, and Mr. Qazi Muhammad Kashif. They always guided me whenever I was in need of that. I also very special thankful to my loving brother Engr. Muhammad Salman.

(Muhammad Haris)

Abstract

Radar Cross Section (RCS) plays a vital role in Radio Detection and Ranging (RADAR) systems to detect enemies' weapons and their movements i.e. aircrafts, missiles, ships, and ground vehicles etc. Since, it is very difficult to conduct practical measurements of RCS for modeling purposes; therefore, to serves this purpose, several simulation platforms have been introduced in the literature to estimate and analyze the RCS of manually designed models/objects. Being one of such platforms, Physical Optics FACET (POFACETS$^{©}$) is a well-established open source simulation software that works on the principles of Physical Optics (PO). This software provides an opportunity to estimate and analyze RCS of any complex object; however, the current version of POFACET (Version 4.2) has the limitation of estimating the RCS of an object for a single incident angle only, and is not capable of providing it for a range of incident angles simultaneously. This thesis presents the functional enhancement of POFACETS$^{©}$4.2. These enhancement include the simultaneous estimation of RCS over the predefined ranges of incident angles and observation angles. This provides a three dimensional space to a user where the RCS of a design model can be taken for any particular incident and observation angle. In this meanwhile the Graphical User Interface (GUI) has also been modified accordingly. The enhanced version carries both the functionalities of computing RCS at a single incident angle and for a range of incident angles. The enhanced POFACETS$^{©}$ version 4.2 is named as EPOFACETS 5.0. In order to analyze the computational functionalities and advantages of EPOFACETS 5.0, the model of largest commercial aircraft A380$^{©}$ is used as the target model to compute the bistatic RCS through EPOFACETS 5.0. For this purpose, the Auto-CAD design of aircraft A380$^{©}$ is acquired and converted to stereolithography (.stl) format. RCS of the designed model is estimated for each incident and observation angle in a three-dimensional space by providing predefined incident and observation angles ranges. Simulation-time efficiency of EPOFACETS 5.0 is compared with that of POFACETS$^{©}$4.2 on a computer with the specifications of 2.50 GHz processor, 256 GB SSD ROM, and 8 GB RAM. It is observed that EPOFACETS 5.0 saves user's time and effort for the estimation of RCS data over a large range

of incident and observation angles. Moreover, the BRCS of the facet-based model of the commercial aircraft Boeing 707$^©$ is computed through the proposed EPO-FACETS 5.0 and FEKO$^©$ software tool. The BRCS simulated results through the proposed EPOFACETS 5.0 software are then compared with the published results of FEKO$^©$ software for results' verification. From the results, it is clear that the BRCS computed through the proposed EPOFACETS 5.0 and FEKO$^©$ software tool are comparatively similar. This work may contribute in various research fields in which RCS is required to be estimated for its onward use in the calculation of reflection coefficients and radar field modeling.

Contents

List of Figures

List of Tables

Abbreviations

BRCS	Bistatic Radar Cross Section
CWR	Continous Wave Radar
DR	Doppler Radar
EM	Electro-Magnetic Wave
GO	Geometric Optics
GTD	Geometrical Theory of Diffraction
GUI	Graphical User Interface
LOS	Line Of Sight
MOM	Method Of Moment
PEC	Perfect Electric Conductor
PO	Physical Optics
POFACETS	Physical Optics FACET
PR	Pulse Radar
PTD	Physical Theory of Diffraction
RADAR	Radio Detection And Ranging
RAM	Radar Absorbent Material
RCS	Radar Cross Section
SBR	Shooting and Bouncing Ray

Symbols

ω Angular Frequency

σ_b Bi-Static RCS

γ Conductivity

ρ Density of charge

R_t, R_r Distance between Transmitter and Receiver

A_{eff} Effective Area of RADAR

η Efficiency

ϵ_o Free space permitivity

μ_0 Free space permeability

E_i Incident Electric field intensity

R Range

R_x Radar Receiver

T_x Radar Transmitter

σ RCS

ϵ_r Relative di-electric constant

G_r Receiving Antenna Gain

n Refractive Index

P_r Received Power

Γ Reflection Co-efficient

E_s Scattered Electric field intensity

G_t Transmitting Antenna Gain

P_t Transmitted Power

J Vector current density

Chapter 1

Introduction

This chapter presents a brief overview of the RADAR (Radio Detection and Ranging) and discusses its types, operations and applications. RADAR Cross Section (RCS) which is the main source of target detection is also discussed in detail.

1.1   Radar and its Working Principle

During the World War II, the radar system was developed by the United States Navy. The radar system uses radio waves to detect the position and speed of the target i.e. Aircrafts, ships, spacecrafts, guided missiles and vehicles. This technology has also been upgraded to various advanced radar system; e.g. weather radar system, marine radar systems, aircraft's anti-collision systems, and ocean surveillance systems etc.

A radar system generally consists of a transmitter, receiver, antenna, duplexer and radar signal processor etc. A typical block diagram representing the main components of the radar system is shown in Fig (1.1). The radar transmitter radiates EM signals in many predefined regions to detect the intruder in its coverage region depends on the user requirements. The radar transmitter signals, when incident on the surface of the object/target, may get reflected/scattered in many directions. Some part of the waves may get penetrated into the object's body while some
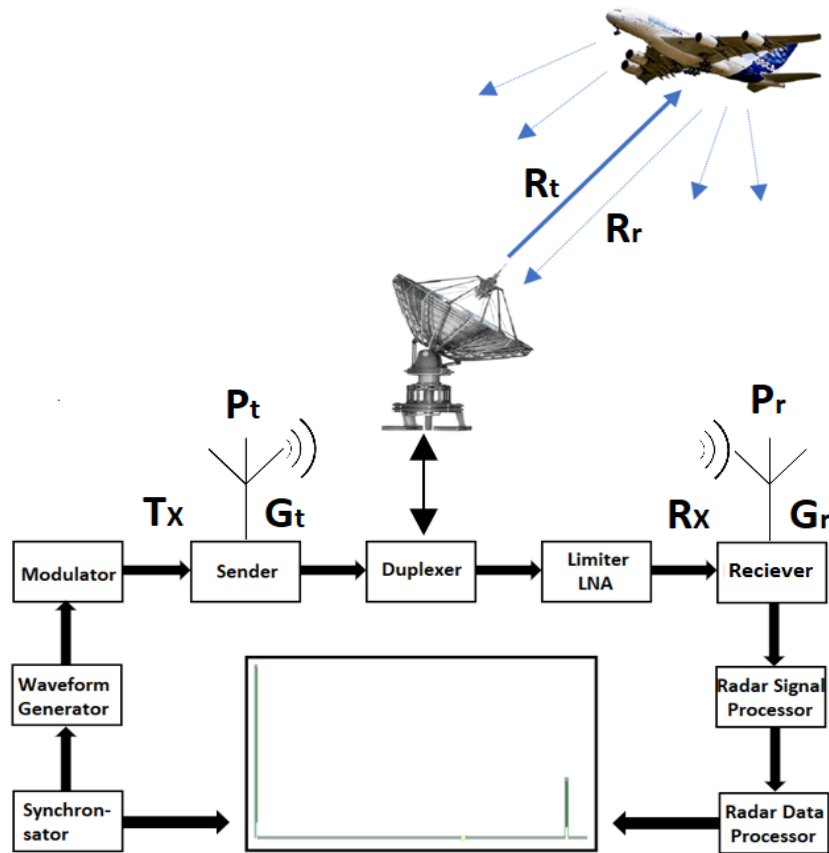
FIGURE 1.1: Typical block diagram of Radar system.

part of the backscattered waves may travel in the direction of the radar receiver. Reflection or absorption of radar signals from the surface of a target towards the radar receiver mainly depends on the electric conductivity of surface material of the target. In cases, when a single antenna i.e. monostatic case, is required to be incorporated to perform both the functions of transmitting and receiving of a signals, then a duplexer is used as a switch between the transmitter and receiver. During the radar signals transmit time, the duplexer acts like a transmitter, while in receiving time it acts like a receiver. The received signals at the radar receiver are then amplified and demodulated for the display. The received signals reflected from the body of an object are also known as a Radar Cross Section (RCS) [1, 2]. The re-radiated power density at the radar is equal to:

$$P_r = \left(\frac{P_t G_t}{4\pi R^2} \right) \left(\frac{\sigma}{4\pi R^2} \right) \left(\frac{G_r \lambda^2}{4\pi} \right) \tag{1.1}$$

Where, P_t is the signal transmitting power of radar, G_t is the antenna gain at radar transmitter and G_r is the antenna gain at radar receiver, σ is the Radar Cross Section (RCS) of the target measured in square of meter (m^2), λ is the radar signal wavelength at which the radar is operated measured in meter (m), and R denotes the radar range between the target and transceiver of the radar.

In Eq (1.1), the first word in bracket indicates the power density of radar at the target. The proceeds form of the first two brackets indicates that how much the power density is received by the radar receiver as a result of scattering or reflection which may occur on the surface of the target. Moreover, in Eq (1.1), the amount of reflected power that is received at the antenna aperture indicates in the third bracket.

In most of the cases the radar transmitter and the receiver are at the same location, which means that $R_t = R_r$ and the term $R_t^2 R_r^2$ can be replaced by R^4, where R is the range. It shows that the received power is inversely proportional to the one-fourth power of the range, which means that the received power from distant targets is relatively very small.

1.2 Radar Cross Section (RCS)

Radar Cross Section (RCS) inherently describes reflection properties of an object which are basically the result of reflected signals returned to the radar receiver. It is normalized to the power density of an incident wave at the target. Therefore it does not depend on the distance of the target/object from the illumination source. Radar Cross Section (RCS) is evaluated from Eq (1.1), and is given as;

$$\sigma = \frac{\text{Power reflected toward source per unit solid angle}}{\text{incident power density}/4\pi} \qquad (1.2)$$

The RCS is a measurement of the reflectivity of a target expressed as 4π times the ratio of power per unit solid angle scattered/dispersed in a particular direction to the power per unit area in a plane wave incident on a scatterer from a particular

direction. So the RCS of a target will become [3, 4].

$$\sigma = \lim_{r \to \infty} 4\pi r^2 \frac{|E_S|^2}{|E_i|^2} \tag{1.3}$$

Where, E_s is the scattered electric field intensity that is reflecting back from the target and E_i is the electric field intensity incident to the target.

A limited amount of radar energy that is reflected from the object towards the radar receiver depends on the following factors:

- Radar Absorbent Material (RAM) used in a target.

- Shape and size of the target.

- Medium between transmitter, target and receiver.

- Wavelength of the illuminating radar signals.

- Incident angle of radar signals, orientation and geometry of the target.

- Frequency and intensity of the incident radar signals.

- Directivity of radar antenna towards the target.

- The reflecting angle of radar signals after hitting the target toward source.

- Polarization of the radiation that are transmitted and received with respect to the geometry of the target.

1.3 Physical Types of Radar

1.3.1 Mono-Static Radar

In monostatic radar, the radar transmitter and receiver are positioned at the same location. Therefore, in this case the transmitter and receiver range/distance are considered identical, i.e. $R = R_t = R_r$. An illustration of monostatic radar is presented in Fig (1.2). If a transceiver is used in monostatic radar, then the

FIGURE 1.2: Mono-static Radar model.

transmitter and receiver gain would be the same i.e. $G = G_t = G_r$. The power received P_r at the radar receiver can be written as follows:

$$P_r = \frac{P_t G^2 \sigma \lambda^2}{(4\pi)^3 R^4} \tag{1.4}$$

1.3.2 Bi-Static Radar

In bistatic radar, the radar transmitter and receiver are positioned at two different locations as shown in Fig (1.3). Therefore, in this case the transmitter and receiver having different antenna gains experience different distances with respect to the target, as compared to the in monostatic case. For the calculation of the received power P_r at the radar receiver in this case, the Eq (1.1) can be rewritten as follows:

$$P_r = \frac{P_t G_t G_r \lambda^2 \sigma_b}{(4\pi)^3 R_t^2 R_r^2} \tag{1.5}$$

Where σ_b is the bistatic radar cross section of the target, R_t and R_r are ranges between the transmitter and receiver towards the target [5].
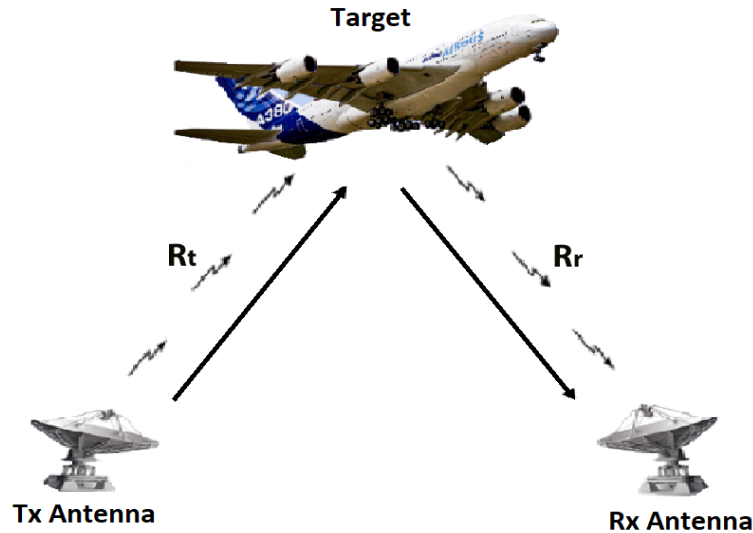
FIGURE 1.3: Bistatic Radar model.

1.4 Electromagnetic (EM) Theory

An electromagnetic (EM) field is generated through the movement of electric charges. The EM field propagates at the same rate as the light travels and interacts with charges and currents. The current carrying wire produces both electric and magnetic fields. This field can be considered a combined electric and magnetic field. Stationary charges in a system result in an electrical field and moving charges in a system result in a magnetic field. The direction has always been perpendicular between the electric and magnetic field. The generated force through the electric field is considerably larger than the force generated through the magnetic field. The way in which charges and currents interact with the electromagnetic field is described by Maxwell's equations and the Lorentz force law [6].

Electromagnetic (EM) field can be considered in two different ways, one is continuous structure and the other one is discrete structure. The electric and magnetic fields are produced through gentle movements of the charged objects. For example, the fluctuations in electric and magnetic fields produced due to oscillating charges that can be seen in a smooth form and in continuous wave form. In that case, the energy is assumed to be shifted continuously through the EM field between two

positions. For example, the metallic atoms of a radio transmitter appears to be transmitting energy continuously.

In a discrete structure the electromagnetic energy carried in packets form called Quanta with a fixed frequency. Radar transmits the electromagnetic (EM) waves in the form of pulses which are used to measure the range and velocity of the target. In this system the Amplitude Modulation (AM) is used, which can measure the time intervals between the transmitted and received pulses for measuring the target range. The Planck's relationship connects the photon energy E with its frequency f throughout the Eq (1.6).

$$E = hf \tag{1.6}$$

Where, h represent the Planck's constant and f denotes the frequency of the photon. Although, modern quantum optics indicates that there is a semi-conventional explanation for the photoelectric effect. The stationary electrons generates electric field where as the moving electrons generates magnetic field. The electrons that is emitted from the metal surfaces exposed to the EM radiation, the photon has been historically (but somewhere not necessarily) used to explain some considerations. It is also observed that the incident radiation intensity increased only if increases the number of electrons that were ejected and there was virtually no effect on the distribution of energy on their ejection. The frequency of the radiation that is only relates with the energy of the discharged electrons.

The charged particles may travel at relative speeds according to near-field propagation speeds, but as Einstein shows, it needs a lot more power which is not possible with electricity, magnetism and space. Also, it is demonstrated that a variable electric field leads to a magnetic field and a variable magnetic field leads to an electric field. When an electromagnetic field travels through different medium, it will change the properties of field due to different boundary condition. The components which

- The refractive angle of an electric field between the two medium depends on the permittivity of individual medium.

- The refractive angle of a magnetic field between the two medium depends on the permeability of individual medium.

1.5   Physical Optics Theory

Physical Optics (PO) are an approximation technique which is commonly used in optics, electrical engineering and applied for physics. The physical optics is used to be more physical than geometric or ray optics. This approximation of ray optics estimates the field on a surface and integrate this field over the surface to calculate the transmitted or scattered field [16].

This technique is also assumed to be suitable in estimating effects of diffraction from surface body. Moreover, this approximation is also used in radio communication to estimate interference, diffraction and polarization effects, however, there is no dependence of diffraction on polarization because this approximation is for high frequency.

In physical optics the estimated optic-ray is integrated over the lens, mirror or aperture to calculate the transmitted or scattered field. From the objects scattering this means that the current is taking on a tangent plane surface at each illuminated point of a material. The current is zero at the shadowed parts mean that these parts are not illuminated. At the radar receiver the resulting field is obtained by taking the integral all these approximated scattered fields. The reflection at the edges or shadowed boundaries are not accurate due to diffraction and refraction.

The difference between Geometric Optics (GO) and Physical Optics (PO), Geometric Optics relates with the refraction and reflection of rays of light without considering the wave or physical nature of light. The geometric optics use the geometrical and graphical methods to find the different positions of images that is formed by mirrors, lenses prism etc. The physical optics explain the objective phenomena of light such as interference, polarization, diffraction etc. and also defines the wave theory of light itself predicts the phenomena of interference and diffraction that are not described through geometric optics.

1.5.1 Physical Optics Based Designing and Modeling of Optical System

To design and analyze the optical systems, many simplified approximations are available. One of the approaches to represent the electric field, that light wave is a single scalar quantity, instead of using a vector quantity such as orthogonal electric vectors and magnetic vectors. The Huygens-Fresnel equation is one of the models to explain the optical system, which was derived in 1815 and based on the assumption that each point on the wavefront generates the other secondary spherical waves that Fresnel combines by using the principle of superposition. By using the Maxwell's equations, the Kirchhoff diffraction equation was derived that puts the Huygens-Fresnel equation. The Fraunhofer diffraction, superposition and refraction phenomena can be found by using the application and the principle of Huygens Fresnel equality [17].

Physical Optics (PO) depends on the electric and magnetic material properties which affects the wave nature of light. In view of these properties, the interaction of the light wave with the metal surface is entirely different from the interaction with dielectric materials.

1.6 Laws of Reflection and Refraction

The law of reflection states that the angle of incidence must be equal to the angle of reflection from a plane incidence surface. This law is valid for when there are no incident losses and also there is no effect of the medium. In other word this law is also called the law of 'Total Internal Reflection'.

In Fig (1.4) the reflecting surface is a plane shining surface, for example plate mirror, P is the incident wave with incident angle θ_1 and Q is the reflecting wave with reflecting angle θ_2, O represents the point where the incident wave hit the plane surface with normal N. The law of refraction states that the incident rays lies on the surface, the sine of the angle of incidence θ_1 divided by the sine of the angle of refraction θ_2.
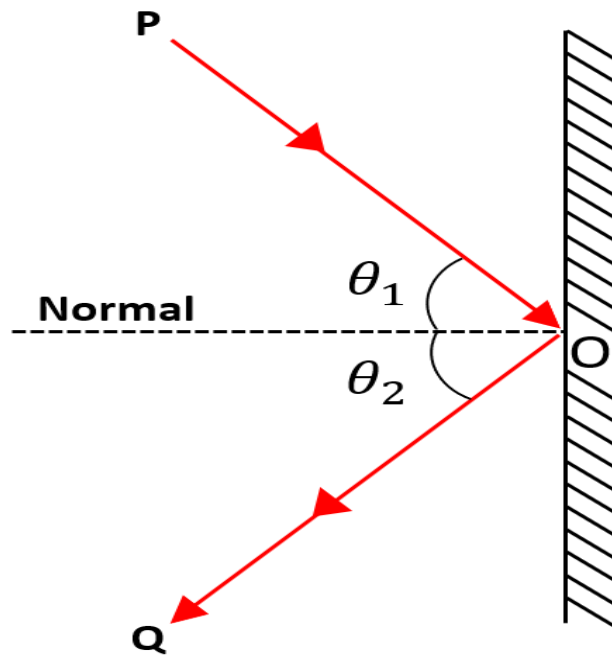
FIGURE 1.4: Reflection from plane surface.

$$\frac{\sin \theta_1}{\sin \theta_2} = n \qquad (1.7)$$

Where, n is the refractive index of second material which is constant for any two materials.

Fig (1.5), shows the law of reflection and the law of refraction from the surface with normal N. These two laws, can be derived from Fermat's principle which stipulates that the path traveled between two points by a beam of light is transversal to the incident path as it passes from one medium to another [7].

1.7 Different Methods for the Prediction of RCS

Radar system uses electromagnetic (EM) waves to detect a target as a result of reflection and scattering of waves from the target surface. In order to analyze the RCS theoretically, the following methods for any 2D or 3D object model Geometrical Optics (GO), Method of Moments (MOM), Finite Element Method (FEM),
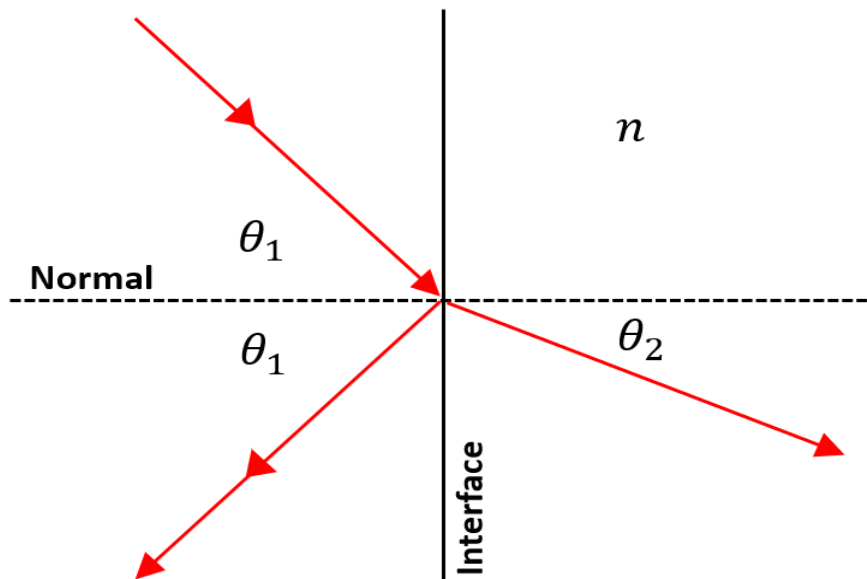
FIGURE 1.5: Laws of Reflection and Refraction.

Physical Theory of Diffraction (PTD), and Physical Optics (PO) are used. These methods are discussed in detail in the coming subsections. However, among all of these methods, the Physical Optics (PO) method is commonly used for the RCS prediction.

1.7.1 Geometric Optics (GO)

Geometric Optics (GO) or Ray Optics (RO), are based on the principles of light propagation in terms of rays. It works on the basis of light propagation, reflection and refraction. The ray in a geometric optics is essentially a conception of the approximate paths along which light travels in certain circumstances. According to Snell's law the ratio of the sines of the angle of incidence to the angle of refraction is a constant depending upon the medium. In geometrical optics, it is assumed that the light rays travel in a straight line when propagating in an homogeneous environment and the angle of reflection is equal to the angle of incidence. Moreover, the ray of light divides and bends in two specific circumstances at the interface of two different medium. Geometrical optics do not take into account some optical effects like diffraction and interference and that practice of is very useful. This

is an approximation when the wavelength is small in relation to the size of the structures that interacts with light. The techniques are specifically valuable to describe geometric aspects of imaging, including optical deviations [8, 9].

1.7.2 Method Of Moment (MOM)

This method is normally preferred when target surface is broken into small number of pieces and to solve its integral equation. In order to obtain the integral equations for a target, MOM use boundary condition and Maxwell's equations respectively. The complex and difficult step is to solve and reduce these integral equations. For the solution of integral equations, linear equations and standard matrix algebra are commonly used. However, this method fails to predict the RCS accurately in practice, if the target size is significant and the signal wavelength is short. Furthermore, it requires high processing speed to solve large matrices [10, 11].

1.7.3 Finite Element Method (FEM)

The Finite Element Method (FEM) is a particular numerical method to solve partial differential equations in two or three space variables (i.e. Some boundary value problems). In FEM the target model is taken into account in order to select the whole body of the target and equally divides its surface in triangular form. This technique splits a large system into smaller and simple parts which are referred to as finite elements depends on the target geometry. This is obtained by a specifically discretization of space within the dimensions of space or sampling the body surface, which is accomplished through the construction of an object mesh. The digital domain of the solution has a limited set of points. The formulation of the FEM of a limit value problem eventually produced a system of algebraic equations which is very difficult to solve these algebraic equations. This techniques is close to the unknown function in the domain. These simpler equations are then model these finite elements of the target model that combined into a bigger system of equations which models the whole target body with limiting area.

1.7.4 Physical Theory of Diffraction (PTD)

This method is related to the fields scattered by perfectly conducting bodies whose surfaces have linear dimensions with sharp edges and have large curvature radii in comparison to the wavelength. The PTD is based on the concept of Elementary Edge Waves (EEW's).

PTD method is used to calculate the edge-diffracted fields. The total scattered field is obtained by adding this edge diffracted field to the PO surface integral. Plotted numeric results supplement the theory and facilitate the visualization of individual contributions of distinct parts of the scattering objects to the total diffracted field [12, 13].

1.7.5 Physical Optics (PO)

The Physical Optics (PO) technique computes the surface current that are induced on an arbitrary body through incident radiation depends on the intensity of incident signals. The body portions that are illuminated directly through incident field, the current is induced which are directly proportional to the incident intensity of the magnetic field and also depends on the absorbing material surface. Moreover, the portions on the surface of the target which are shadowed, the value of current at that portions are approaches to zero and only the non shadowed area considered for scattering region. The radiation integrals for current is subsequently used in order to calculate the scattered field far from the target.

In this technique, the PO currents are changed by the use of a variable unit vector over the scatters surface [14, 15]. These current elements are produced for the reflector, which is powered by a remote electric line source. The scattering integral is expressed by the use of these currents and estimated in an asymptotic manner with the steady-state method.

The current is then utilized as a part of the radiation integrals to figure the scattered field a long way from the objective. PO is a high-recurrence estimation strategy that gives best results for electrically huge bodies ($L \geq 10\lambda$).

1.8   Research objectives

The objective of this research work is to explore various methods for estimating RCS and select the most commonly used method out of them, investigate its feature and enhance its functionality if needed.

1.9   Thesis Organization

The rest of thesis is divided into five chapters. The Chapter 2 presents the literature survey for all kinds of simulators that can estimate the RCS of an object and problem formulation. Chapter 3 presents the present version of POFACETS©4.2 and its limitations. Chapter 4 presents the proposed version of POFACETS©4.2 which is the Enhanced version of POFACETS, i.e EPOFACETS 5.0. Chapter 5 presents the simulation results and parametric analysis. Chapter 6 concludes the research work and explains how its findings can be explained to facilitate the future research in the area.

Chapter 2

Literature Survey and Problem Formulation

This chapter briefly discusses the literature survey of Radar Cross Section (RCS) simulation tools and presents their comparative analysis in section 2.1 and 2.2. In section 2.3, the problem formulation is presented. Section 2.4 discusses research methodology of the thesis and section 2.5 lists the thesis contributions.

2.1 Literature Survey

The Radar Cross Section (RCS) is a fundamental quantity in the radar system to detect the presence of an intruder in its region. RCS is the reflection properties of an object which is the basic requirements of the radar receiver to properly detect the target. It is basically the result of reflection and scattering of electromagnetic (EM) waves from the surface of an object base on the directivity of a radar transmitter. As discussed in chapter 1, the RCS depends on the geometrical shape of an object, surface material of the target and the incident electric field intensity. In order to predict and analyze the RCS of an object according to the user requirements, different types of simulators have been used which are based on PO, MLFMM, FEM, GO, PTD, FIT etc., which are listed below.

2.1.1 Physical Optics FACETS (POFACETS©4.2)

The Physical Optics FACETS (POFACETS©) version 4.2 is a MATLAB© based simulation software that was developed by David C. Jenn in 2004 at the Naval Postgraduate School [18]. This simulation tool works on the principle of Physical Optics (PO). It is an open source, user friendly and easy to use software to estimate the RCS. This software tool facilitates the user to predict RCS by modifying surface roughness, material properties and incident angles with respect to observation angles. The Graphical User Interface (GUI) of POFACETS©4.2 helps a user to load and run the simulation software more conveniently [19].
The RCS was computed based on the PO and PTD methods for the surface and edge integral to the RCS estimation for large and complex obstructions. An adaptive subdivision scheme that depends on the situation of incident shadowing, reflection shadowing, scattering shadowing and multiple reflections, was developed [20].

2.1.2 FEKO©

FEKO© is an electromagnetic simulation software tool that was developed by the US ANSYS company based on the Computational Electromagnetic (CEM) techniques used to find the RCS of a large object in a defined 3-D range. This software is also used for the electromagnetic compatibility (EMC) analysis, scattering analysis and antenna designing etc. It is a commercial software provided by the Altair community [21]. They can also allow a user to access the free license student version of this software but have some limitations according to the model geometry. Basis of the Feko solver is the Method of Moments (MoM) technique. Meanwhile, it also combined other techniques such as the Multilevel Fast Multipole Method (MLFMM), the Finite Element Method (FEM) Uniform Theory of Diffraction (UTD), Geometrical Optics (GO) and Physical Optics (PO). The FEKO© software is further categorized in three main components: CADFEKO, POSTFEKO and EDITFEKO. In order to create and mesh the geometry of an object, the

CADFEKO is used and also used to specify the solution settings and calculation requirements in a graphical environment. POSTFEKO is used to creates and displayed the 2D and 3D result graph and reads the results from the binary output file (*.bof). And EDITFEKO is used to developed a large and complicated models through high level scripting language. The bistatic RCS measurements of an object at a fixed bistatic angle in a compact range is performed. The scaled model of Boeing 707$^©$ and canonical missile are used for these bistatic measurements. These targets were illuminated with a uniform plane waves that were created by a parabolic dish reflector. The bistatic scattering of the targets were measured by placing a receive antenna at a fixed bistatic angle and finite distance in the compact range. The measured analysis of a complex targets was performed in anechoic chamber. For simulation analysis, the FEKO$^©$ software tool used the Multi Level Fast Multipole Method (MLFMM) for the RCS simulations and then compared with the measured results [22, 23].

The RCS data computation and analysis for complex target are the specific requirements for radar engineer. The target can be detected and obtained by 1-D PDF and 2-D RCS intensity. The RCS data can be calculated by 2D-IFFT by varying the incidence angles and excitation frequency. In [24], FEKO$^©$ simulation software tool is used to compute the RCS of a missile and presents the 1D, 2D and Inverse Synthetic Aperture Radar (ISAR) image.

In [25], the RCS of F-35 aircraft model is analyzed at 5 GHz frequency. For simulation purpose, the FEKO$^©$ software tool is used to compute the monostatic and bistatic RCS of a target model by using the Physical Optics (PO) method. The three different configurations is performed for the transmitter and receiver polarization i.e., Vertical-Vertical (VV), Vertical-Horizontal (VH) and Horizontal-Horizontal polarization.

By considering a large moving object, wind turbine affects the performance of the weather radar. So, for the identification of wind farm clutter, it is important to analyzed the electromagnetic scattering characteristics of wind turbine. The RCS of a large object is changed by moving or rotating the wind turbine blades which is due to changing the incident angle properties targeted on turbine blades. In [26],

the Radar Cross Scattering (RCS) of wind turbine is computed using FEKO$^{\text{©}}$ electromagnetic simulation software tool. The efficiency of this software tools is compared with the existing mathematical formulas of cylinder and cone to calculate the wind turbine RCS by changing their frequencies.

The development of radar technology gives significance to each country in the field of military engagements in order to develop the possessing aircrafts' stealth behavior with small RCS, due to which the enemy would not be able to easily detect these aircrafts' but the Radar Absorbent Material (RAM) of the taget take into account. In military aircrafts' designing, the computational electromagnetics (CEM) method becomes an important factor in simulating the behavior of an aircraft geometry through its RCS when it is illuminated by EM waves.

In [27], the simulation of RCS was performed through FEKO$^{\text{©}}$ electromagnetic simulation software using Unmanned Combat Aerial Vehicles (UCAV) and carried out the factors that were affecting the RCS values. Moreover, the impacts of these factors were analyzed by changing the computational methods, radar frequency and the target coating material. From the results it shows that, by increasing frequency, the greater computational resources is required due to which a large number of meshes is formed and required greater memory and a very high amount of time for simulation.

The scattering characteristics of stealth aircrafts' for monostatic and bistatic radar system provides a great significance in an aircraft's detection. In order to analyze the scattering characteristics of stealth aircrafts, the FEKO$^{\text{©}}$ software is used to compute the monostatic and bistatic RCS in different polarization ways i.e., HH and VV polarization. In [28], the EM scattering calculation method includes the MOM, PO, MLFMM and UTD methods etc.

During the last decade, several simulation software for computing the RCS of a target were introduced. In [29], the sphere and square flat plate models are used to compute the RCS at 10 GHz frequency. For this purpose, the three commercial RCS simulation software are used i.e., HFSS$^{\text{©}}$, CST$^{\text{©}}$ and FEKO$^{\text{©}}$, and then their simulation results are compared. The comparative analysis of these software was discussed in terms of accuracy, run time calculation and memory requirements.

2.1.3   Computer Simulation Technology (CST$^{©}$) Studio Suite 2019

Computer Simulation Technology (CST$^{©}$) studio suite is an electromagnetic (EM) software tool that can be used to find the RCS of an object. This simulating tool also used for designing the 3D models of any object, PCB designing, plane models, antenna designing etc. The CST$^{©}$ studio suite software is an open source simulating tool that can be easily accessible and easy to use as compared to other simulating tools which are not open source. Different simulating methods, including Finite Element Method (FEM), Finite Integration Technique (FIT), Transmission Line Matrix (TLM), and Particle in Cell (PIC) are used in this software tool.

The detection and location of the moving target are dependent on the bistatic RCS and the design parameters of the radar, which in our experimental study used the LTE signal as a Passive Bistatic Radar (PBR) source. The moving target that may also be categorized into positions from different bistatic radar angles using conventional processing approaches that we have carried out using CST$^{©}$ Microwave Studio (CST-MWS) simulation [30].

RCS is a major significant metric in the area of stealth and anti-stealth radar. This paper introduced a variety of full-wave simulation methods, and the RCS of the S-shaped input is computed respectively, using these methods implanted in the commercial software CST$^{©}$ Microwave Studio (CST-MWS) [31].

High-frequency methods are well known as a convenient approach for treating EM problems regarding electrically large structures. In this paper, this method is proposed as a proper tool for computing the mono-static RCS of a relatively small complex structure. These computations have been carried out by employing the integral equation and asymptotic solver of CST$^{©}$ Microwave Studio (MWS) [32]. This paper describes the analysis and prediction of the RCS for simple target shapes such as circular flat plate, triangular flat plate, ellipsoid and sphere etc. Moreover, this paper explained precisely PO approximation in measuring the monostatic RCS far field for different simple models varying in size through with the MATLAB$^{©}$ programming to compute the resultant graphs, and the computed

results were compared with more precise data that is obtained by CST$^©$ that uses the stochastic solver in the RCS calculation of these objects [32].

RCS is an significant parameter that provides an indication of the spatial waveform of the target return signal to the radar (Echo) that may be supposed as a signature. For any physical objects the signature measurements for the RCS like aircraft, tanks, and vessels is more complex and costly processes. The Computer Simulation Technology (CST$^©$) software is used to compute the RCS for many target materials as well as for various angles [33–35].

2.1.4 Computer Solution (COMSOL$^©$) Multiphysics

COMSOL$^©$ Multiphysics is a simulation platform that encompasses all of the steps in the modeling workflow of defining geometries, material properties, and the physics that describe specific phenomena to solve and post processing models for producing accurate and trustworthy results. For designing the stealth antenna using the COMSOL$^©$ multi-physics application to analyze Frequency Selective Surface (FSS) structures. The RCS of antenna is reduced because it possesses the dual filter concept of frequency and polarization for electromagnetic waves.

In [36], the stealth aircraft F-117 nighthawk fighter is considered as a target object and also measured the RCS for analysis. It was noted that the RCS is an important parameter for radar and its aspect angles that are varied with respect to target movements and also the reflected outcomes are received at radar receiver. The CAD model of F-117 is developed and the RCS of this model is measured in COMSOL$^©$ Multi-physics software [36, 37]. The incident radar signals were transmitted to the target and the RCS has been measured. Moreover, it has been analyzed that better RCS can be obtained with the high frequency band and this detectability can be increased.

COMSOL$^©$ Multi-physics software is utilized to simulate the interaction between incident electromagnetic wave and the cloaks. The material designed model are then imported into this software to computes its RCS. This software based on the Finite Element Method (FEM) to simulate monostatic and bistatic RCS of a

target model. Monostatic and bistatic RCS is calculated to show the scattering suppression effect at radar receiver. The results show that meta-materials have an excellent performance in reduction of the scattering [38].

2.1.5 Computer Aided Design Radar Cross Section (CADRCS©)

Computer Aided Design Radar Cross Section (CADRCS©) is the RCS simulation tool which is used for designing a graphical model of an object in triangular dimensions. The model is then further exported to other software for different purposes. The CADRCS software was sold as a simulation tool for military and industrial applications to teach the main concept of RCS. The three different types of the target models are created and observed in CAD software and then are imported to CADRCS software for simulation [39]. The CADRCS simulate the effects of reflectivity of a material on the RCS of a target by using the Physical Optics (PO) method. This software is not only able to find the RCS of an object, but it also finds and show the high and low reflective area on the surface of that object material.

The RCS of a CAD© model of the stealth bomber B-2 Spirit was simulated through the CADRCS software [40, 41]. The aim of this study was to examine that how the shape may influence the RCS of an aircraft and how the use of Radar Absorbent Material (RAM) can further reduce its RCS. This software, like other simulation tools, combines physical optics with Ray Tracing (RT) techniques to calculate the RCS of a target.

The RCS simulations of a heat searching air-to-air missile model have been carried out using the CADRCS© software [40]. The frequency of 10 GHz has been considered in these simulations, the missile surface was referred to as a Perfect Electric Conductor (PEC) and covered with a Radar Absorbing Material (RAM). The simulation results comparison demonstrates how different portions of the missile can contribute with the RCS. Furthermore, it is demonstrated that how the RCS of the missile is minimized through the use of radar absorbing materials.

The commercially available CADRCS$^{©}$ software, sold as a simulation tool for military and industrial applications. Models of objects and targets are created in CAD$^{©}$ and then imported to CADRCS$^{©}$ for simulation [42]. The commercial software CADRCS$^{©}$ was used in the simulations. It combines ray-tracing techniques with physical optics to calculate the RCS of an object. Shadowing of rays is also taken into account, resulting in accurate RCS calculations for objects greater than the radar wavelength [43].

2.1.6 Finite Difference Time Domain (FDTD$^{©}$) 3D Electromagnetic Simulation Software

The Finite Difference Time Domain (FDTD$^{©}$) method is used in 3D electromagnetic simulation software for finding the RCS of hellfire missile. The accurate calculation of the RCS of millimeter wave frequency required the geometrical representation of the target and physical modeling techniques that capture the scattering and reflecting effect of small facets of the target [44]. REMCOM is the supplier company of providing the RCS simulators based on the Physical Optics (PO) method, and Method of Equivalent Current (MEC). The three directions (XY, XZ, YZ) of hellfire target are observed and predict its RCS. The geometry of this target consists of 11,536 facets and modeled as Perfect Electric Conductor (PEC) material. No need of simplification is required in target geometry because there are no spaces between each of the target facets. For the simulation the X3D RCS model is selected by applying both the methods of Physical Optics (PO) and Method of Equivalent Current (MEC). The simulation is performed on a sinusoidal wave of 10 GHz frequency.

Three-Dimensional (3-D) MATLAB$^{©}$-based codes are developed for RCS Modeling and Simulation (MODSIM) using Method of Moments (MOM) and Finite-Difference Time-Domain (FDTD) approaches [45]. A novel, accelerated, and parallelized Finite-Difference Time-Domain (FDTD) based RCS prediction tool which predict the RCS of complex targets [46].

In [47], the rapid and precise calculation of the RCS has an important meaning

for the search for the complex military target. FEKO$^{©}$ is a software for electro-magnetic simulation that can rapidly and accurately compute the radar scattering character of a complex military target particularly for large multi-conductor 3D electric bodies. The arithmetic analysis is based on the MOM, FDTD and PO methods, and the RCS is computing for the complex military target through FEKO$^{©}$ software.

2.1.7 Computer Aided Software Testing (CAST$^{©}$)

CAST$^{©}$ is a simulation software tool used for prediction and analysis of RCS simulation. This simulation tool is capable to find the monostatic and bistatic RCS of a model, it also finds the amplitude, phase and distance figure for complex 3D objects over a user specified frequency and angle ranges [48]. In this paper, they introduce CAST$^{©}$ application and its techniques to compute RCS of different sized objects and their surroundings CAST$^{©}$ provide the estimation that how the radar signature would be strong to detect the different direction at different frequencies. It is introduced to the design process of different military vessels to analyze and improve their stealth capabilities and also be used for analyzing the various radar reflectors in order to develop the optimal radar reflectors to improve the maritime safety. During the planning process the CAST$^{©}$ can estimate the RCS of a vessel. Using the Applied Physical Optics (APO) in combination with Physical Theory of Diffraction (PTD) to predict the RCS.

2.1.8 EPSILON$^{TM©}$

An EPSILON$^{TM©}$ software tool developed by ROKE in the UK in 2008 which is designed to predict the Radar Cross Section (RCS) directly from the target geometrical parameters. Moreover, it is the analysis tool that gives support for the radar system modelling that allows a designer to assess the radar signature of a design and also study the relationship between the signature and the shape and direction of the design [49]. The radar signature management is required

for the clients who design the platforms like ships, flat plane, aircraft or radar system. In the military platforms the designer needs to minimize the RCS to reduce the probability of detection of targets based on radar sensors. This paper describes a Network Application Interface, Network (API) that has been added to the EPSILON$^{TM©}$ RCS prediction code. EPSILON$^{TM©}$ is a well established Physical Optics (PO) based prediction code with Shooting Bouncing Ray (SBR) multiple scattering and Physical Theory of Diffraction (PTD) edge scattering facilities [50, 51].

EPSILON$^{TM©}$ is a multi-purpose tool, that approaches actual scenario models, allowing customers to rapidly assess target signatures and to study these signatures vary depending on the shape, geometry and direction of its conception. It estimates the RCS electrically of large targets based on computational model of the target [52].

2.1.9   PUMA-EM$^{©}$

PUMA-EM$^{©}$ is an open-source simulating tool that can be used for designing of a model and then find its RCS using desire angles and frequencies. PUMA-EM$^{©}$ is a LINUX operating system software tool which is much harder to use for simulating the object RCS. It is used to compute the RCS of a target model for only single incident angle. This software is based on coding that allows the computation of different EM quantities when an object (target) is incident by an electromagnetic source. These quantities are actually the scattered fields and the target surface current, which can compute the monostatic and bistatic RCS for different required angles [53].

The method used for the RCS calculation is the boundary element method also known as Method of Moments (MOM). The main limitation of this software is that, it can only compute the RCS of a simple model. This software is not used for complex model As discussed that the RCS depends on the surface material of a target, so, for this purpose the Perfect Electric Conductor (PEC) material of a target was assumed for better RCS estimation [54].

2.2 Comparative Analysis of Various Simulators

This section provides comparative analysis of well-known Radar Cross Section (RCS) estimation software that can be used to predict the RCS according to the requirements of the user. Among them, some software is open-source whereas most of them are commercial software which require high subscriptions.

Although, open-source software is easily accessible; however, their ease of operability varies from software to software. Therefore, in this work, a user friendly programming language based open-source software POFACETS$^©$4.2 is preferred to estimate RCS. The POFACETS$^©$4.2 provides an open-source copyright to users and allow them to modify the MATLAB$^©$ codes according to their requirements. The comparison of currently available RCS software is presented in Table (2.1):

The comparative analysis is based on the user facility to interact with these RCS software tools. Among these software, the POFACETS$^©$4.2, FEKO$^©$, and CST$^©$, are the tools which are easily accessible and open source software. All the other software are commercial and need resources to interact with these software which are much difficult for the users.

In order to use the POFACETS$^©$4.2 software tool, the RCS of a target model is computed for only a single incident angle and takes much more time to computes the RCS for a range of incident angle.

In order to use the student crack version of FEKO$^©$ software tool, the RCS of a target is computed for a range of incident angles with respect to observation angle. By considering the limitations of student crack version, the RCS is computed for the less number of model facets, due to which the RCS is not much accurately as compared to other software related to the model parameters. Also, it required more memory to stored RCS data and facet model.

In order to use the CST$^©$ software tool, the problem of facets limitation is appeared wile using for the computation of RCS of a complex target. This software tool is used for a simple model. This simulating tool is also used for designing the 3D models of any object etc. The simulation run time for the RCS computation for a range of incident angle is much more as compared to POFACETS$^©$4.2.

TABLE 2.1: Comparative analysis of RCS simulators

Name of Simulator	Principle/Technique Used	Source File	Single/Range of Angles	Facets Limitations	Simulation Time/Memory Requirements	GUI Window/Codes
POFACETS©4.2	Physical Optics (PO)	Open Source	Single Incident	No	Low Time/Lesser Memory	GUI Window
FEKO©	Multi Level Fast Multipole Method (MLFMM), (PO), (FEM), (MOM)	Open Source and Commercial	Range of Incident	Yes	High Time/Higher Memory	GUI Window
CST© Studio Suite	Finite Element Method (FEM), Finite Integration Technique (FIT), Transmission Line Matrix (TLM)	Open Source	Range of Incident	Yes	High Time/Higher Memory	GUI Window
COMSOL©	Physical Theory of Diffraction (PTD)	Commercial	Single Incident	Yes	Low Time/Higher Memory	GUI Window
CADRCS©	Method of Moment (MOM)	Commercial	Single Incident	Yes	High Time/Lower Memory	GUI Window
FDTD 3D©	Method of Equivalent Current (MEC), (PO)	Commercial	Range of Incident	Yes	High Time/Higher Memory	GUI Window and Codes
CAST©	(PO), (MOM), (PTD)	Commercial	Single Incident	Yes	Low Time/Lesser Memory	GUI Window
EPSILON™©	Physical Optics (PO)	Commercial	Range of Incident	Yes	High Time/High Memory	GUI Window
PUMA-EM©	Method of Moment (MOM)	Open Source	Single Incident	No	Low Time/Lesser Memory	Coding Base Simulation

2.3   Problem Formulation

Although, the existing simulation software POFACETS©4.2 provides sufficient RCS results to analyze the reflective properties of the targeting object. However, the existing version estimates RCS with respect to a single incident angle. In order to estimate RCS over a range of incident angles, the same procedure of POFACETS©4.2 is repeated for each incident angle one-by-one. In such scenario, estimation of RCS through POFACETS©4.2 become cumbersome and time consuming for a user. Therefore, an enhanced version of POFACETS©4.2 is required to be establish to reduce the working and time consumption of a user.

2.4   Research Methodology

In order to enhance the functionalities of the existing version of POFACETS©4.2, the Graphical User Interface (GUI) and POFACETS©4.2 codes are upgraded to accommodate the range of incident angles. A self-guiding GUI is established separately to input the range of incident angles to guide the user and avoid any mistake. The related MATLAB© codes are developed for RCS estimation and linked with the GUI. The GUI automatically adjusts its related scenario and provides estimated RCS of any input model.

2.5   Thesis Contribution

The major contributions of this thesis are given as under:

- The present version of POFACETS©4.2 is upgraded, so that it can compute the bistatic RCS of an object with a range of incident angles.

- Designing the GUI in MATLAB© which contains the range of incident angles, the range of incident angles and parameters similar like POFACETS©4.2 named as EPOFACETS 5.0.

- EPOFACETS 5.0 compute the range of incident angles in a single step which are reducing simulation run time to 39.251% compare with POFACETS©4.2.

- The computing RCS data are then stored in cells arrays in MATLAB© file which contains RCS estimating plots with respect to observation angles, incident and observation angles, frequency. The simulation data are then used in approximating the shape of an object and also used to find the reflection co-efficient of that object.

Chapter 3

POFACETS©4.2 and its Limitations

This chapter gives a detailed overview of the existing POFACETS© version 4.2 and explains a step-by-step procedure to design an object and to find its Radar Cross Section (RCS). Moreover, the limitations of the POFACETS©4.2 are listed at the end of this chapter.

3.1 Physical Optics FACETS (POFACETS©)

3.1.1 Background

Physical Optics (PO) based MATLAB© simulation software POFACETS©4.2 is a well-known RCS estimation tool that has been developed by David C. Jenn in 2004 [19]. This software facilitates users through its Graphical User Interface (GUI) and allows them to input all the required informations at one place [55]. This software facilitates users to design a facet-based model following the specific requirements to the designed model. Additionally, this software also allows users to design models through other software tools such as CAD©, AutoCAD©, Epsilon©, COMSOL© etc. and to import the designed model into POFACETS©4.2 for RCS

estimation. Moreover, this tool allows users to adjust surface materials properties such as surface roughness, surface resistivity and type of material. Once a model is designed, the user is able to estimate the RCS of the model at specific range of observation angles at fixed single incident angle.

3.1.2 Physical Optics (PO) Method

This section describes the theoretical working of the Physical Optics (PO) approximation technique that are used in POFACETS©4.2 software tool. The following sets of calculations are involved in this method.

3.1.2.1 Scattered Field Calculation of an Arbitrary Body

In order to understand the Physical Optics (PO) method, consider an arbitrary object whose scattered field formula is derived using triangular facets. In PO method, the surface currents on the facets are incident due to which the surface of the material will excite to produce the scattered field which can be calculated through Taylor series. The model for which the calculation is expanded to perform the computation of the scattered field using various facets combinations of the target model.

3.1.2.2 Radiation Integral of the Scattered Field from the Arbitrary Body

The scattering field from an arbitrary body is the specific case of a scattering field from a triangular surface. A mathematical formula can be derived for the scattered field from a triangular facet through the given arbitrary body. Let the arbitrary scattering body is placed in (x, y, z) plane centered at the origin having the coordinates (u, v, w) as shown in Fig (3.1). In order to calculate the RCS of the body, take into account that the observation point at an area far from the target [56], where, R and r vectors can be considered nearly parallel. The whole
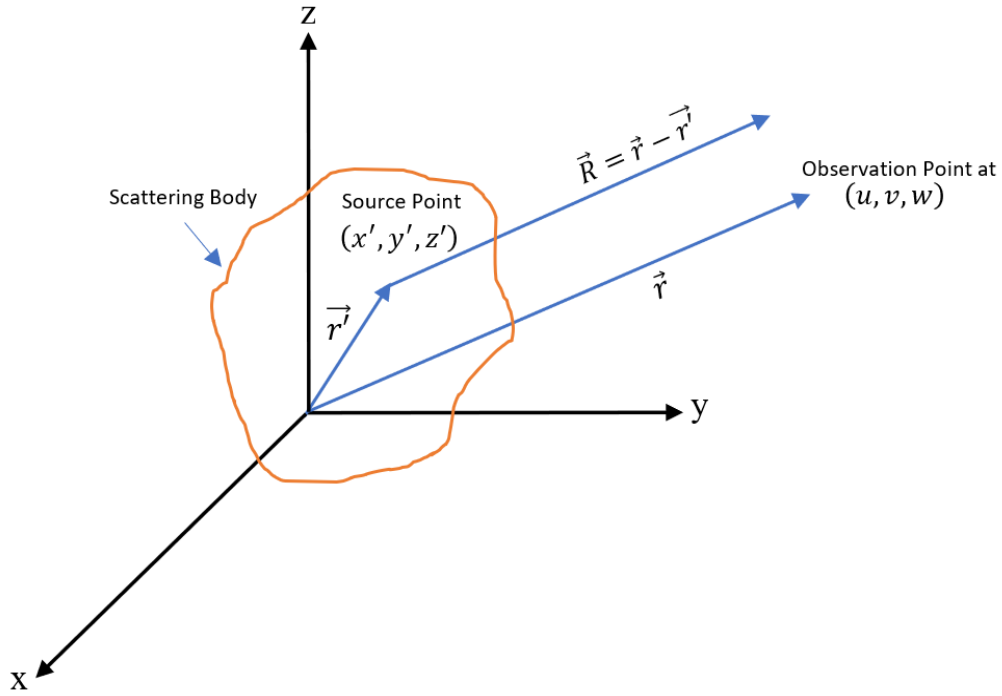
FIGURE 3.1: Scattering field from an arbitrary body.

arbitrary body is subdivided into extremely small volume points v', out of which one source point is lying at the (x', y', z') coordinates. The source point position vector is indicated as:

$$\vec{r'} = \hat{x}x' + \hat{y}y' + \hat{z}z' \tag{3.1}$$

Where, $(\hat{x}, \hat{y}, \hat{z})$ be the unit vectors of the co-ordinate axes. These unit vectors are in the direction of observation point whose position vector can be written as:

$$\hat{r} = \hat{x}u + \hat{y}v + \hat{z}w \tag{3.2}$$

where

$$
\begin{aligned}
u &= \sin\theta\cos\phi \\
v &= \sin\theta\sin\phi \\
w &= \cos\theta
\end{aligned}
\tag{3.3}
$$

As assumed at the shadowed region, the total current are supposed to zero and no reflection is received. Here, the observation point is located at the far finite distance from the target and according to the observation point, the spherical
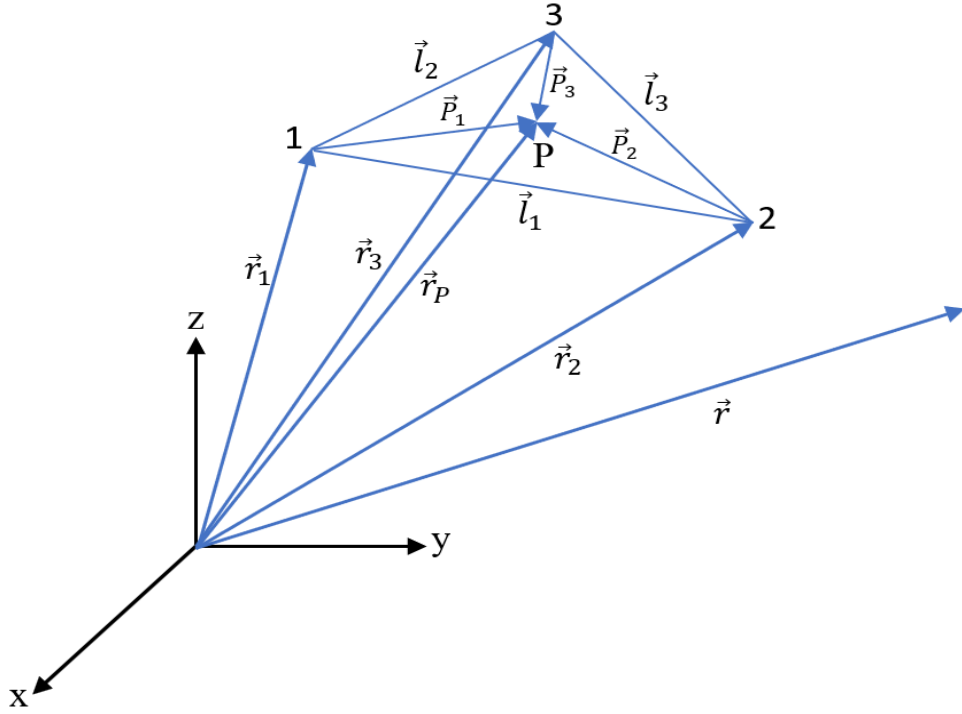
FIGURE 3.2: Facets geometry of the arbitrary body.

coordinates are θ and ϕ. In order to considered $J_m = 0$, which is the magnetic volume current in the body, the field scattered from the arbitrary body is given by:

$$\vec{E}_s(r, \theta, \phi) = E_\theta(r, \theta, \phi)\hat{\theta} + E_\phi(r, \theta, \phi)\hat{\phi} = \frac{-jkZ_0}{4\pi r}e^{-jkr}\int\int\int_v \vec{J}e^{jkg}\mathrm{d}v' \qquad (3.4)$$

Where, J depicts the electric volume current, Z_0 explains the space intrinsic impedance, $k = \frac{2\pi}{\lambda}$ and g is the dot product of $\vec{r'}$ and $\vec{r}$ that yields:

$$g = \vec{r'}.\hat{r} = x'u + y'v + z'w \qquad (3.5)$$

3.1.2.3 Radiation Integral of a Triangular Facets

Consider, triangular facet of an arbitrary body with an arbitrary direction of the vertices 1, 2, and 3, as shown in Fig (3.2). In this case, the integrating point P whose coordinates are (x_p, y_p, z_p) corresponding to the (x', y', z') coordinates of the integration point of the arbitrary body. The triangular facet position vector is:

$$\vec{r_p} = x_p\hat{x} + y_p\hat{y} + z_p\hat{z} \tag{3.6}$$

After substituting the values of the triangular facets of the two-dimensional object shown in Fig (3.2), the Eq (3.4) becomes a surface integration. Since, in the triangular surface only the surface current is flowing; therefore, the Eq (3.4) becomes:

$$\vec{E}_s(r, \theta, \phi) = \frac{-jkZ_0}{4\pi r}e^{-jkr} \int\int_A \vec{J}_s e^{jkg} \mathrm{d}s_p \tag{3.7}$$

Where, J_s denotes the surface current, A is the triangular surface area, ds_p describes the differential surface area, and the term g may be calculated from the dot product of $\vec{r_p}$ and $\hat{r}$ i.e.

$$g = \vec{r_p}.\hat{r} = x_p u + y_p v + z_p w \tag{3.8}$$

Fig (3.2), represents the single facet geometry with an arbitrary direction. The vertices of the facet are known according to their Cartesian coordinates (x_n, y_n, z_n) for taking n=1,2,3. The vertices of the position vectors are given by:

$$\vec{r_n} = x_n\hat{x} + y_n\hat{y} + z_n\hat{z} \tag{3.9}$$

Subsequently, the side vectors may be calculated using coordinates of the node as shown below:

$$\vec{l_1} = \vec{r_2} - \vec{r_1}, \ \vec{l_2} = \vec{r_3} - \vec{r_2}, \ \vec{l_3} = \vec{r_1} - \vec{r_3} \tag{3.10}$$

The facets upper normal may subsequently derived by using the cross product of every possible two side vectors in a right direction. For example:

$$\hat{n} = \frac{\vec{l_1} \times \vec{l_3}}{|\vec{l_1}||\vec{l_3}|} = n_x\hat{x} + n_y\hat{y} + n_z\hat{z} \tag{3.11}$$

The vertices with this direction, the facet outer side is referred to like the front side when its value equal to 1, while the facet opposite side shows its back side when its value is equal to 0. The vector of propagation for a plane is formed, when it is incident at the angle (θ_i, ϕ_i), and is propagating back towards the origin, so

the propagation vector becomes:

$$\hat{k}_i = -\hat{r} = -(\hat{x}u_i + \hat{y}v_i + \hat{z}w_i) \tag{3.12}$$

where, (u_i, v_i, w_i) denotes the cosines angles between the vectors and the three coordinate axes and $\hat{r}$ expresses the directional unit vector that is originating at the origin towards source at (θ_i, ϕ_i). A upper side of the facet is illuminated once the following condition is satisfied:

$$-\hat{k}_i.\hat{n} \geq 0 \tag{3.13}$$

The observed scattered field from a single facet is derived through two simple problems:

- The calculation of the surface current J_s flowing over the facet surface through PO methods.

- The calculation of radiation integral of a triangular surface in Eq (3.7).

3.1.2.4 Surface Current Computation Through Physical Optics (PO)

In Physical Optics (PO), the target surface is illuminated directly through incident field. The magnetic field intensity is directly proportional to the amount of induced current on the target's body. The current is set to zero at portions where the target is not illuminated, which is given by:

$$\vec{J}_s = \begin{cases} 2\hat{n} \times \vec{H}_i & \text{illuminated facets} \\ 0 & \text{shadowed facets} \end{cases} \tag{3.14}$$

Where, J_s denotes the surface current of the targeted body, H_i explains the intensity of the magnetic field induce on the target surface. Generally, the intensity of the electric field E_i can be expressed as:

$$\vec{E}_i = (E_{i\theta}\hat{\theta} + E_{i\phi}\hat{\phi})e^{-j\vec{k}_i.\vec{r}} \tag{3.15}$$

Assuming that $\hat{r}_p = \hat{r}$ and $\vec{k}_i = k\hat{k}_i = -k\hat{r}_i$, for a point (x_p, y_p, z_p) on the surface, so the Eq (3.15) becomes:

$$\vec{E}_i = (E_{i\theta}\hat{\theta} + E_{i\phi}\hat{\phi})e^{jk\hat{r}_i.\vec{r_p}} \tag{3.16}$$

The magnetic field intensity H_i becomes:

$$\vec{H}_i = \frac{\vec{k}_i \times \vec{E}_i}{Z_0} = \frac{1}{Z_0}(E_{i\phi}\hat{\theta} - E_{i\theta}\hat{\phi})e^{jk\hat{r}_i.\vec{r_p}} \tag{3.17}$$

Therefore, the surface current flowing on the facet can be calculated as:

$$\vec{J}_s = 2\hat{n} \times \vec{H}_i = \frac{2}{Z_0}(E_{i\phi}\hat{\theta} - E_{i\theta}\hat{\phi})e^{jkh} \tag{3.18}$$

Where h is defined as:

$$h = \vec{r_p}.\hat{r}_i = x_p u_i + y_p v_i + z_p w_i \tag{3.19}$$

3.2 Working Principle of RCS Estimation Using POFACETS$^©$4.2

As discussed earlier, POFACETS$^©$4.2 is an open source well-established simulation tool that works on the principles of Physical Optics (PO). This uses a MATLAB$^©$ code to develop Graphical User Interface (GUI) in order to facilitate a user while estimating RCS of an object according to the user requirements. In order to estimate RCS through POFACETS$^©$4.2, a facet-based model of the object is required. Also a facet-based model is designed in other software tool and then import into POFACETS$^©$4.2 for RCS computations. The Superposition theorem and Taylor series are then implemented to compute the scattered fields reflected from the targets' surface. The scattered field of each facet is then evaluated and then the scattered field vectors are summed to compute the total field at the required incident and observation angle. For all incident and observation angles, the same procedure is repeated to get the target RCS. A step by step working principle of POFACETS$^©$4.2 in term of flow diagram is explained in Fig (3.3).
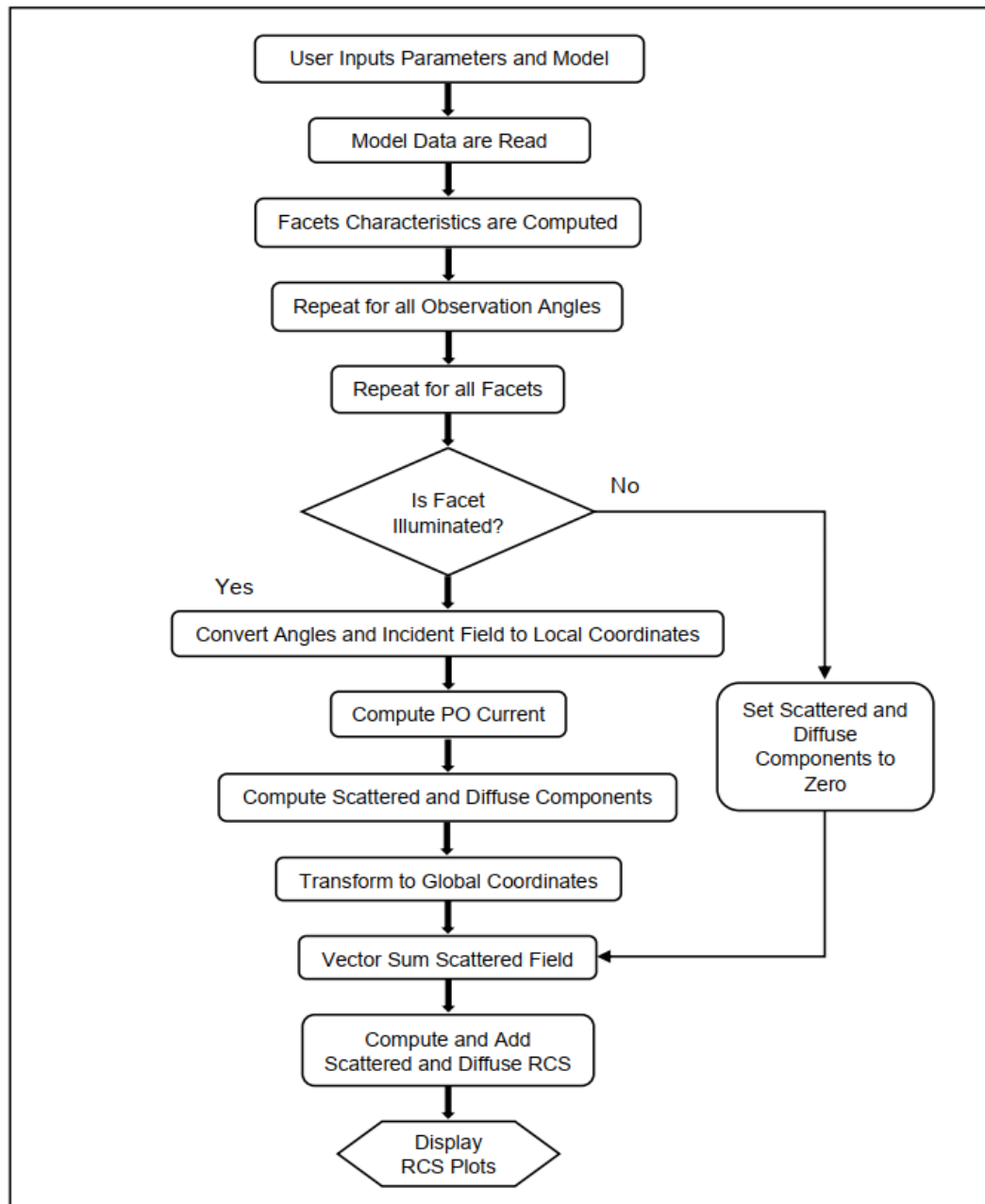
FIGURE 3.3: Flow chart for RCS calculation.

3.3 Graphical Components of POFACETS©4.2 Main Window

3.3.1 POFACETS©4.2 Main Window

The main screen GUI of POFACETS©4.2 has been categorized into three main functions blocks i.e. Design Model, RCS calculation and Utilities, as shown in Fig

(3.4). The design block includes options to design a model manually and graphically. A user can select one of the options depending upon requirement. The second block includes options of calculating monostatic and bistatic RCS. The third block includes utilities option to convert the present version of POFACETS©3.0 to old version of POFACETS©2.3 and also a user can convert GUI 3.0 version into non-GUI 2.3 version and vice versa. The button "About" acknowledges the contribution of authors. In GUI, each box is linked to a predefined set of MATLAB© codes to perform the related operation.

3.3.1.1 Manual Model Designing

In order to manually design a triangular facet-based model of an object, a user has to provide facets related information's such as number of vertices and number of facets. The GUI window of manual design is shown in Fig (3.5). The window has been designed in three main blocks representing the steps of manual model designing. In the first step, vertices of model plan are taken and checked the
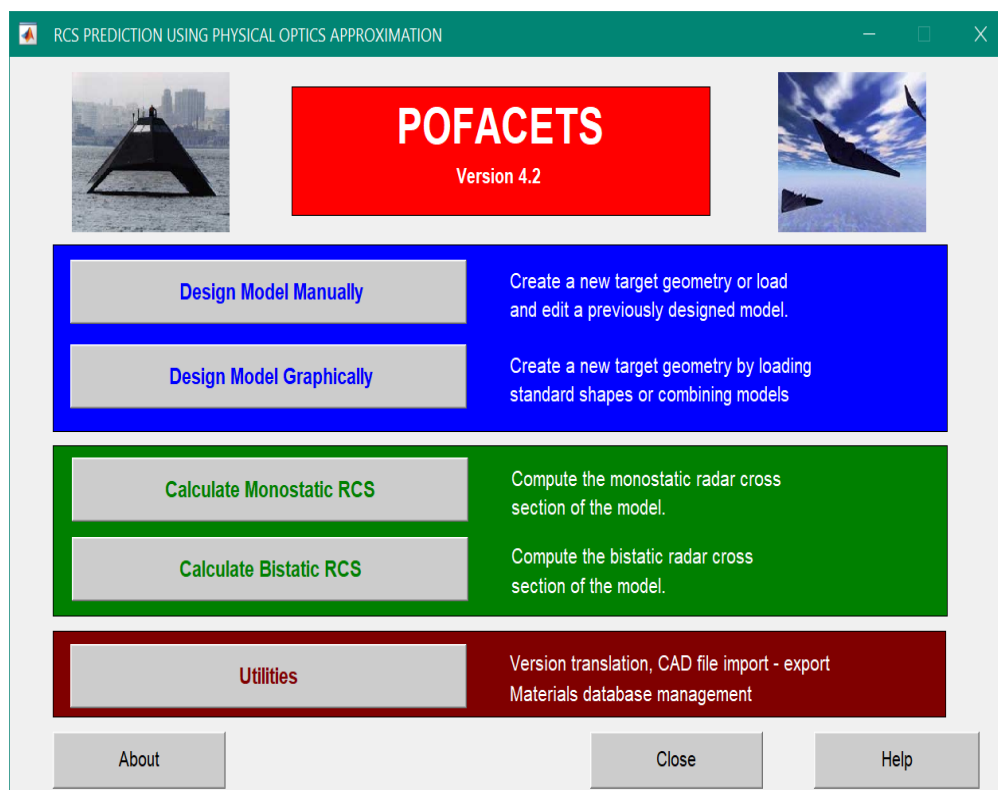

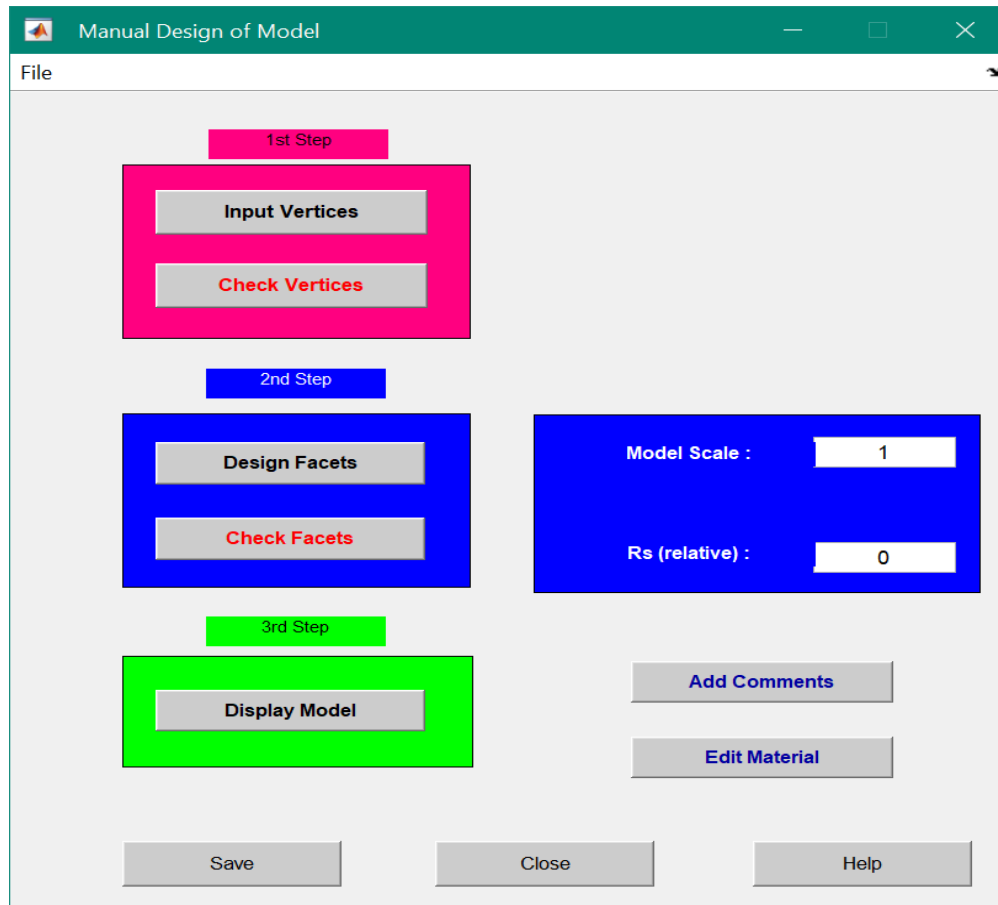FIGURE 3.4: Main screen GUI of POFACETS©4.2.

FIGURE 3.5: GUI of manual model design.

correct input. In the second step, the facets are designed and checked by taking facet points. In the third step, the model is checked for finalization. In manual design, the maximum number of facets and vertices are allowed to be 40. However, this number of vertices is not adequate to design a complex model. Normally manual design of model is not considered good as a user has to manually obtain the vertices of model and has to store them in an array, as shown in Fig (3.6). After putting the vertices, the number of facets can then enter in row and column by using the vertex number. The user can able to edit the number of facets by changing the size of the matrix shown in Fig (3.7). The two rows in figure specify the number of facets and the first three columns denote the vertices of the facets. If Column 4 is set 1, denote that the facet illuminated on front side and if column 4 is set 0, denote that the facet illuminated on both sides (front and back). Column 5 indicates that the facet is Perfect Electric Conductor (PEC) when it set 0. After completing all the facet definition, the designed model is displayed by clicking the
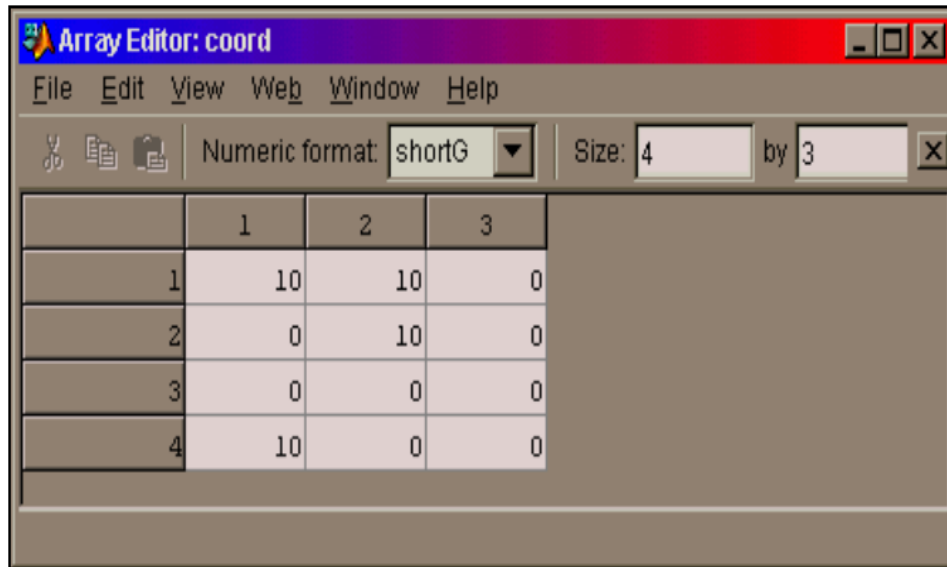
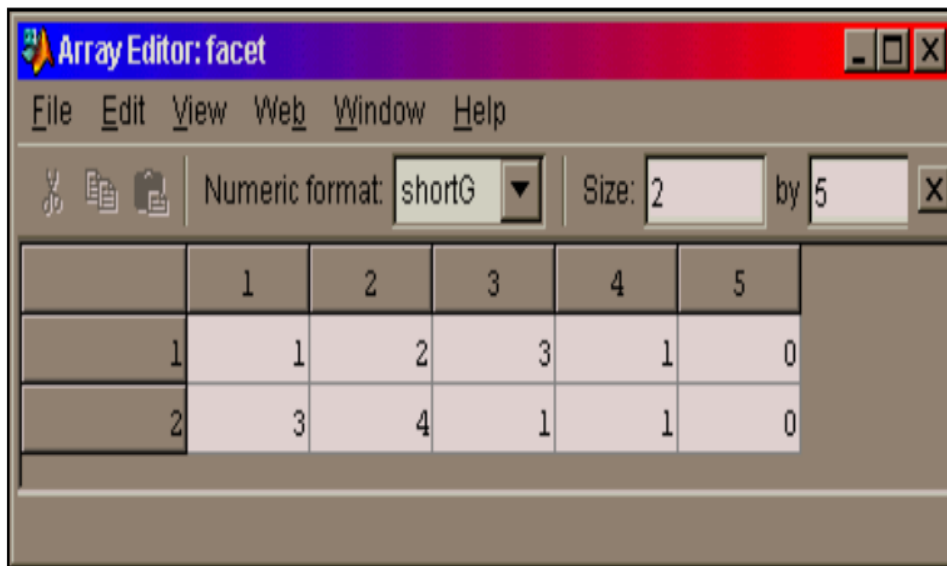FIGURE 3.6: GUI of input vertex coordinate.

FIGURE 3.7: GUI of input facets vertices.

third step, which is called Plate model displayed in a triangular GUI window shown in Fig (3.8). The user can be able to change any vertices of facets and coordinates of the model after completing and displayed model. Also, the user can change the view of 2D plate model into 3D and to label the facets and coordinates vertices of the plate model that are clearly mentioned in the GUI manual model display. Once the model design, the user can save it easily and compute the RCS of the designed Plate model. Using this model user can import another model in this triangular surface and combine with plate model. Complex models are designed
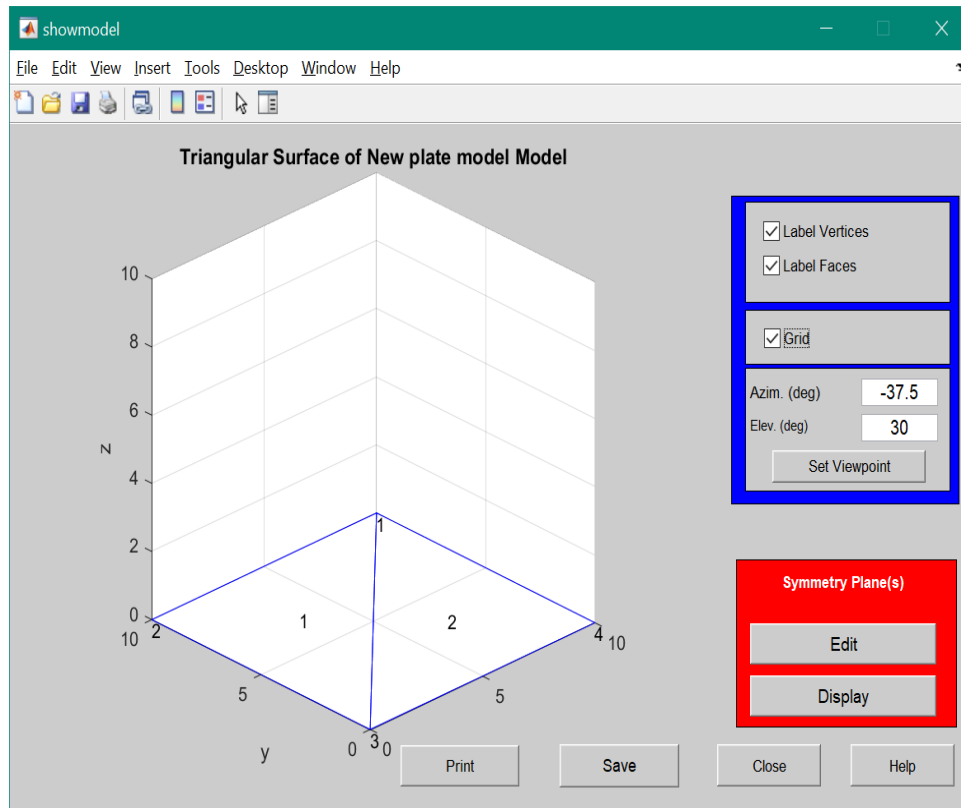
FIGURE 3.8: GUI of plate model.

by importing another model in same triangular surface for making it a complete model, but note that in a complex model like increases the number of facets, the simulation execution time for computing the RCS will increase.

3.3.1.2 Graphical Model Formulation

In Graphical model formulation, complex models are designed which cannot be drawn manually by obtaining vertices. The graphical shapes such as sphere, cone, ellipse, box, fuselage, cylinder, etc. are provided to create different shapes. These geometrical models may be used to build the other new model or we may able to make changes to the current models. All these geometrical models are described with the mathematical equations and many of them are implemented through standard MATLAB© codes. The existing graphical shapes in GUI form are shown in Fig (3.9) and Fig (3.10).

All these graphical shapes are easy to adjust, rotate or change their positions, orientations and to change their number of facets. As discussed earlier that the
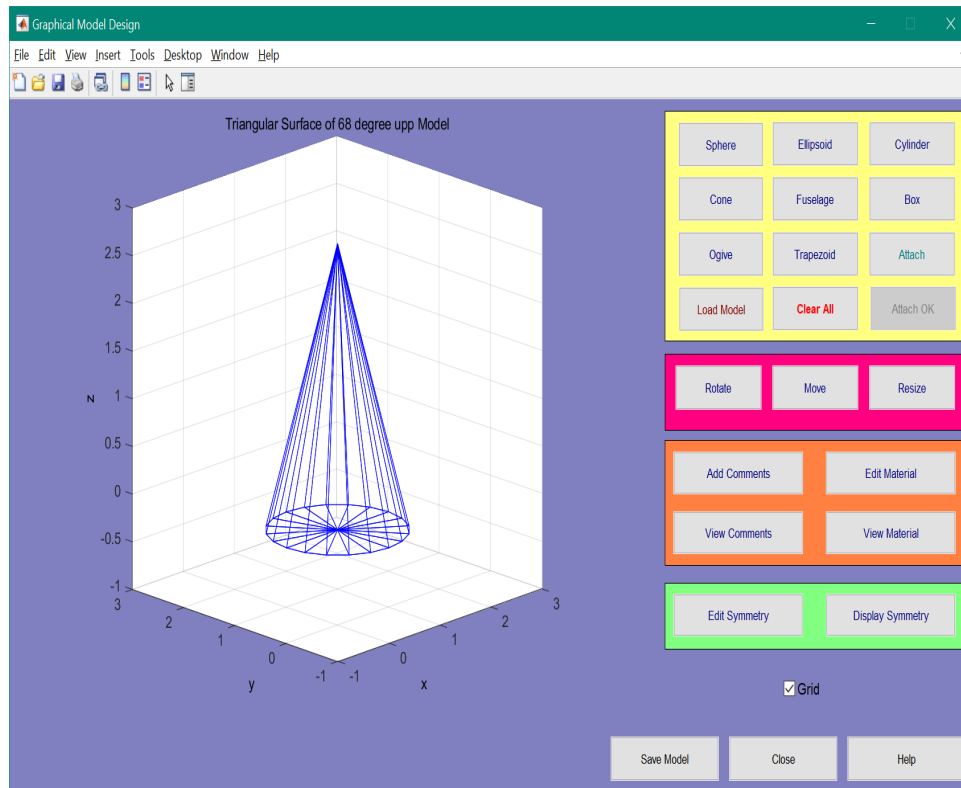
FIGURE 3.9: GUI of graphical cone.

increase in number of facets consumes more simulation time as compared to plate model that has less number of facets.

3.3.1.3 Mono-Static RCS Calculation

As discussed earlier in chapter 1, an RCS is termed monostatic, when both the transmitter and receiver antennas of the radar are located at the same location. The RCS calculation is performed according to the observation angles θ and ϕ at fixed frequency. The GUI shown in Fig (3.11), is used to find the monostatic RCS versus observation angle. In order to compute the RCS, click on "Load File" to select the model first for which it is needed to compute the RCS. Then enter the observation "Starting Angle" and "Ending Angle" values and put the frequency in GHz. The user has options to select different graphs, such as polar graph and 3D graph. By clicking on "Calculate RCS" button, the user would be able to calculate the desired RCS. The RCS estimated for values, $0°\leq\theta\leq360°$ with increment of $3°$ for $\phi=0°$ is shown in Fig (3.11) and the estimated RCS is shown in Fig (3.12).
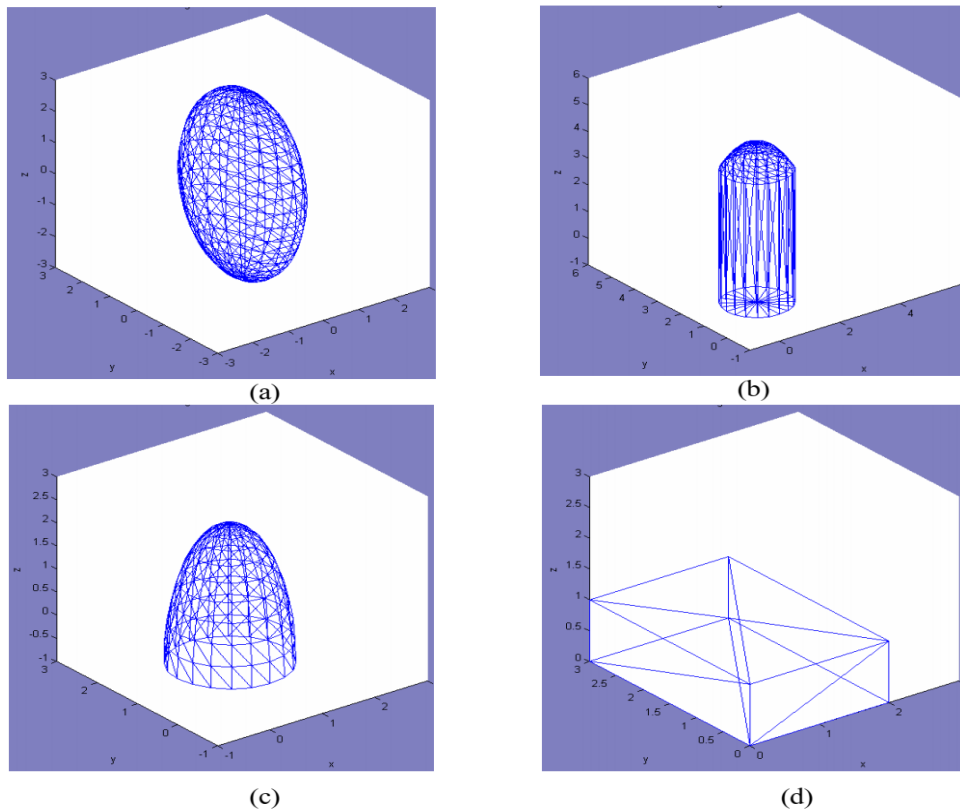
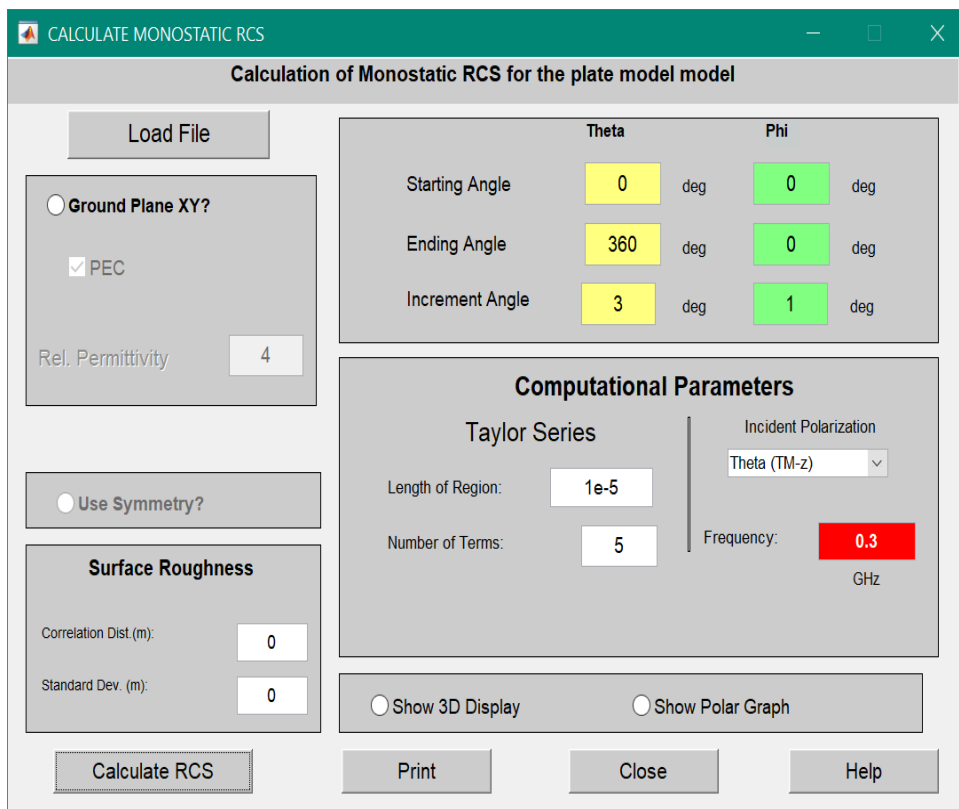FIGURE 3.10: Graphical Shapes (a) Ellipsoid (b) Fuselage (c) Ogive (d) Box.

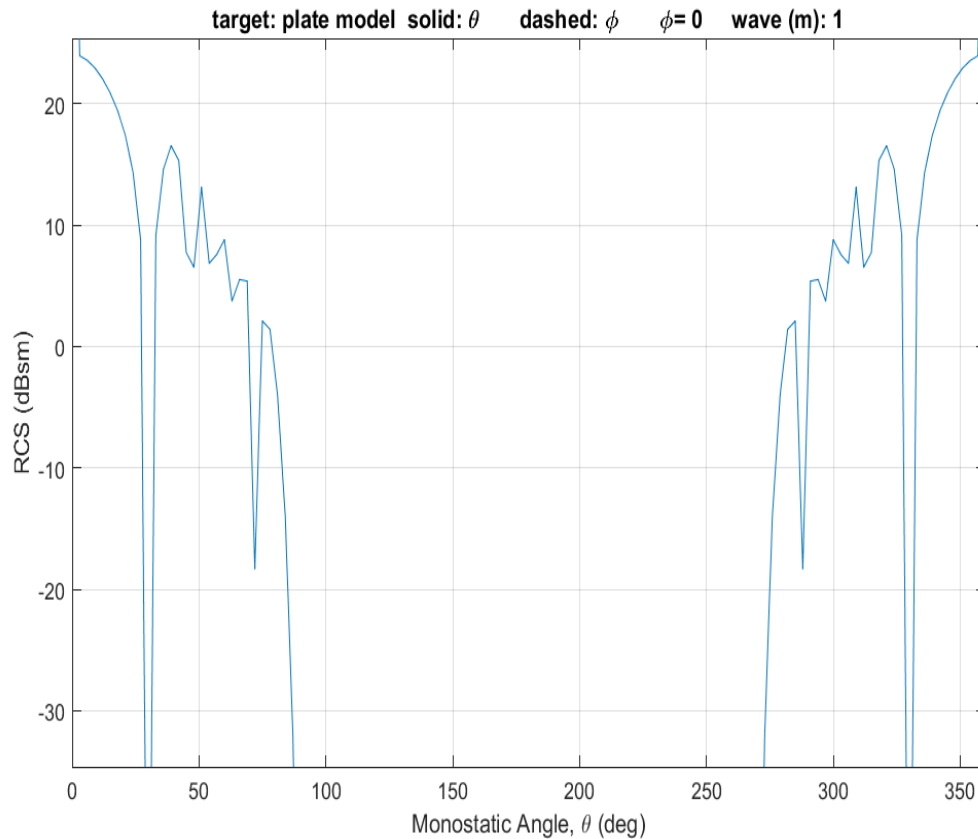FIGURE 3.11: GUI of monostatic RCS calculation vs observation angle.

FIGURE 3.12: RCS of a plate model in monostatic case.

3.3.1.4 Bi-Static RCS Calculation

In the bistatic radar case, both the transmitter and receiver antennas are located at two different positions to detect a target. Some of the parameters are same in bistatic case as compared to monostatic case. In bistatic case the users have an option to input their desire incident angles and observation angles. In both cases, the transmitter of the radar is positioned at a fixed location with reference to the position of the target but the required observation angles are changed. As discuss earlier, that RCS simulation time depends on the number of facets and also depends on the observation angles. The values that mention in the bistatic GUI are set initially in MATLAB© code. The procedure for RCS calculation is same as in the case of monostatic RCS. The GUI window to find bistatic RCS versus observation angle is shown in Fig (3.13). The obtained RCS result are shown in Fig (3.14) which is obtained by putting incident angle (θ=30°) and (ϕ=0°) and by keeping the frequency at (f=0.3 GHz).
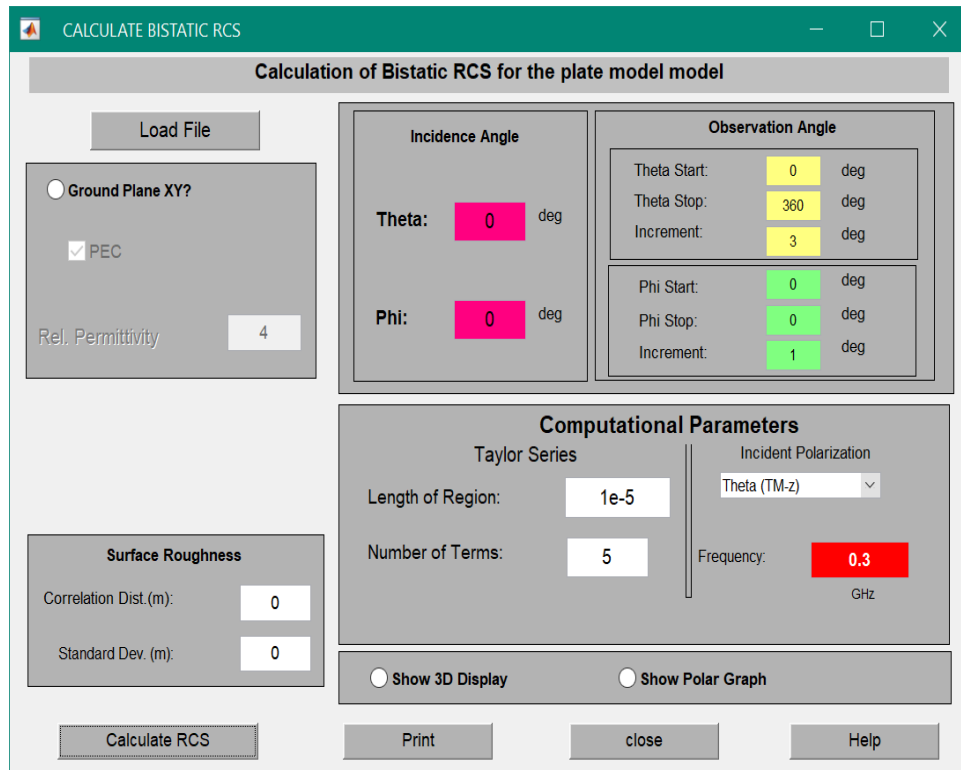
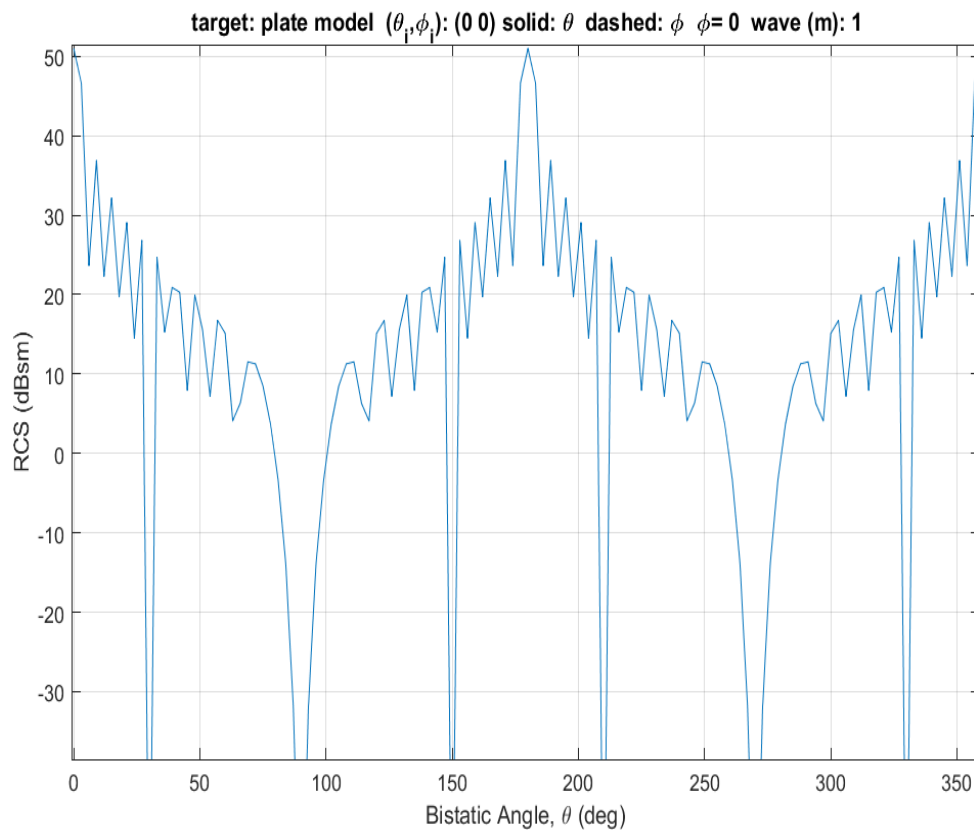FIGURE 3.13: GUI of bitatic RCS calculation vs observation angle.

FIGURE 3.14: RCS of a plate model in bistatic case.

3.3.1.5 Utilities (Import/Export of Models)

POFACETS©4.2 facilitates users to import or export designed models from other designing software tools. For example, the AutoCAD© software can be used to design complex models and can be imported into POFACETS©4.2 for the RCS estimation. Import of different file formats facilitates users to work efficiently on their desired designing software.

3.4   POFACETS©4.2 Limitations

The POFACETS©4.2 has the following limitations.

- It does not provide the flexibility to estimate the RCS of a model over a range of incident angles.

- This requires a huge amount of time and effort of a user when the RCS is required to be estimated at multiple incident angles.

Chapter 4

Proposed Enhanced Version of POFACETS©4.2 and its Limitation

This chapter presents an upgraded version of POFACETS©4.2, named as EPO-FACETS 5.0 (Enhanced-POFACETS), and briefly discusses all the steps involved in the establishment of the Graphical User Interface (GUI) of EPOFACETS 5.0. Moreover, the limitations of EPOFACETS 5.0 are also discussed at the end of this chapter.

4.1 The Proposed EPOFACETS 5.0

4.1.1 Introduction

EPOFACETS 5.0 is a MATLAB© based simulation software, that works on the same principles of electromagnetics (EM) which have been used in POFACETS©4.2. If it is required to estimate the RCS of an object at several incident angles', then in POFACETS©4.2, a user has to input all the incident angles' one by one to estimate the RCS. This procedure becomes cumbersome and time consuming when
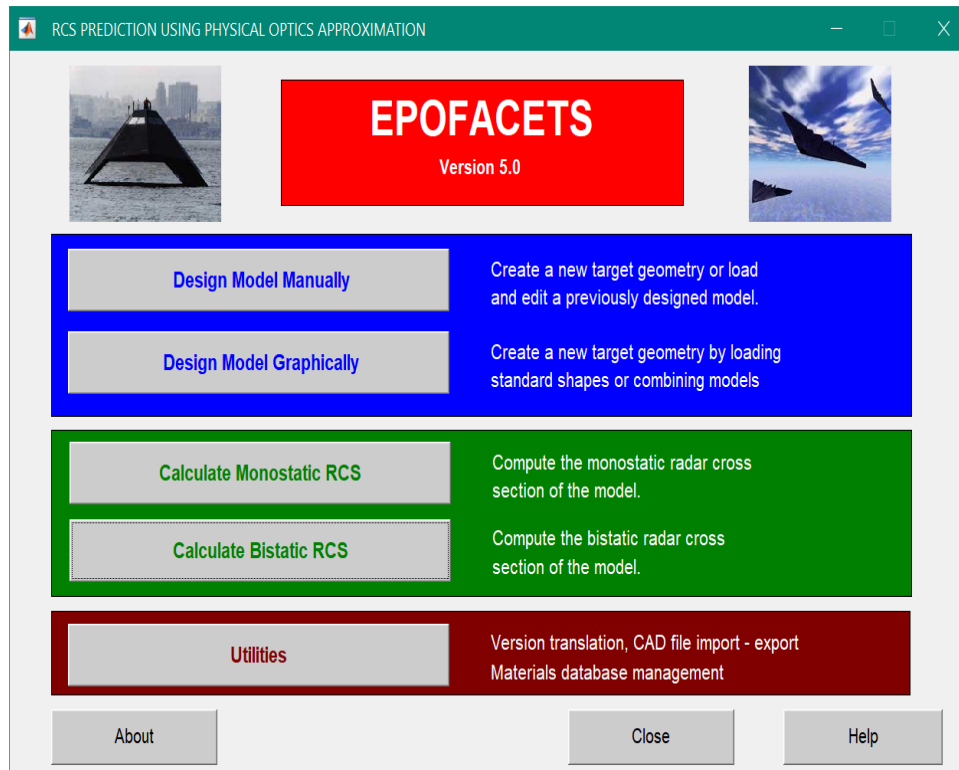
FIGURE 4.1: Main screen GUI of EPOFACETS 5.0.

RCS is required at several angles'. The enhanced version of POFACETS©4.2, i.e. EPOFACETS 5.0, removes this limitation and enables a user to estimate RCS over a defined range of incident angles'. The detailed procedure and steps involved in the designing of EPOFACETS 5.0 are explained in subsequent subsections.

At first, the main screen of EPOFACETS 5.0 GUI is generated which provides options to estimate the monostatic and bistatic RCS of a model as shown in Fig (4.1). In order to estimate the bistatic RCS, click on the "Calculate Bistatic RCS" option, the bistatic designed window is appeared as shown in Fig (4.2).

4.1.2   EPOFACETS 5.0 GUI Designing Procedure

In order to design the GUI of EPOFACETS 5.0, the "guide" function is used in MATLAB© command window. A blank window, as shown in Fig (4.3), would appear with options of "Create New GUI" and "Open Existing GUI", select the option "Create New GUI" to select the option "Blank GUI" and press "OK". A Blank GUI template would appear as shown in Fig (4.4). On the left side of the
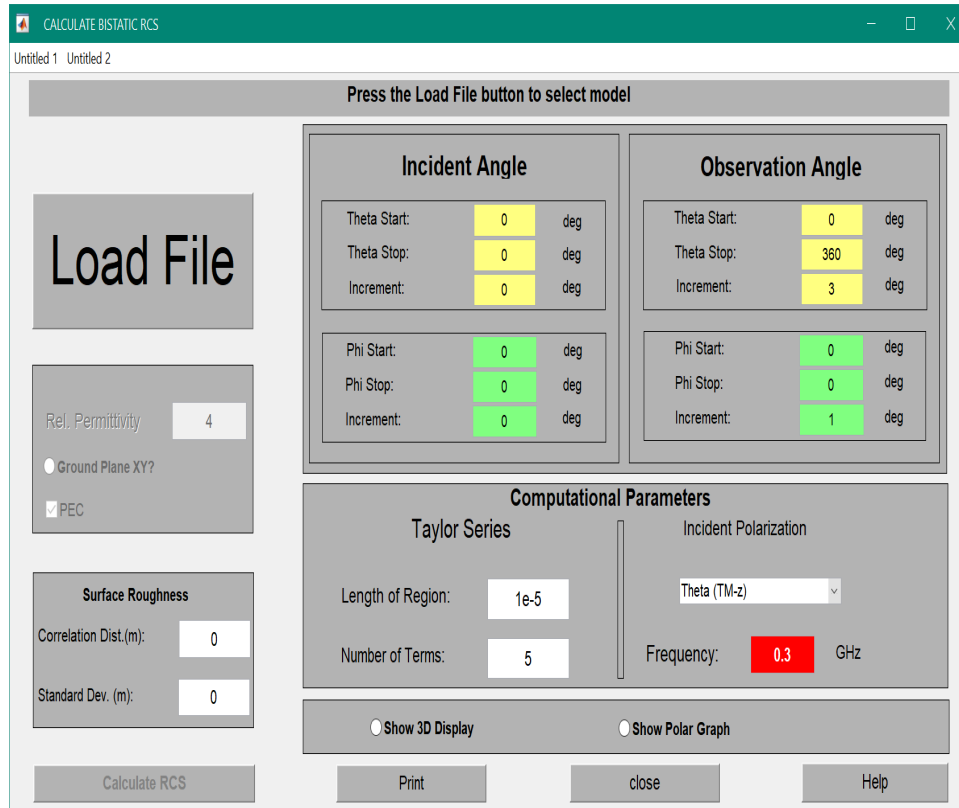
FIGURE 4.2: GUI of bistatic RCS using EPOFACETS 5.0.

layout, Editor Component Palette would also be displayed with various options such as Push Button, Slider, Radio Button, Edit Text and Static Text etc. A user can also resize its window size in the grid layout editor. The EPOFACETS 5.0 GUI window is designed by using the following components:

4.1.2.1 Push Button

In EPOFACETS 5.0, five push buttons are added to operate function of "Load File", "Calculate RCS", "Print", "Close" and "Help". From the component palette a user can drag a button into the layout area and can position them according to the work requirement as shown in the following Fig (4.5). The push button component is used to generate some user-defined buttons which have been circled as shown in Fig (4.5), e.g. "Load File", "Calculate RCS", "Print", "Close", and "Help". In order to change the push button properties, the property inspector option is used to label the push buttons and to change the other related functional parameters such as callback, create function, tag and text size etc.
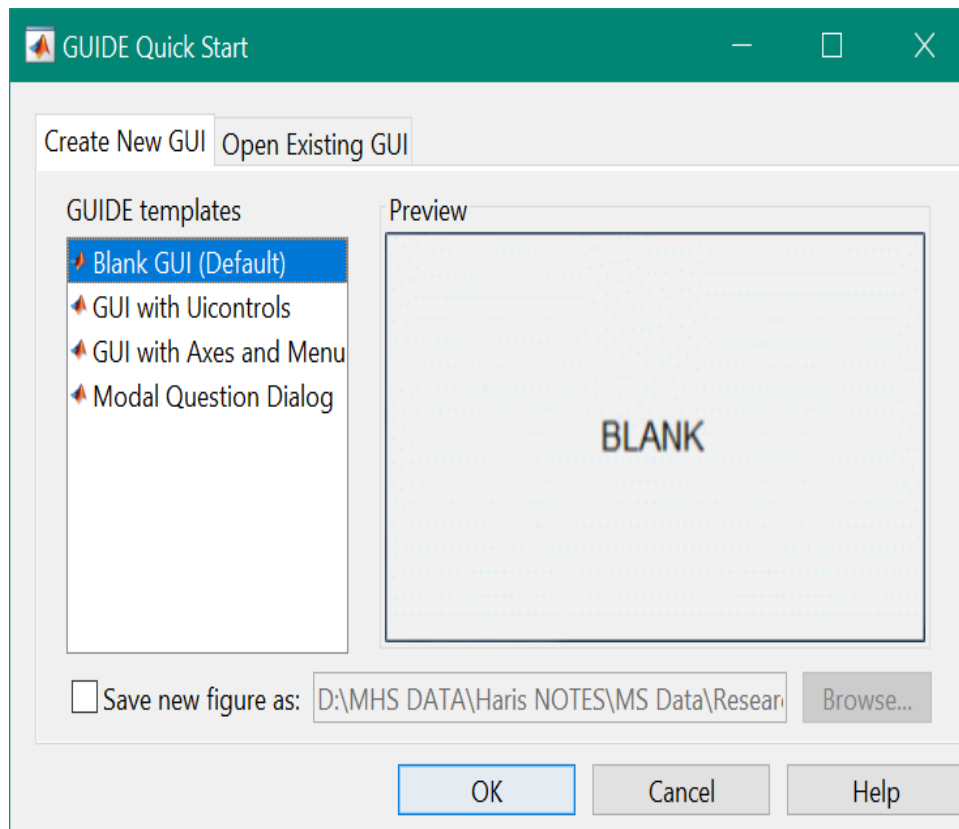
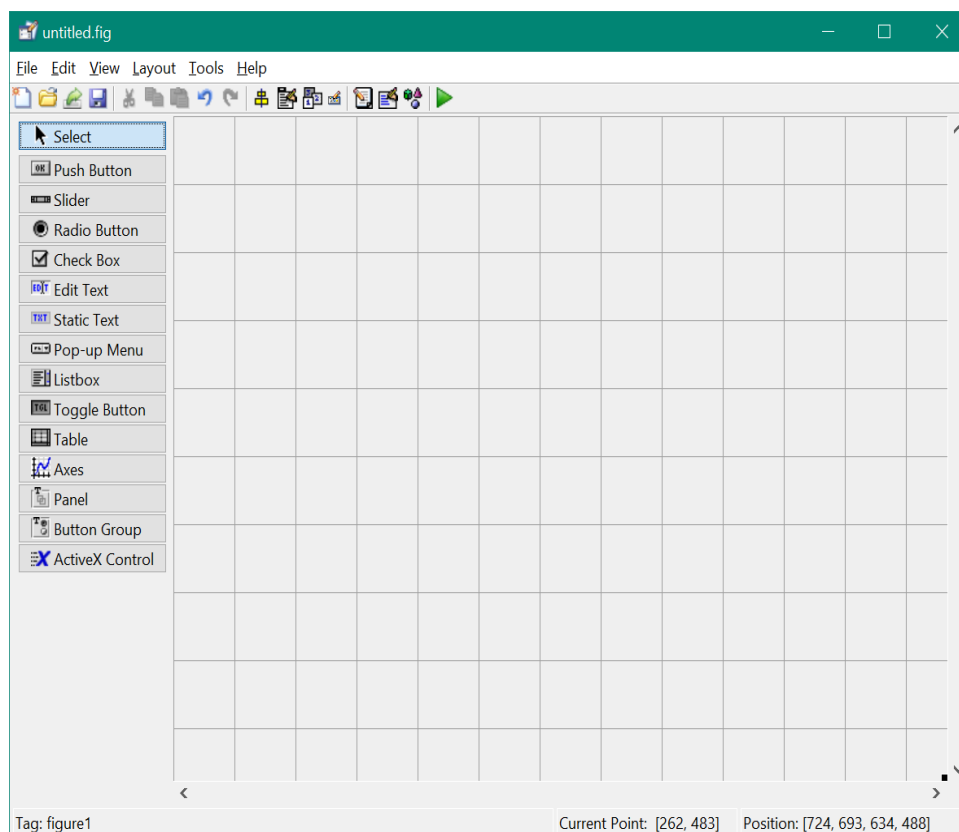FIGURE 4.3: Guide tool window.

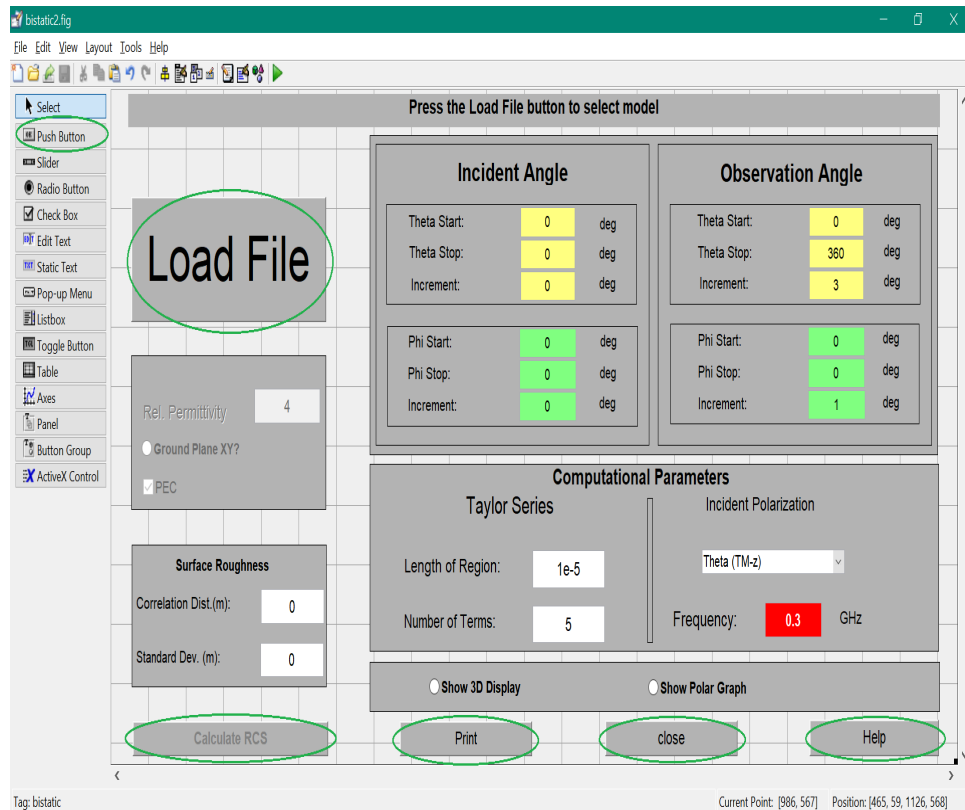FIGURE 4.4: Creating GUI blank window.

FIGURE 4.5: Push button component.

4.1.2.2   Radio Button

Radio Button is similar to the Check Box component, which is intended to be used for mutually exclusive options i.e. only one option can be selected from a group of available option. The radio buttons have both selected and unselected states. In order to enable a radio button, simply press the button. In EPOFACETS 5.0, radio button component is used to provide some user-defined options which have been circled as shown in Fig (4.6), e.g. "Ground Plane XY", "Show 3D Display", and "Show Polar Graph". Similarly, in order to change the radio button component properties, the property inspector option is used to label the radio buttons and to change the other related functional parameters.

4.1.2.3   Edit Text Component

The Edit Text control fields facilitates a user to input different values at the time of running a program. A user can also put a default value in edit text control. The
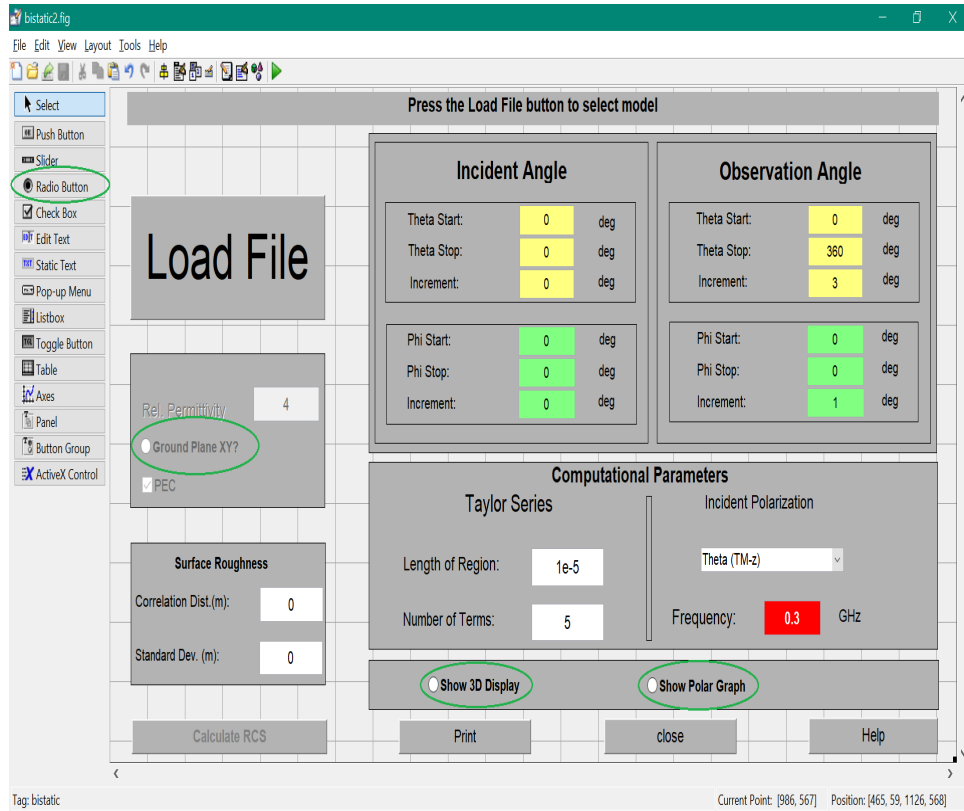
FIGURE 4.6: Radio button component.

string property holds the text input by the user. In order to get the string entered by the user, fetch the string property from the recall function. In EPOFACETS 5.0, the "Edit Text" component is used to generate some user-defined text boxes which have been circled as shown in Fig (4.7), e.g. "Incident Angle" values, "Observation Angle" values, "Relative Permittivity", "Surface Roughness" values, "Frequency" and "Taylor Series" values. In order to change the "Edit Text" component properties, the property inspector option is used to label the "Edit Text" and change the other related functional parameters.

4.1.2.4   Static Text Component

The Static Text control option displays descriptive text in the GUI window. Static text is usually used for labeling commands, providing instructions to the user, or indicating values associated with a cursor. In EPOFACETS 5.0, the "Static Text" component is used to generate some user-defined texts which have been circled as shown in Fig (4.8), e.g. "Incident Angle", "Observation Angle", "Theta Start" and
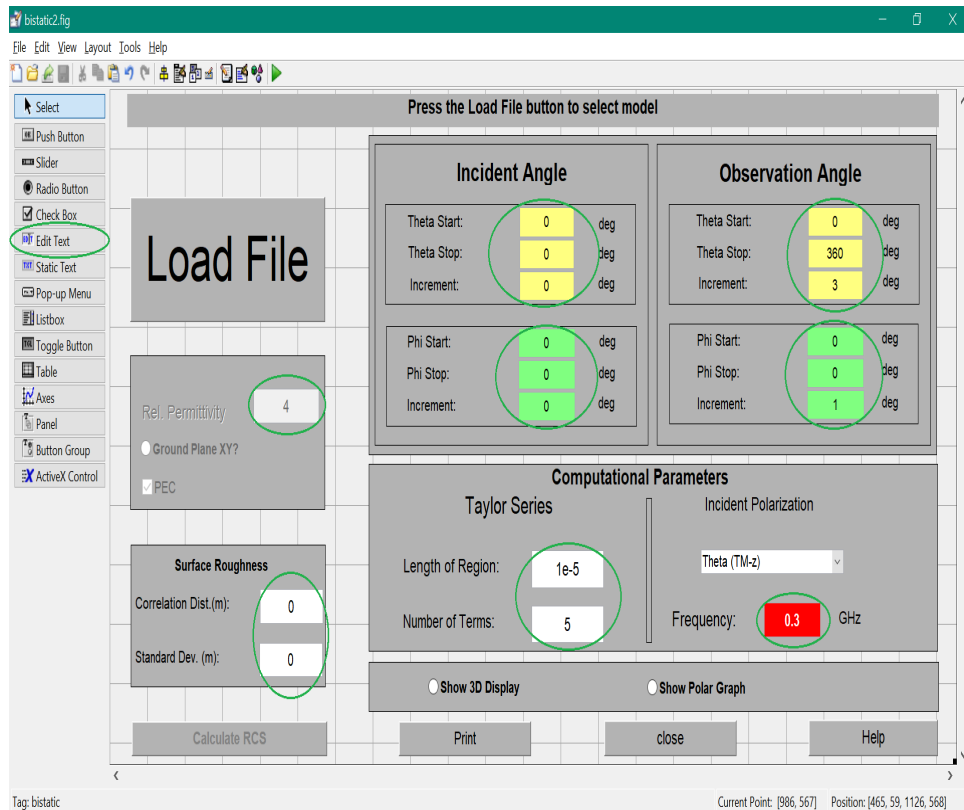
FIGURE 4.7: Edit text component.

"Stop", "Increment", "Computational Parameters" etc. To change the properties of a "Static Text" component, the property inspector option is used to label the static text and change the font size, text location or text style.

4.1.2.5 Pop-Up Menu Component

The Pop-Up menu open provides a selection list (options) for a user by means of a direct arrow button. The string property provides the list of string displayed in the pop-up menu. The "Property Inspector" is used to modify with the addition of more items to the "Pop-Up" menu through typing one option per line in the string edit box. Furthermore, the "Pop-Up" menu text and background color can also be changed. In EPOFACETS 5.0, the "Pop-Up" menu component is used to generate an option box of incident polarization which has been circled as shown in Fig (4.9), i.e. "Incident Polarization" values. In order to change the properties of the "Pop-Up" menu component, the property inspector option is used to edit the options label in "Pop-Up" menu.
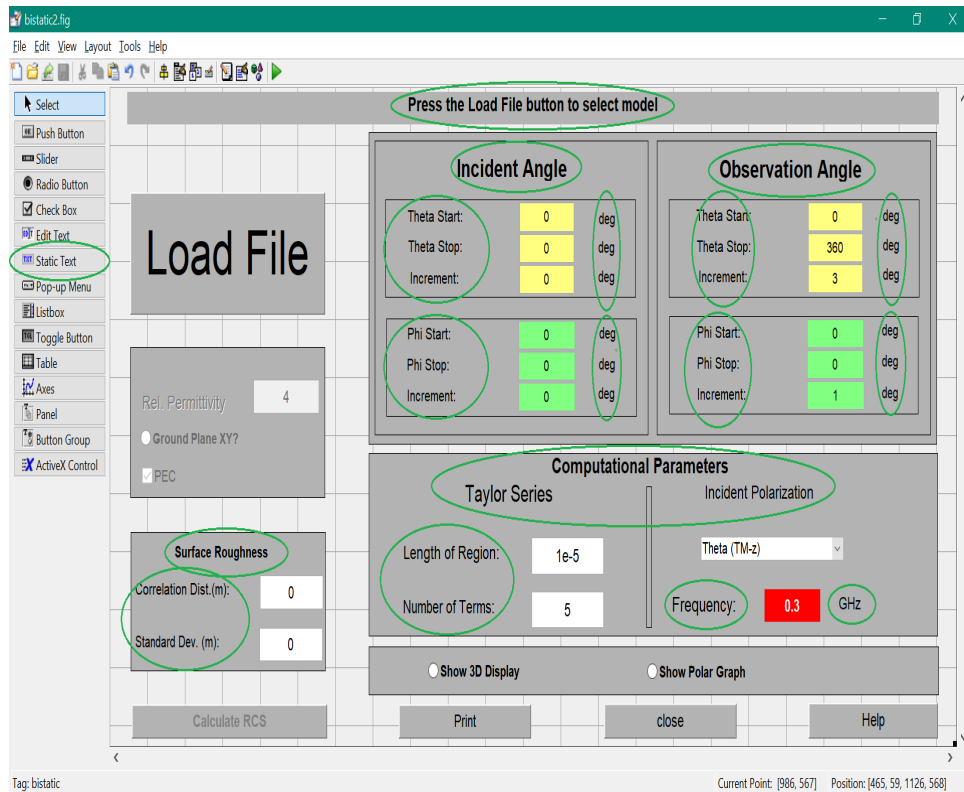
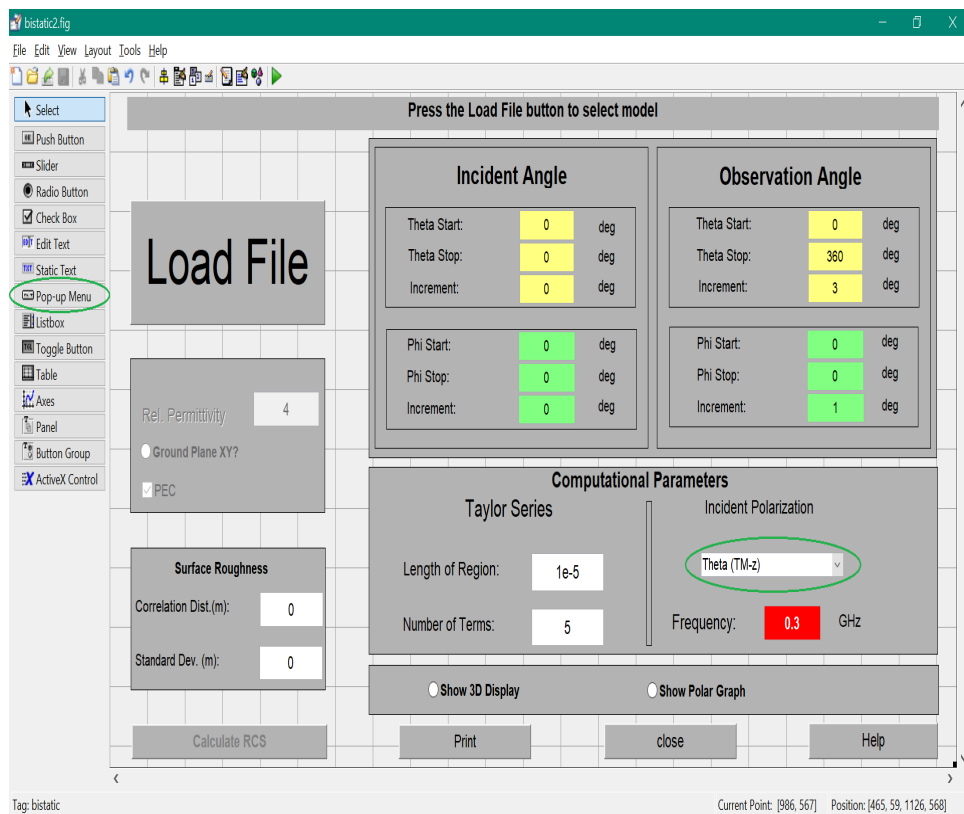FIGURE 4.8: Static text component.

FIGURE 4.9: Pop-Up menu component.

4.2   Incident angles' Cases Implemented in EPOFACETS 5.0

Since, the primary objective of EPOFACETS 5.0 is to estimate RCS for a specified range of incident angles'; therefore, to resolve and adjust this issue four main cases are developed. These cases are categorized on the basis of the incident angles' specification provided by the user and the adjustment of the MATLAB$^©$ codes. The EPOFACETS 5.0 simulation software understands the requirements of the user and performs actions accordingly over the required range of incident angles'. These cases are discussed as follows:

4.2.1   Case 1 (Fixed θ and ϕ)

The EPOFACETS 5.0 software is designed to facilitate user by providing option of inserting start, stop and increment value, as shown in Fig (4.10). In order to obtain RCS at fixed incident angles', a user is required to input the same start and stop angles' or to input start angle with zero increment. This process will provide RCS at fixed incident angle which turns this software at the same level of POFACETS$^©$4.2. After computing the RCS, it provide the RCS plot and MATLAB$^©$ file which contains the following information.

- (**itheta**): Incident θ-angle value

- (**iphi**): Incident ϕ-angle value

- (**theta**): Observation θ-angle value (fixed value in our case at 90°)

- (**phi**): Observation ϕ-angle values (varies from 0° to 360°)

- (**freq**): Frequency of incident wave (selecting 0.12 GHz in our case)

- (**Sth**): RCS plot with respect to observation θ-angle values

- (**Sph**): RCS plot with respect to observation ϕ-angle values
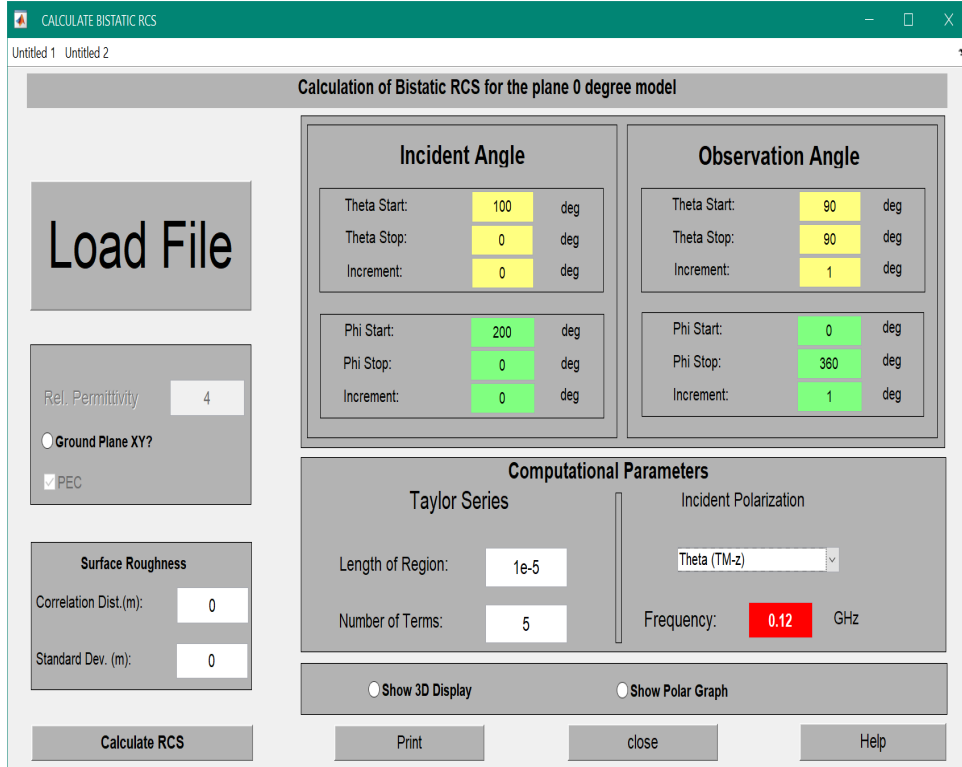
FIGURE 4.10: GUI of EPOFACETS 5.0 case 1.

4.2.2   Case 2 (Varying θ and Fixed ϕ)

This case occurs when it is required to vary θ incident angle for obtaining RCS while keeping fixed angle of ϕ. In this case, a user has to provide range of incident θ angle with specific increment value. Furthermore, it is required to fix the ϕ incident angle by providing the same "Phi Start" and "Phi Stop" angle or by giving "Phi Start" angle with 0 increment as shown in Fig (4.11).

The required RCS values at all the predefined incident angles' are saved in structure arrays of MATLAB$^{©}$ in "TSim" data file of length (M×1), where M denotes the number of incident θ angles' and each (1×1 struct) structured cell contains the following information.

- (**itheta**): Incident θ-angle value

- (**iphi**): Incident ϕ-angle value

- (**theta**): Observation θ-angle value (fixed value in our case at 90°)

- (**phi**): Observation ϕ-angle values (varies from 0° to 360°)

FIGURE 4.11: GUI window of EPOFACETS 5.0 case 2.

- (**freq**): Frequency of incident wave (selecting 0.12 GHz in our case)

- (**Sth**): RCS plot with respect to observation θ-angle values

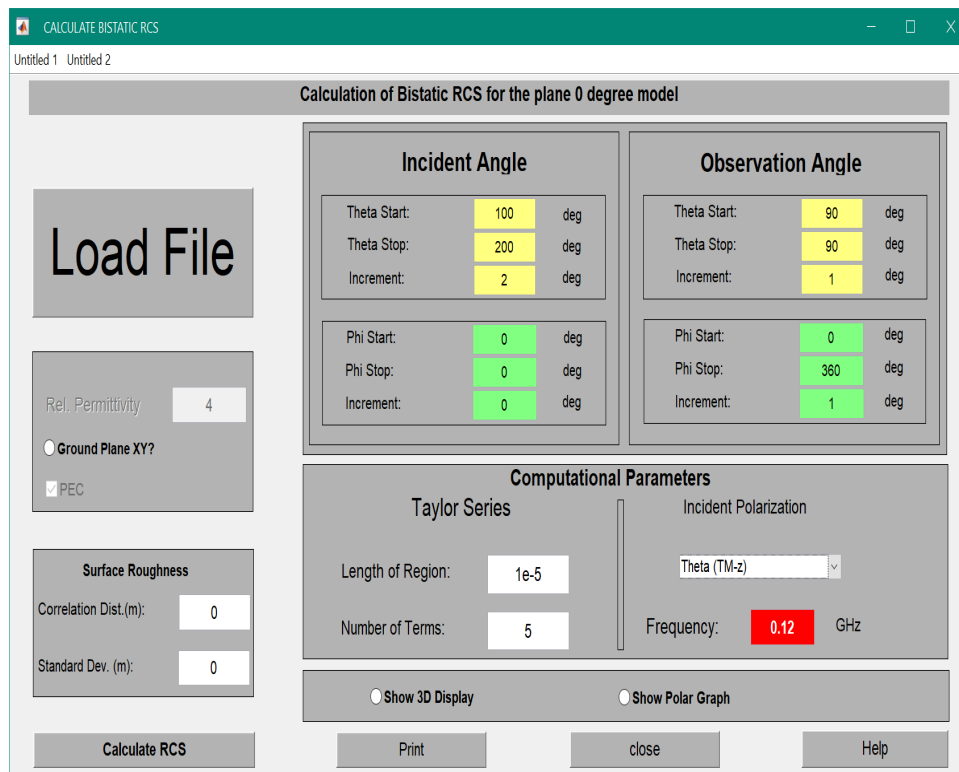- (**Sph**): RCS plot with respect to observation ϕ-angle values

4.2.3 Case 3 (Fixed θ and Varying ϕ)

This case occurs when it is required to vary ϕ incident angle for obtaining RCS while keeping fixed angle of θ. In this case, a user has to provide range of incident ϕ angle with specific increment value. Furthermore, it is required to fix the θ incident angle by providing the same "Theta Start" and "Theta Stop" angle or by giving "Theta Start" angle with 0 increment as shown in Fig (4.12).

The required RCS values at all the predefined incident angles' are saved in structure arrays of MATLAB© in "TSim" data file of length (1×N), where N denotes the number of incident ϕ angles' and each (1×1 struct) structured cell contains the following information.
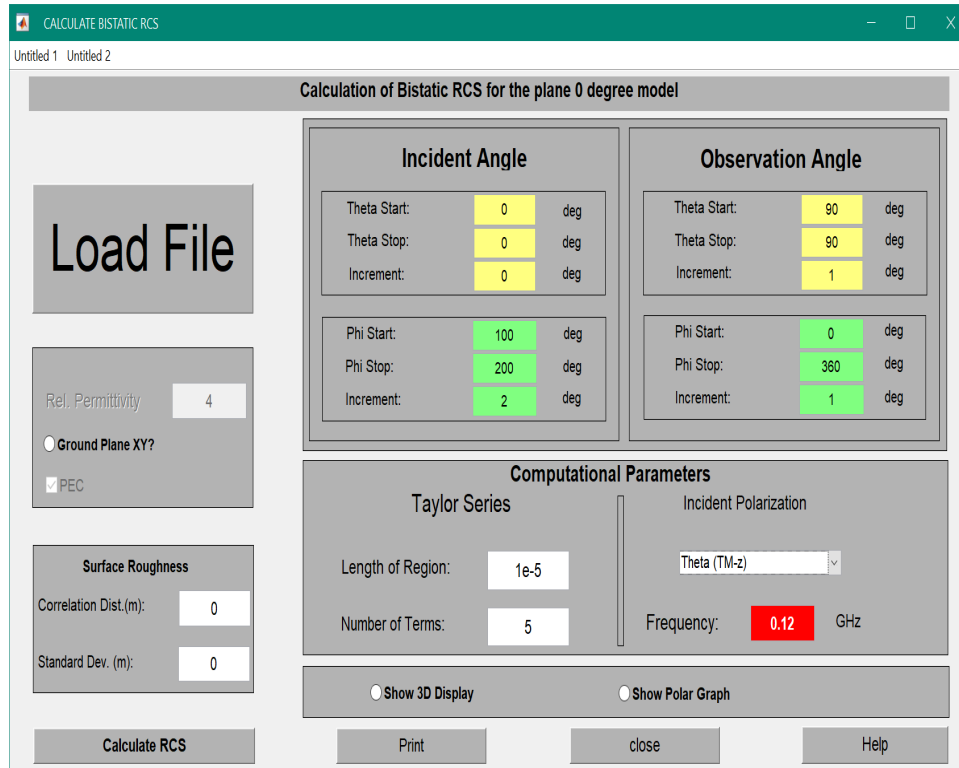
FIGURE 4.12: GUI window of EPOFACETS 5.0 case 3.

- (**itheta**): Incident θ-angle value

- (**iphi**): Incident ϕ-angle value

- (**theta**): Observation θ-angle value (fixed value in our case at 90°)

- (**phi**): Observation ϕ-angle values (varies from 0° to 360°)

- (**freq**): Frequency of incident wave (selecting 0.12 GHz in our case)

- (**Sth**): RCS plot with respect to observation θ-angle values

- (**Sph**): RCS plot with respect to observation ϕ-angle values

4.2.4 Case 4 (Varying θ and ϕ)

The major application of EPOFACETS 5.0 is discussed in case 4 as shown in Fig (4.13). This case occurs when it is required to vary θ and ϕ incident angle values for obtaining RCS over a range of incident angles'. In this case, a user has
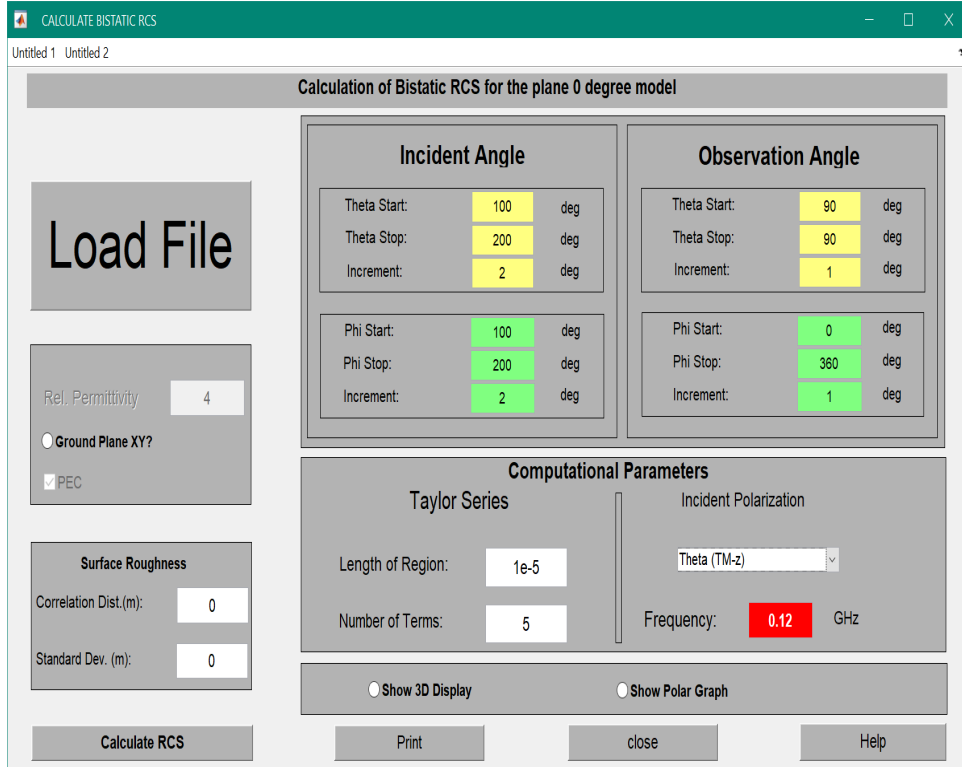
FIGURE 4.13: GUI window of EPOFACETS 5.0 case 4.

to provide range of incident θ and ϕ angles' with specific increment values. The incident start and stop angle values must be kept different for (θ and ϕ), if these angle values are same then it becomes case 1. Furthermore, it is required that the increment value must be greater or equal to 1 depend on user requirements. Each for the single incident θ-angle value the whole cycle of ϕ-angle values will be executed. These simulations for the RCS calculation of a model are then performed in a single run by providing all required incident angle values.

The required RCS values at all the predefined incident angles' are saved in structure arrays of MATLAB© in "TSim" data file of length (M×N), where M denotes the number of incident θ angles' and N denotes the number of incident ϕ angles' as shown in Table (4.1) and each (1×1 struct) structured cell contains the following information.

- (**itheta**): Incident θ-angle value

- (**iphi**): Incident ϕ-angle value

- (**theta**): Observation θ-angle value (fixed value in our case at 90°)

TABLE 4.1: Bistatic RCS computation using EPOFACETS 5.0

S/N	1	2	3	4	$\cdots$	N
1	(1×1) struct	(1×1) struct	(1×1) struct	(1×1) struct	$\cdots$	(1×1) struct
2	(1×1) struct	(1×1) struct	(1×1) struct	(1×1) struct	$\cdots$	(1×1) struct
3	(1×1) struct	(1×1) struct	(1×1) struct	(1×1) struct	$\cdots$	(1×1) struct
4	(1×1) struct	(1×1) struct	(1×1) struct	(1×1) struct	$\cdots$	(1×1) struct
$\vdots$	$\vdots$	$\vdots$	$\vdots$	$\vdots$	$\vdots$	$\vdots$
M	(1×1) struct	(1×1) struct	(1×1) struct	(1×1) struct	(1×1) struct	(1×1) struct (M×N)

- (**phi**): Observation ϕ-angle values (varies from 0° to 360°)

- (**freq**): Frequency of incident wave (selecting 0.12 GHz in our case)

- (**Sth**): RCS plot with respect to observation θ-angle values

- (**Sph**): RCS plot with respect to observation ϕ-angle values

4.3   EPOFACETS 5.0 Angular Specifications

In this section the angles' measurements are discussed which are used in EPO-FACETS 5.0 or POFACETS©4.2. The angles' that are taken in EPOFACETS 5.0 is different which is used in normal cases [56]. Fig (4.14), shows the angular coordinates in four quadrants used in EPOFACETS 5.0 and Fig (4.15), shows the 2-D angle coordinates system.

4.4   EPOFACETS 5.0 Limitations

Although the functionalities of EPOFACETS 5.0 have been improved to reduce the time and effort of a user; however, there are still some limitations that are listed below:
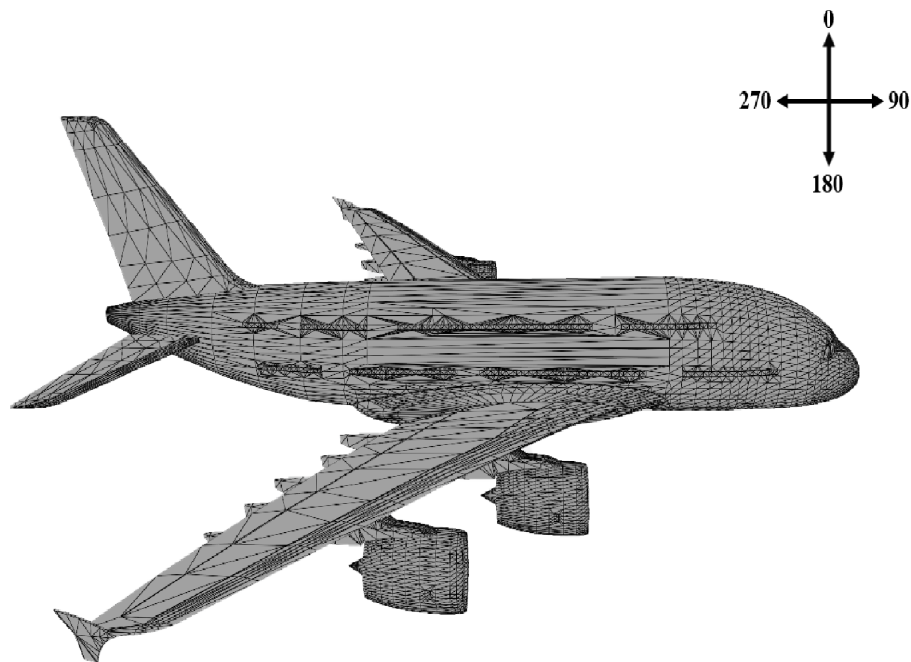
FIGURE 4.14: Angles' coordinates in EPOFACETS 5.0.

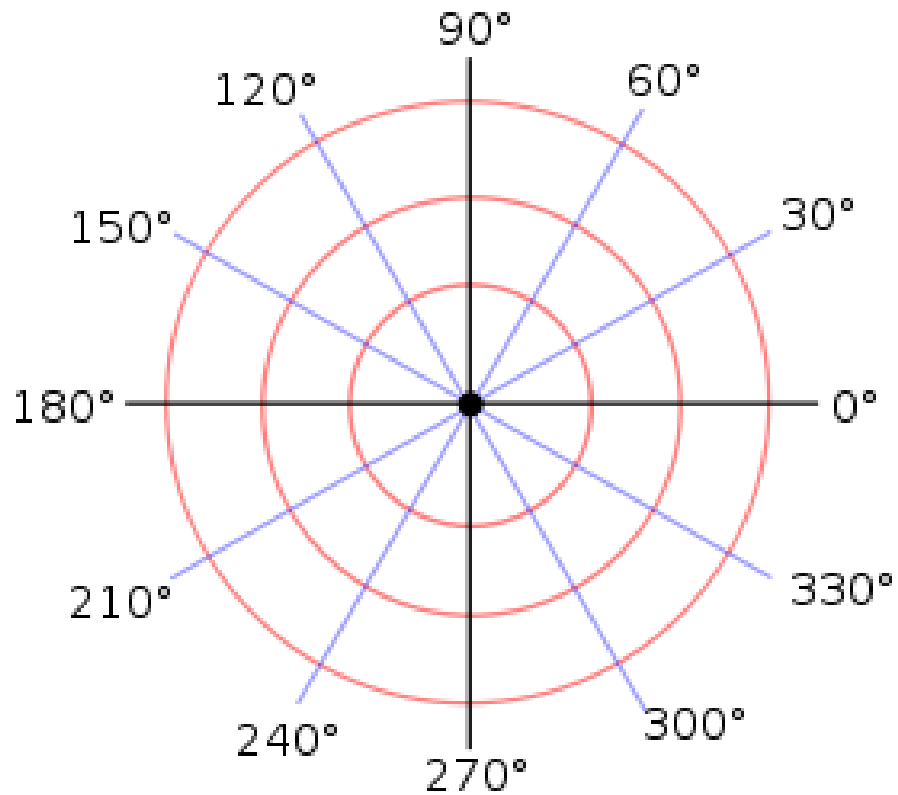FIGURE 4.15: Normal angles' Coordinates.

- A high performance dedicated computer with (Large RAM and high processor speed) is required to run and save the estimated RCS results or data.

- Keeping in view the power outage issues in Pakistan, an Uninterruptible Power Supply (UPS) may be required to run and complete the simulation process if the RCS is needed to be estimated over a wide range of incident angles'.

Chapter 5

Simulation Results and Performance Analysis of EPOFACETS 5.0

This chapter provides simulation results of obtaining BRCS through EPOFACETS 5.0 and discusses its performance in comparison to POFACETS©4.2.

5.1 Bi-Static RCS Computation of Aircraft A380© Model using EPOFACETS 5.0

In our simulation, the largest commercial aircraft A380© model is used as a target to compute the bistatic RCS through EPOFACETS 5.0. Since, EPOFACETS 5.0 requires a facet-based model to predict the RCS; therefore, AutoCAD© design of aircraft A380© is acquired [57, 58] and converted to stereolithography (.stl) format by using AnyCAD© software. The RCS of the designed model is estimated for a range of incident angles from 0° to 360° and azimuthal plane is considered for observation angles. The facet-based model of aircraft A380© imported in EPOFACETS 5.0 is shown in Fig (5.1). Once the model is loaded, the parameters as per the user requirements can be changed. A user can also
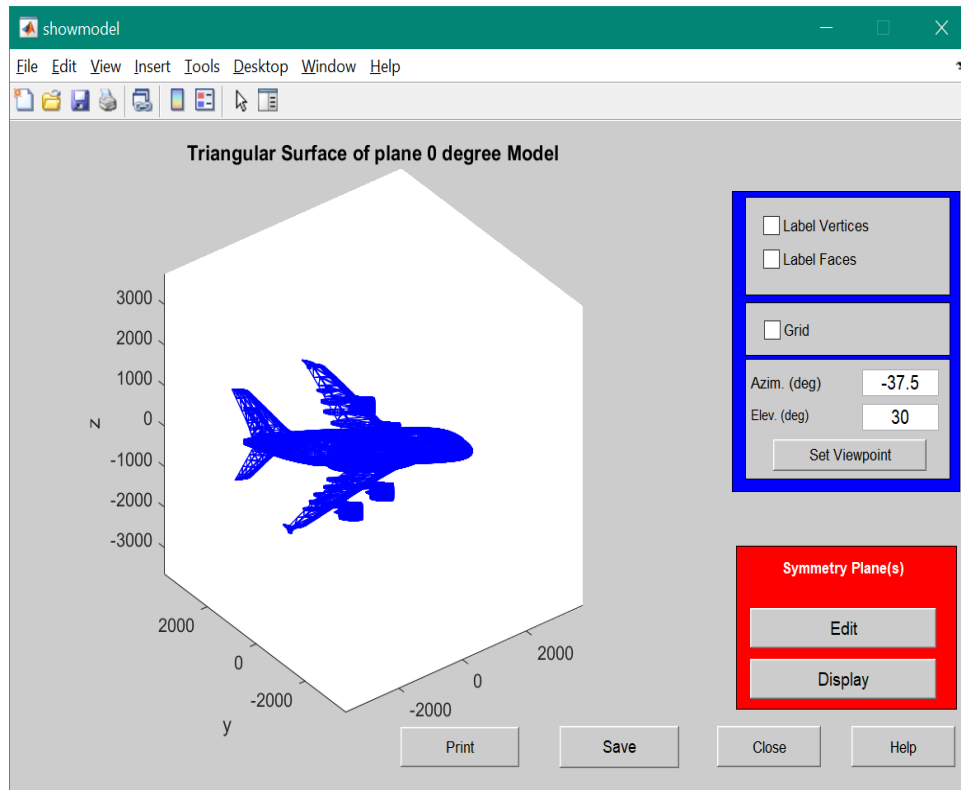
FIGURE 5.1: Facet-based model of Aircraft A380©.

modify surface properties of the model according to its own requirements. The surface parameters should be inserted intelligently, because RCS depends upon the scattered fields reflected from the surface of the model. The computational parameters include incident polarization and Taylor series. A user may select incident polarization θ (TM-z) that corresponds to vertical polarization, or ϕ (TE-z) that corresponds to horizontal polarization. Using a single incident angle (θ-Start=100° and ϕ-Start=180°), observation angles (θ-Start=90°, θ-Stop=90°, Increment=1), (ϕ-Start=0°, ϕ-Stop=360°, Increment=1) and keeping the frequency of 0.12 GHz as shown in Fig (5.2).

Fig (5.3) and Fig (5.4), shows the RCS estimates of aircraft A380© both in linear and polar plots respectively. RCS simulation results are saved in MATLAB© structure cells array. The structured cells array contains the range of incident angles with respect to observation angles, and the RCS of a target model at every incident and observation angles with constant frequency. The results are basically the RCS approximation of a target which are used in military engagements to detect and intercept intruders in Modern Electronic Warfare.
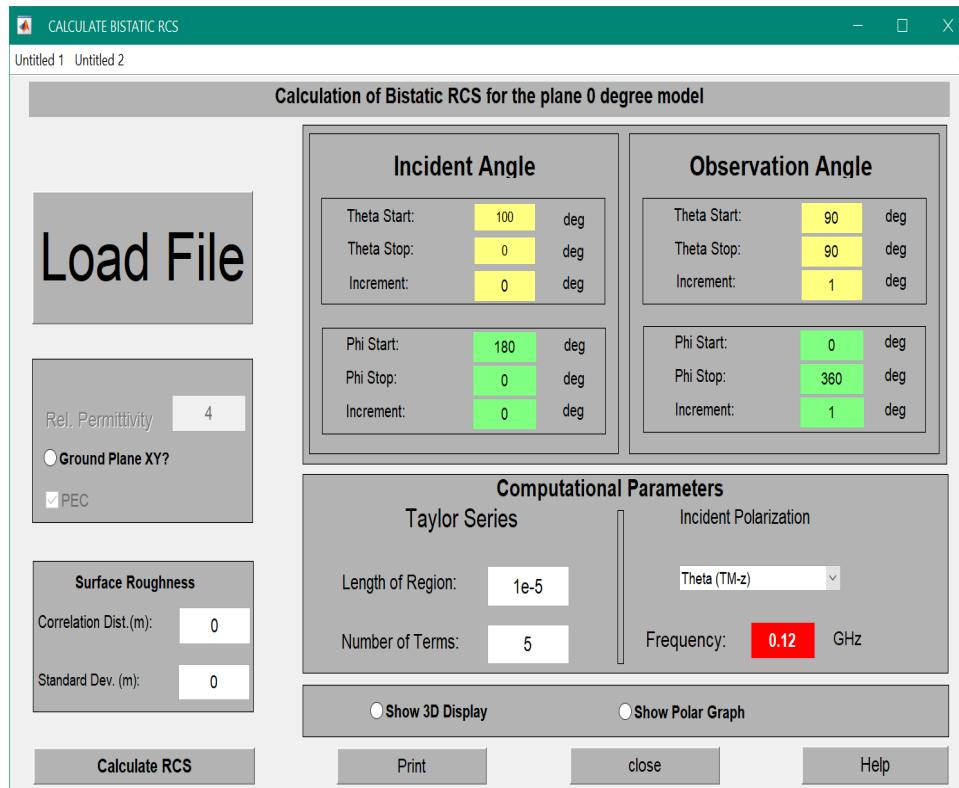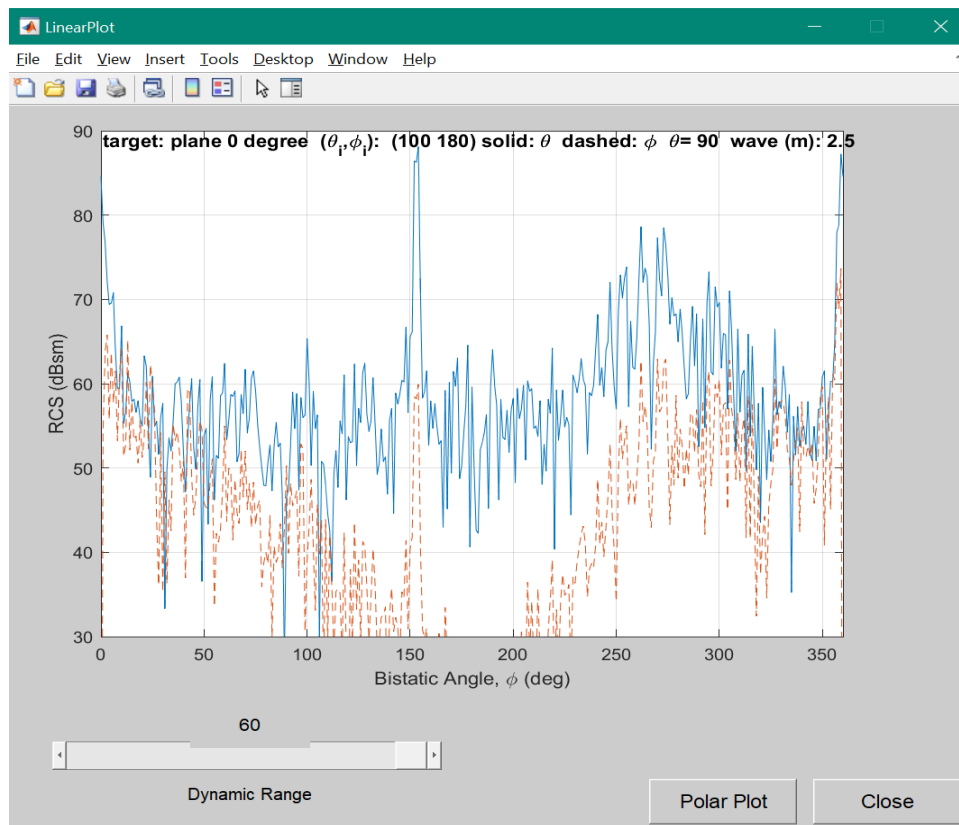
FIGURE 5.2: GUI of bistatic RCS model parameters.
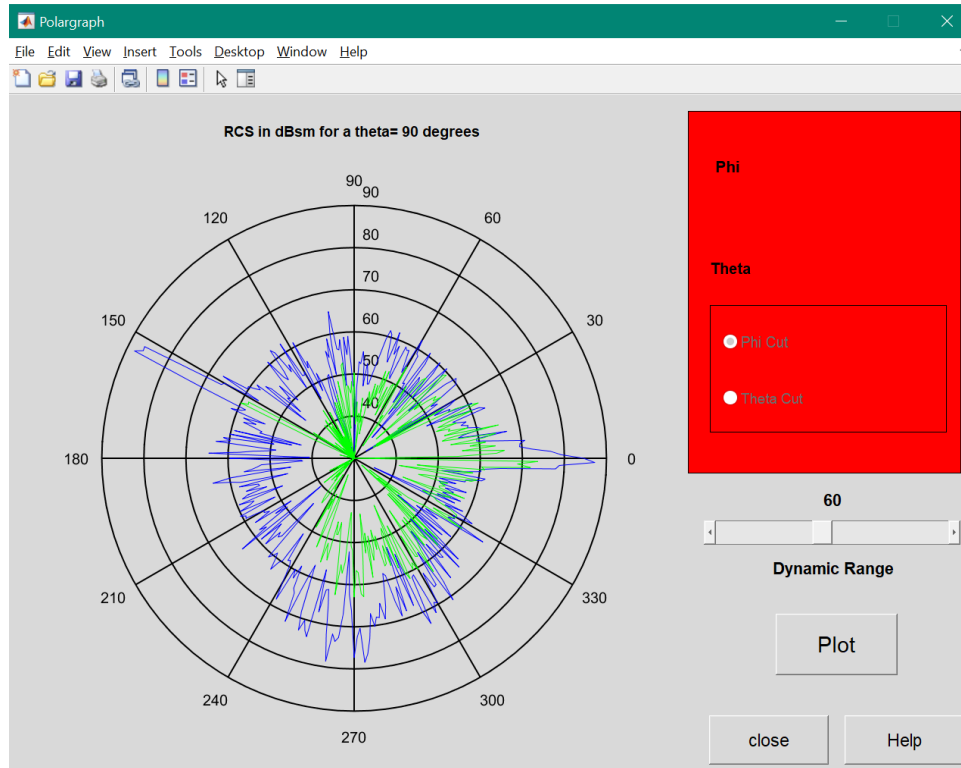

FIGURE 5.3: RCS linear plot of Aircraft A380© model.

FIGURE 5.4: RCS polar plot of Aircraft A380© model.

5.2 RCS Computation of a Target Aircraft A380© Model

As discussed earlier, the main objective of EPOFACETS 5.0 is to decrease simulation burden of a user when it is required to estimate BRCS over a wide range of incident angles. In this section, BRCS of aircraft A380© is estimated over the range of incident angles from 0° to 360° as shown in Fig (5.5). Since, BRCS estimation requires high processing time; therefore, for simplicity and to ease the system an increment value of 2 is chosen. As per requirements, a user can select different increment values.

In case when a continuous electricity backup is not available, a user may split the simulation process by dividing incident angles range i.e. 0° to 90°, 90° to 180°, 180° to 270°, and 270° to 360°. BRCS estimation through EPOFACETS 5.0 over the range from 0 to 360 with increment 2 will provides the estimated result in a structured cells array of dimension (181×91) and each structured cell array contain the data information about the RCS, incident angle, observation angle, frequency
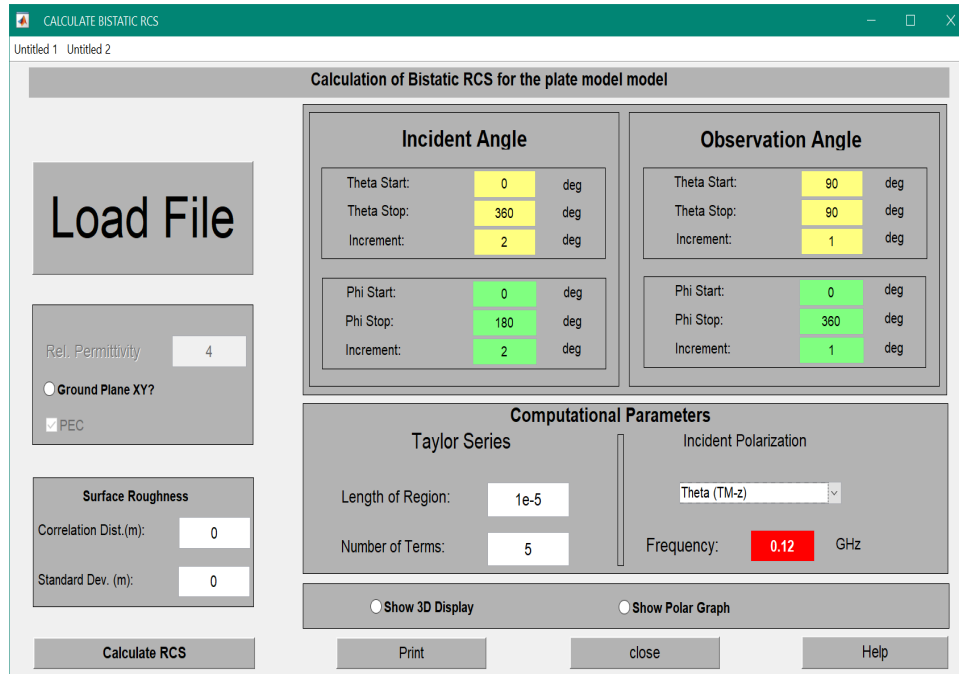
FIGURE 5.5: GUI window of EPOFACET of Aircraft A380$^{©}$ model.

and other parameters. This means the BRCS simulation will be executed 16471 times.

5.3   BRCS Results Comparison of EPOFACETS 5.0 and POFACETS$^{©}$4.2

In order to verify BRCS estimation obtained through EPOFACETS 5.0, the results are compared with the estimates of POFACETS$^{©}$4.2. Incident angles θ=180° and ϕ=264° are considered for both the versions as shown in Fig (5.6) and Fig (5.7). In Fig (5.8), "Theta Stop", "Phi Stop" and "Increment" are kept "0". In order to observe RCS the observation angles are kept at azimuth plane i.e. θ=90° and 0°≤ϕ≤360°.

Since, POFACETS$^{©}$4.2 doesn't estimate RCS over a range of incident angles; therefore, the results are estimated and compared for a single incident angle. The estimated BRCS results estimated through POFACETS$^{©}$4.2 and EPOFACETS 5.0 are shown in Fig (5.7) and Fig (5.9) respectively. From the results it is clear that both the versions work the same.
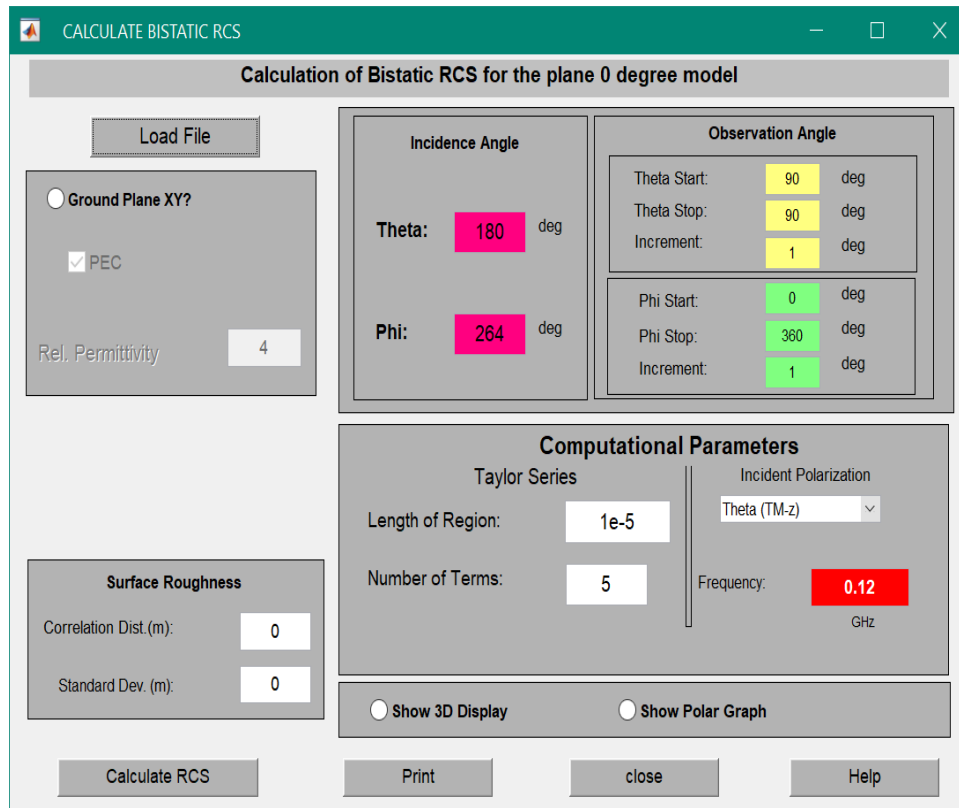
FIGURE 5.6: GUI window of bistatic RCS calculation using POFACETS©4.2.

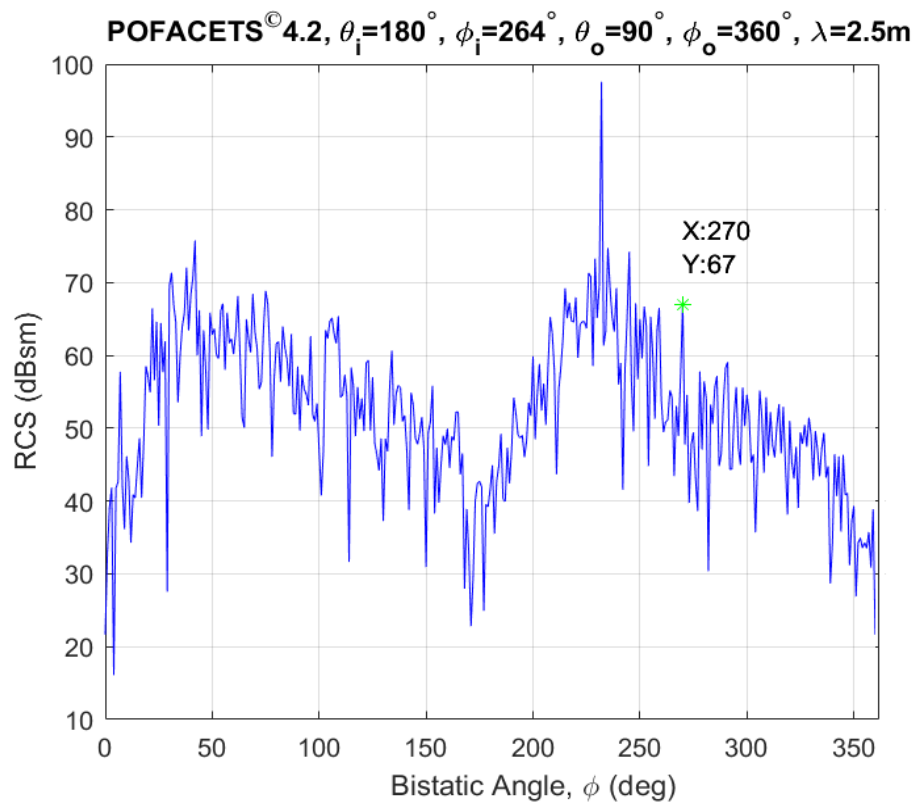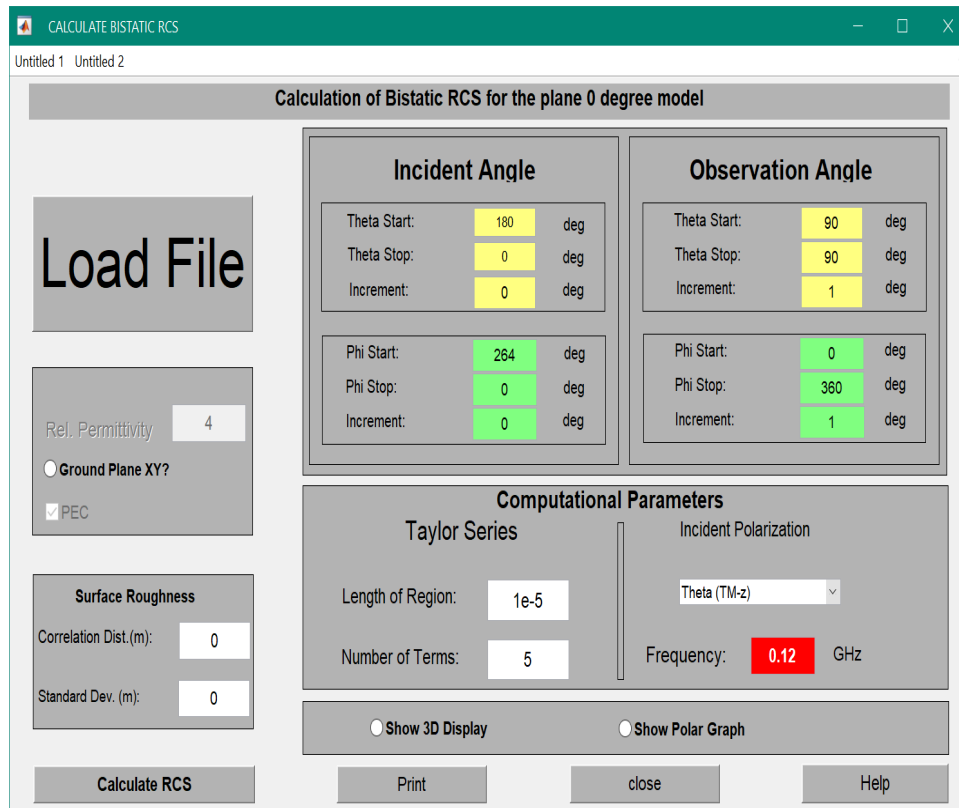FIGURE 5.7: RCS plot using POFACETS©4.2.

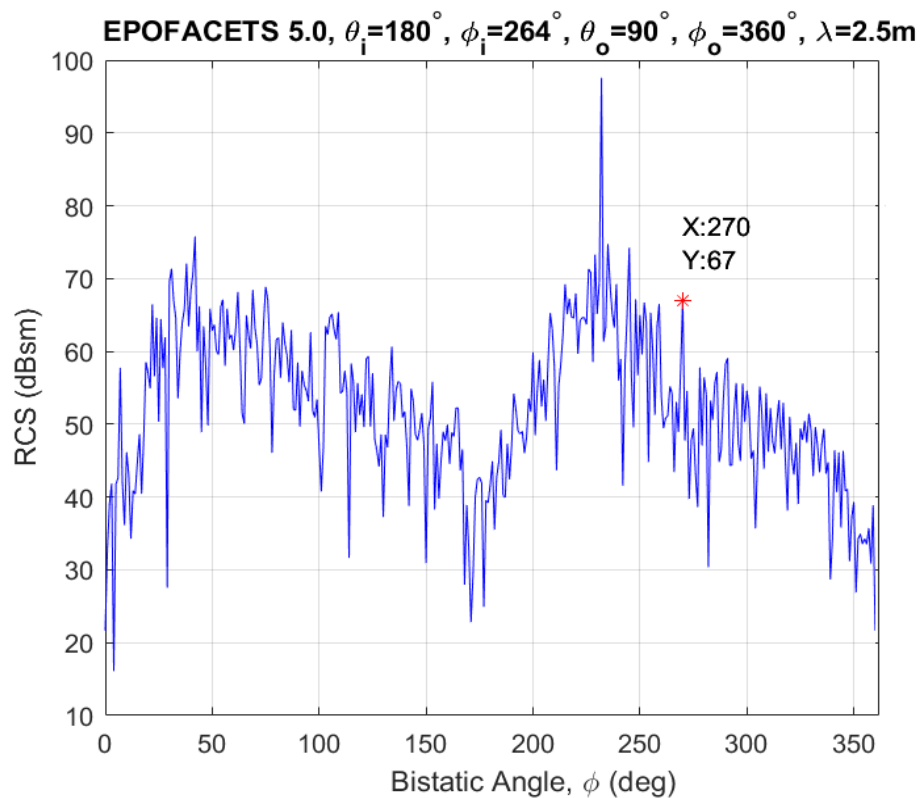FIGURE 5.8: GUI window of bistatic RCS calculation using EPOFACETS 5.0.

FIGURE 5.9: RCS plot using EPOFACETS 5.0.

TABLE 5.1: Simulation time comparison between POFACETS©4.2 and EPO-FACETS 5.0

Time (Hours/Days)	POFACETS©4.2	EPOFACETS 5.0
Model Loading	1 min and 12 sec	1 min and 12 sec
GUI Parameters Input	32 sec	45 sec
For Single Incident Angle	2 min and 45 sec	2 min and 45 sec
Requirement for a Range $0°\leq\theta_i\leq90°$, $0°\leq\phi_i\leq180°$, Inc.=2 (Including Model Loading and Parameters Input Time)	279 Hrs. (11.628 Days)	169.8477 Hrs. (7.076 Days)
Requirement for a Range $0°\leq\theta_i\leq180°$, $0°\leq\phi_i<360°$, Inc.=2 (Including Model Loading and Parameters Input Time)	1116 Hrs. (46.5 Days)	679.3903 Hrs. (28.3079 Days)

5.4 Simulation Based RCS Time Analysis

5.4.1 Simulation Time Comparison between POFACETS© 4.2 and EPOFACETS 5.0

Since, the one objective of this work is to reduce simulation time for estimating RCS over a range of incident angles; therefore, in this section, RCS simulation time comparison between EPOFACETS 5.0 and POFACETS©4.2 is provided. For a single incident angle, both the versions consume approximately the same time, whereas, for a range of incident angles the EPOFACETS 5.0 surpass the existing version with a huge time difference. In EPOFACETS 5.0, all the required incident angles are inputs at one time with respect to the observation angles. A comparison of simulation time consumed for estimating RCS at each step is listed in Table (5.1).

The POFACETS©4.2 requires a very high amount of time for estimating RCS for a range of incident angles because it demands to enter incident angles manually for each simulation run and repeat the same process again and again for range of incident angles. In contrast, the EPOFACETS 5.0 requires to enter incident angles range for a single time and hence saves the power and the time of a user.
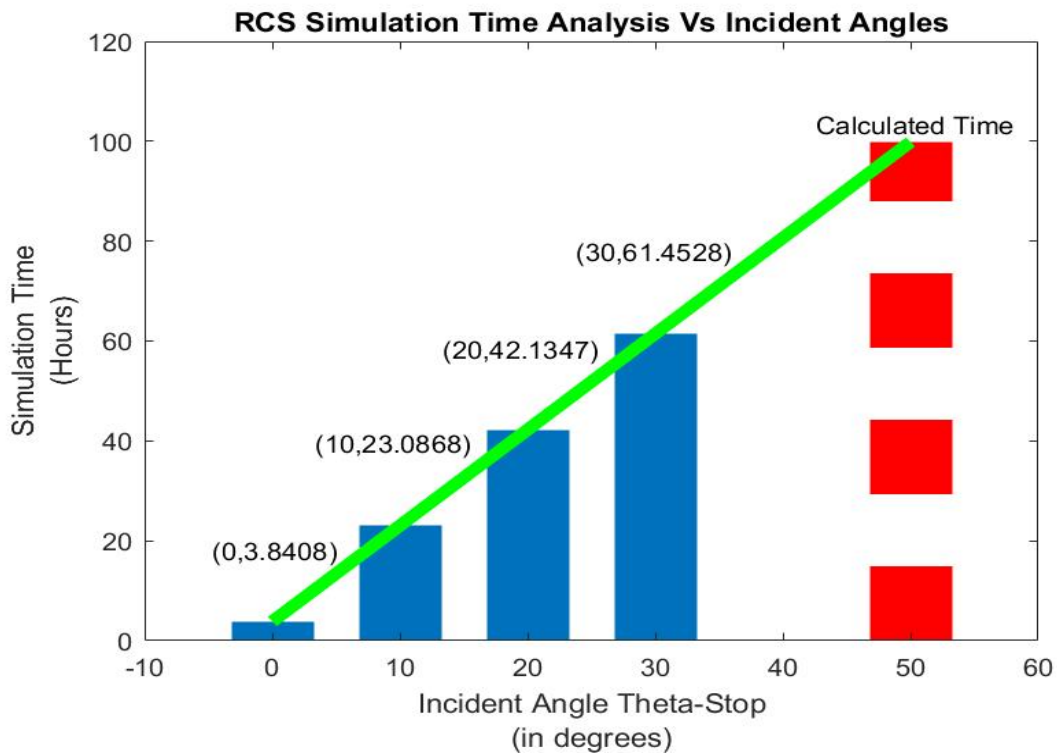
FIGURE 5.10: RCS simulation time analysis for different ranges of incident angle using EPOFACETS 5.0.

5.4.2 Simulation Time Estimation of EPOFACETS 5.0

In this section, simulation time consumed by EPOFACETS 5.0 is analyzed to obtain an estimated time duration for completing a task. For this purpose, simulation is run for four different scenarios of incident angle ranges, θ_i-Start=θ_i-Stop=$0°$, $0°\leq\theta_i\leq10°$, $0°\leq\theta_i\leq20°$ and $0°\leq\theta_i\leq30°$, whereas the incident angles range of ϕ is kept fixed i.e. $0°\leq\phi_i\leq180°$.

For simulation ease, the increment size is assumed 2. The complete details along with simulation time consumed during each scenario is listed in Table (5.2). The simulation is performed on a computer with the specifications of 2.50 GHz processor, 256 GB SSD ROM, and 8 GB RAM.

By analyzing simulation time consumed by each scenario, it is observed that the consumption of simulation time increases linearly. Therefore, a linear line can be fitted to these values that may provide a projected time duration of a task as shown in Fig (5.10).

In case, when a simulation is required to be run for $0°\leq\theta_i\leq50°$ and $0°\leq\phi_i\leq180°$,

TABLE 5.2: RCS simulation time analysis of EPOFACETS 5.0 for different range of incident angles

Simulation	Incident θ-Angle Range	Incident ϕ-Angle Range	Simulation Time
Simulation 1	θ-Start=0°, θ-Stop=0°, Increment=0	ϕ-Start=0°, ϕ-Stop=180°, Increment=2	3.8408 Hrs.
Simulation 2	θ-Start=0°, θ-Stop=10°, Increment=2	ϕ-Start=0°, ϕ-Stop=180°, Increment=2	23.0868 Hrs.
Simulation 3	θ-Start=0°, θ-Stop=20°, Increment=2	ϕ-Start=0°, ϕ-Stop=180°, Increment=2	42.1347 Hrs.
Simulation 4	θ-Start=0°, θ-Stop=30°, Increment=2	ϕ-Start=0°, ϕ-Stop=180°, Increment=2	61.4528 Hrs.

and the required increment value is 2, then the projected time can be calculated approximately through general empirical formula that are shown in Eq (5.1), which would be around (98.7158 Hrs.).

$$
\text{Time (minutes)} \approx 60 \times (1.9 \times \theta_i) + (\frac{\phi_i}{2} + 1) \times 2.45
$$
$$
\text{Time (Hrs.)} \approx (1.9 \times \theta_i) + (\frac{\phi_i}{2} + 1) \times 0.0408
$$
$$(5.1)$$

5.5 Validation of RCS Results through Well-established Radar Simulator FEKO©

In this section, RCS simulation of commercial aircraft Boeing 707© is computed through the proposed EPOFACETS 5.0 and FEKO© software tool. As discussed earlier, FEKO© software is based on the Multi-Level Fast Multipole Method (MLFMM), Physical Optics (PO), Uniform Theory of Diffraction (UTD), and Method of Moment (MOM); whereas EPOFACETS 5.0 is based on the Physical Optics (PO) method to compute monostatic and bistatic RCS.

In [22], the bistatic RCS of a large target is performed at fixed bistatic angle in
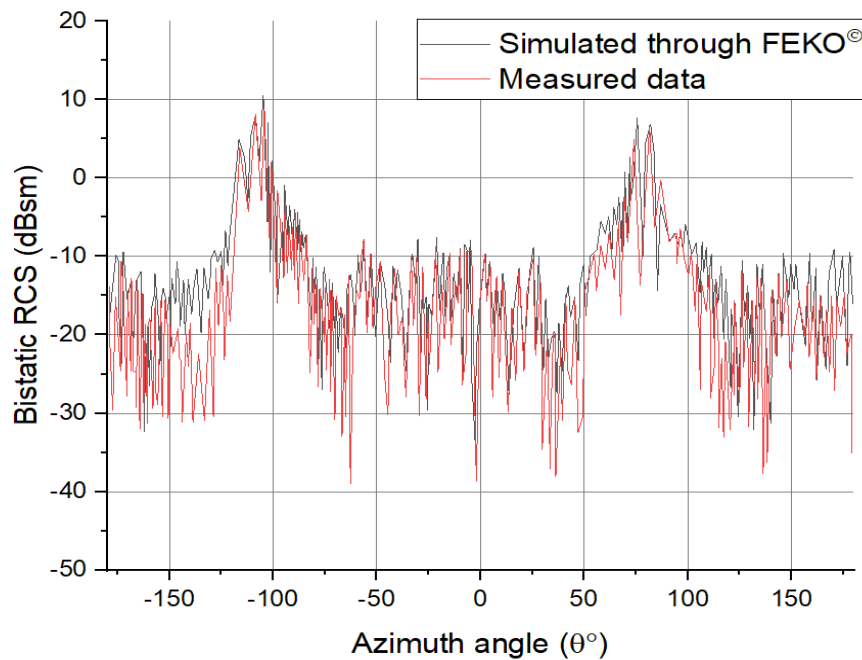
FIGURE 5.11: RCS plot of measured and simulated data of Boeing 707$^{©}$ aircraft through FEKO$^{©}$ software.

a compact range. The target scaled model of Boeing 707$^{©}$ was illuminated with a uniform EM plane wave which was created by a parabolic dish reflector. The bistatic scattering of the target is measured by the radar receiving antenna placed at fixed bistatic angle with a finite distance in compact range. The measured analysis of the model is performed in anechoic chamber by rotating in azimuth direction with fixed bistatic angle of 30.8°. In order to check the accuracy of bistatic RCS measured analysis performed in the compact range, the measured data is compared with the full wave simulations. These simulations were performed through FEKO$^{©}$ software using Multi-Level Fast Multipole Method (MLFMM) algorithm at 3.6 GHz frequency as shown in Fig (5.11).

In order to compare the RCS simulated results of the proposed EPOFACETS 5.0 with the published results of FEKO$^{©}$ software for results' verification, the same facet-based model of the commercial aircraft Boeing 707$^{©}$ is being used. The commercial aircraft Boeing 707$^{©}$ target facet-based model (.stl) format was imported in EPOFACETS 5.0 in order to compute the bistatic RCS for a range of incident angles from -180° to 180° over the same frequency of 3.6 GHz.

In this simulation, the target was illuminated by considering the azimuthal plane
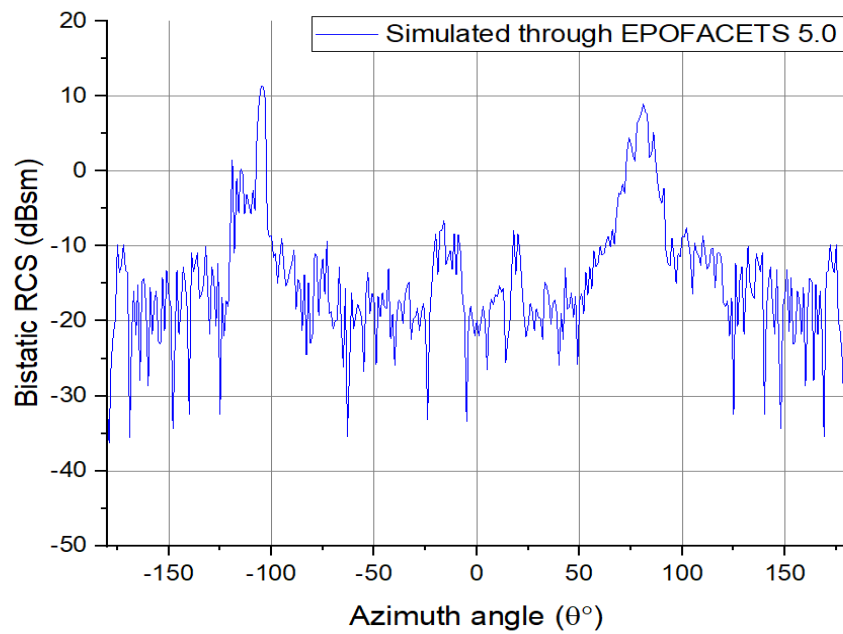
FIGURE 5.12: RCS plot of Boeing 707© aircraft through EPOFACETS 5.0.

for incident and observation angles to keep fixed bistatic angle of 30.8°. The computed RCS result at every incident angle with respect to observation angle is calculated to keep the constant difference of 30.8° between them. The simulated bistatic RCS results are shown in Fig (5.12). The estimated BRCS results of the target model Boeing 707© through EPOFACETS 5.0 and FEKO© software are compared as shown in Fig (5.13).

From the results, it is clear that the RCS computed through EPOFACETS 5.0 and FEKO© software tool are comparatively similar. This verifies that the proposed EPOFACETS 5.0 can be utilized for any flying object for the prediction of its RCS before it is observed by a realistic radar.

Moreover, as discussed earlier, that the RCS is changed by varying the incident frequency and the number of facets of the target model. Due to which the model Boeing 707© commercial aircraft that are used in FEKO© software having less number of facets as compared to the same model with greater number of facets used in EPOFACETS 5.0.

The error estimation of RCS results computed through FEKO© and EPOFACETS 5.0 with the measured data is shown in Fig (5.14). In order to reduced the number of facets in EPOFACETS 5.0, the estimated error is decreased as compared

to FEKO$^©$ results with measured data.

Fig (5.15) and Fig (5.16), shows the rate of accuracy of the estimated error in RCS computed through the FEKO and EPOFACETS 5.0 compared with measured results.

From the results, it is clear that in FEKO result, the rate of occurrence is higher with some offset in the estimating RCS upto 5 degree, but in EPOFACETS 5.0 results, the mean values are very closed to zero, which shows a natural error phenomena. However, a higher value of variance may be decreased by using a sophisticated estimation algorithm.

Hence, it is concluded that the open source EPOFACETS 5.0 software may used to computed the RCS of a target model over a range of incident angles and takes less RCS simulation time as compared to other software tools.

Furthermore, the facets model and RCS data after simulation is stored, occupied very less memory as compared to FEKO and other simulation software tools.

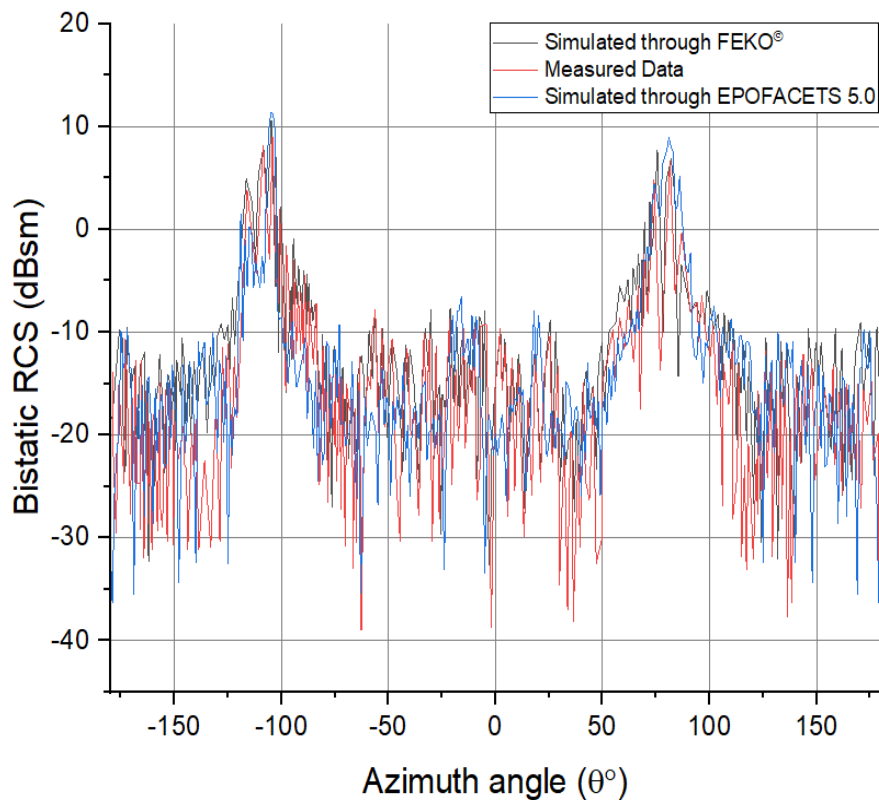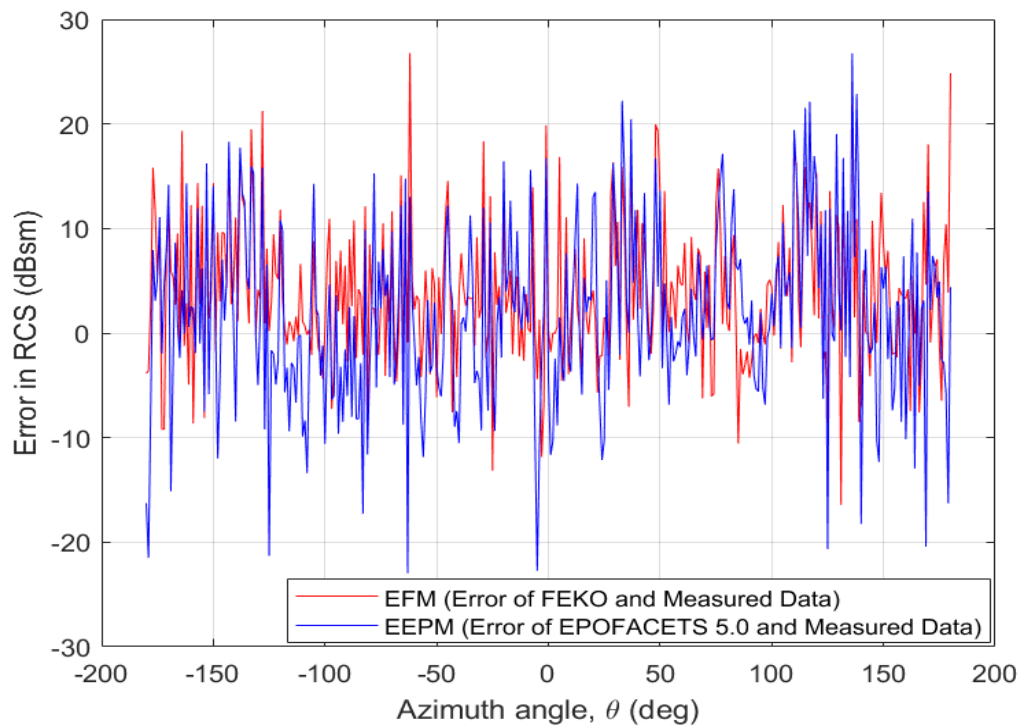FIGURE 5.13: Combined RCS plots of Boeing 707$^©$ aircraft through FEKO$^©$ and EPOFACETS 5.0.

FIGURE 5.14: Error estimation in RCS of Boeing 707© aircraft computed through FEKO© and EPOFACETS 5.0 with measured data.
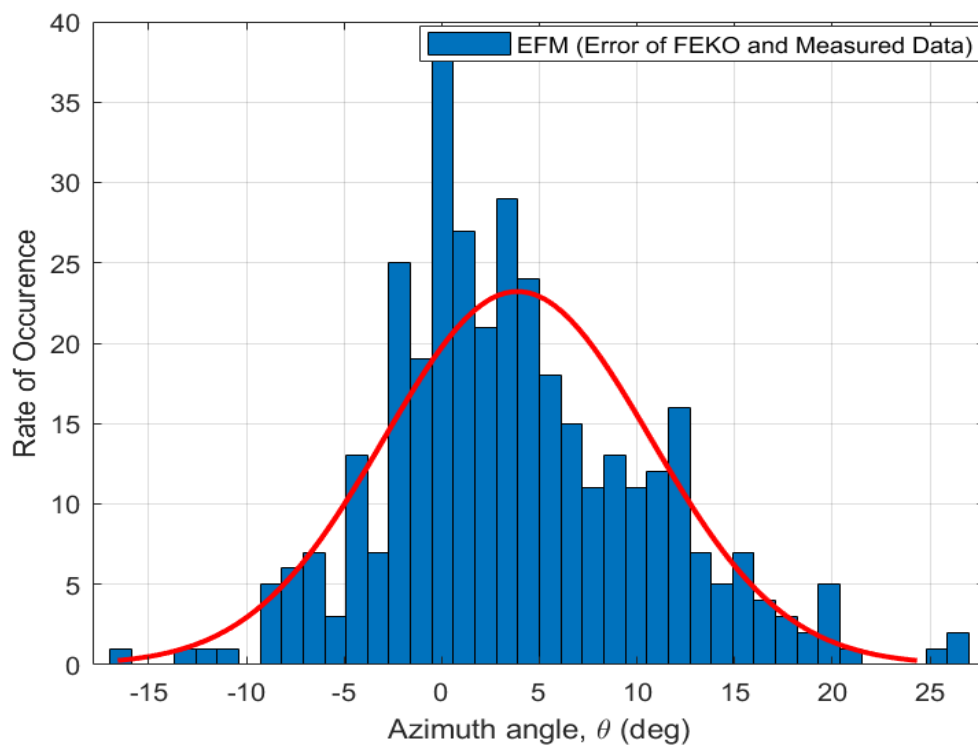
FIGURE 5.15: Error estimation Histogram of RCS computed through FEKO© with measured data.
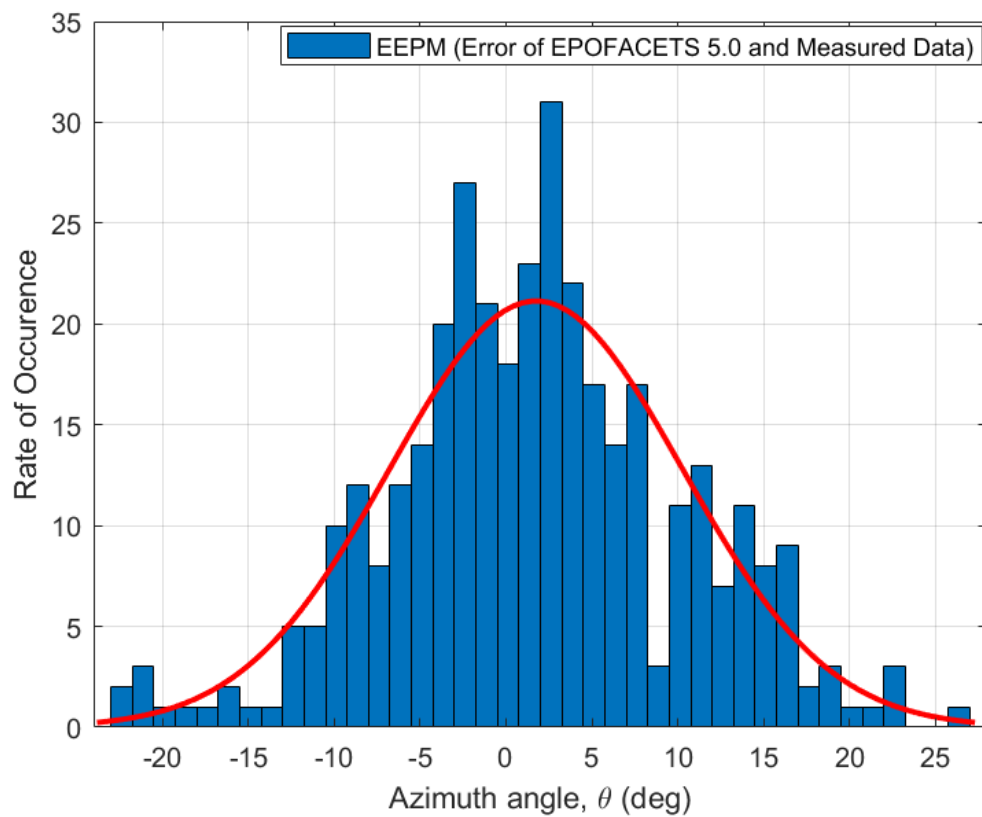
FIGURE 5.16: Error estimation Histogram of RCS computed through EPO-FACETS 5.0 with measured data.

Chapter 6

Conclusion and Future Work

This chapter gives a brief discussion of the conclusion of the thesis in section 6.1 and in section 6.2, the further possible future works on this thesis is discussed.

6.1 Conclusion

The current version of POFACETS$^©$ i.e. Version 4.2, has been limited to estimate bistatic RCS of an object for a single incident angle and has not been able to provide RCS for a predefined range of incident angles. In this research work, the Enhanced version of POFACETS$^©$4.2 has been designed named as EPOFACETS 5.0 which have capabilities of estimating bistatic RCS of a target model over a range of predefined incident angles. In order to enhance the functionalities of the existing version of POFACETS$^©$4.2, the Graphical User Interface (GUI) and POFACETS$^©$4.2 codes have been upgraded to accommodate the range of incident angles. A self-guiding GUI have been established separately to input the range of incident angles and to guide the user to avoid any mistake. The related MATLAB$^©$ codes have been developed for RCS estimation and linked with EPOFACETS 5.0 GUI. The GUI automatically adjusts its related scenario and provides estimated RCS of any input model.

For analysis, the largest commercial aircraft A380$^©$ model has been used to

77

compute the bistatic RCS through EPOFACETS 5.0. For this purpose, the AutoCAD$^©$ design of aircraft A380$^©$ has been acquired and converted to stereolithography (.stl) format. The bistatic RCS of the designed model have been estimated for each incident and observation angle in a three-dimensional space by providing incident and observation angles ranges. Simulation time performance and RCS estimation of EPOFACETS 5.0 over POFACETS$^©$4.2 have been evaluated on a computer with 2.50 GHz processor, 256 GB SSD drive ROM and 8GB RAM. It has been evaluated that EPOFACETS 5.0 provides advantage in terms of simulation time. The resultant RCS plots of the target model have been stored in MATLAB$^©$ structured cells array. The comparative analysis of the resultant RCS has been carried out which compares the RCS results taken either by using EPOFACETS 5.0 or POFACETS$^©$4.2 for a required incident angle. Moreover, the RCS simulation time have been analyzed for different range of incident angles and observed that the consumption time for each range of incident angles have been approximately linearly increased.

Furthermore, the BRCS of the facet-based model of the commercial aircraft Boeing 707$^©$ has been computed through the proposed EPOFACETS 5.0 and FEKO$^©$ software tool. The BRCS simulated results through the proposed EPOFACETS 5.0 software have been compared with the published results of FEKO$^©$ software for results' verification. From the results, it has been cleared that the BRCS computed through the proposed EPOFACETS 5.0 have been comparatively similar to results computed through FEKO$^©$ software tool. This verifies that the proposed EPOFACETS 5.0 can be utilized for any flying objects for the prediction of its RCS before it has been observed by a realistic radar.

6.2   Future Work

Although, the functional capabilities of EPOFACETS 5.0 have been improved to reduce the total simulation time and effort of a user; however, there are one limitation that should be removed in future. The EPOFACETS 5.0 estimates bistatic RCS for varying observation angles θ and ϕ values or keeping fixed value of θ or ϕ

angle values for a given range of incident angles which may takes much more time during simulation; therefore, it can be further improved in future, the symmetric functions will be required in EPOFACETS 5.0 for computing bistatic RCS in order to reduce simulation run time and user effort, and also to reduce the backup power usage time for RCS simulation over a wide range of incident angles.

The proposed EPOFACETS 5.0 has been designed to run sequentially. However, its performance in terms of simulation time can be substantially enhanced if parallel computing mechanism is integrated with its working. Moreover, the proposed EPOFACETS 5.0 MATLAB$^{©}$ codes can be upgraded if more advance high level programming language is employed e.g. Python. The proposed EPOFACETS 5.0 can also be used to estimate the RCS of a missile on the basis of its predicted trajectory.

Bibliography

[1] X. Shaojian, C. Bing, and Z. Ping, "Radar-communication integration based on DSSS techniques," in *2006 8th international Conference on Signal Processing*, vol. 4. IEEE, 2006.

[2] R. E. N. EN SET, "Knowledge-based radar signal and data processing," 2007.

[3] E. E. Garrido Jr, "Graphical user interface for a physical optics radar cross section prediction code," Naval Postgraduate School Monterey CA, Tech. Rep., 2000.

[4] M. C. Budge and S. R. German, *Basic RADAR analysis*. Artech House, 2015.

[5] M. I. Skolnik, "An analysis of bistatic radar," *IRE Transactions on Aerospace and Navigational Electronics*, no. 1, pp. 19–27, 1961.

[6] W. Feng, M. Dong, and X. Zhangsui, "Electro-magnetic field calculating based on wavelet-MoM," in *2007 8th International Conference on Electronic Measurement and Instruments*. IEEE, 2007, pp. 3–923–3–926.

[7] P. Zhang, S. Gong, and R. Mittra, "Beam-shaping technique based on generalized laws of refraction and reflection," *IEEE Transactions on Antennas and Propagation*, vol. 66, no. 2, pp. 771–779, 2017.

[8] A. Di Simone, W. Fuscaldo, L. M. Millefiori, D. Riccio, G. Ruello, P. Braca, and P. Willett, "Analytical models for the electromagnetic scattering from isolated targets in bistatic configuration: Geometrical optics solution," *IEEE*

Transactions on Geoscience and Remote Sensing, vol. 58, no. 2, pp. 861–880, 2019.

[9] Z. Li, T. J. Cui, X. J. Zhong, Y. B. Tao, and H. Lin, "Electromagnetic scattering characteristics of PEC targets in the terahertz regime," *IEEE Antennas and Propagation Magazine*, vol. 51, no. 1, pp. 39–50, 2009.

[10] D. C. Schleher, *Electronic warfare in the information age.* Artech House, Inc., 1999.

[11] J. Su, X. Xu, and M. He, "Hybrid PMM-MOM method for analyzing the RCS of finite array," in *2011 IEEE International Conference on Microwave Technology and Computational Electromagnetics.* IEEE, 2011, pp. 497–500.

[12] A. K. A K Ozturk, "Implementation of physical theory of diffraction for radar cross section calculations," Ph.D. dissertation, bilkent university, 2002.

[13] M. Vespe, S. Selleri, and G. Pelosi, "Parallel implementation of a high frequency code for the prediction of the RCS from complex targets using the parallel virtual machine," in *IEEE Antennas and Propagation Society Symposium, 2004.*, vol. 4. IEEE, 2004, pp. 4515–4518.

[14] U. U Yalcin, "Scattering from a cylindrical reflector: modified theory of physical optics solution," *JOSA A*, vol. 24, no. 2, pp. 502–506, 2007.

[15] M. Sarnik and U. Yalcin, "Modified theory of physical optics and solution for scattering fields from a perfectly conducting parabolic reflector," in *2016 IEEE International Conference on Mathematical Methods in Electromagnetic Theory (MMET).* IEEE, 2016, pp. 349–352.

[16] R. Hasaba, K. Ito, and M. Ando, "Estimation of radar cross section in multiple reflection ducts by combination of modified-physical optics and iterative physical optics," in *2011 IEEE International Conference on Microwave Technology and Computational Electromagnetics.* IEEE, 2011, pp. 380–383.

[17] Y. Z. Umul, "Modified theory of physical optics solution of impedance half plane problem," *IEEE transactions on antennas and propagation*, vol. 54, no. 7, pp. 2048–2053, 2006.

[18] D. Jenn, *Radar and laser cross section engineering*. American Institute of Aeronautics and Astronautics, Inc., 2005.

[19] F. Chatzigeorgiadis and D. C. Jenn, "A MATLAB physical-optics RCS prediction code," *IEEE Antennas and Propagation Magazine*, vol. 46, no. 4, pp. 137–139, 2004.

[20] S. Shi and H. Kobayashi, "RCS calculation software for large and complex obstacles," in *2011 International Conference on Electronics, Communications and Control (ICECC)*. IEEE, 2011, pp. 975–978.

[21] Altair HW FEKO software 3D view. [Online]. Available: https://shareappscrack.com/altair-hw-feko/?token=35215790

[22] M. Potgieter, J. W. Odendaal, C. Blaauw, and J. Joubert, "Bistatic RCS measurements of large targets in a compact range," *IEEE Transactions on Antennas and Propagation*, vol. 67, no. 4, pp. 2847–2852, 2019.

[23] M. Pienaar, J. W. Odendaal, J. Joubert, C. Pienaar, and J. C. Smit, "Bistatic RCS measurements in a compact range," in *2017 International Conference on Electromagnetics in Advanced Applications (ICEAA)*, 2017, pp. 1199–1202.

[24] X. Wang, C. Wang, and Y. Liu, "RCS computation and analysis of target using FEKO," in *Proceedings of 2014 3rd Asia-Pacific Conference on Antennas and Propagation*, 2014, pp. 822–825.

[25] D. L. Herda, J. Suryana, and A. Izzuddin, "Radar Cross Section of F35: Simulation and Measurement," in *2020 6th International Conference on Wireless and Telematics (ICWT)*, 2020, pp. 1–6.

[26] W.-k. He, C.-d. Ji, Z.-f. Huo, X.-l. Wang, and R.-b. Wu, "RCS calculation of wind turbine mast for weather radar," in *2016 CIE International Conference on Radar (RADAR)*, 2016, pp. 1–4.

[27] J. Sijabat and T. Indriyanto, "Radar Cross Section analysis of unmanned combat aerial vehicle (UCAV) using FEKO software," *AVIA*, vol. 2, 03 2021.

[28] L. Zhu, X. Liang, J. Li, and R. Li, "Simulation analysis on static scattering characteristics of stealth aircraft," in *2016 IEEE Advanced Information Management, Communicates, Electronic and Automation Control Conference (IMCEC)*, 2016, pp. 1774–1778.

[29] N. Jafari, "Comparison of various full-wave softwares in calculating the RCS of simple objects," 10 2018.

[30] A. A. N. Hafizah, M. Y. H. Hazwan, A. R. N. Emileen, R. A. R. S. Azmir, O. K. Azura, and S. Asem, "RCS analysis on different targets and bistatic angles using LTE frequency," in *2015 16th International Radar Symposium (IRS)*. IEEE, 2015, pp. 658–663.

[31] D. Yu and M. Zhang, "Comparison of various full-wave methods in calculating the RCS of inlet," in *2008 International Conference on Microwave and Millimeter Wave Technology*, vol. 2. IEEE, 2008, pp. 1018–1021.

[32] A. B. Gorji, B. Zakeri, and R. C. Janalizadeh, "Physical optics analysis for RCS computation of a relatively small complex structure," *Applied Computational Electromagnetics Society Journal*, vol. 29, no. 7, pp. 530–540, 2014.

[33] A. M. Ahmed, I. H. Ali, and H. R. Hatem, "Bi and mono-static Radar Cross Section computation for various target's materials," *International Journal of Engineering and Technology*, vol. 8, no. 1.5, pp. 513–516, 2019.

[34] V. I. Sizov, M. Cherniakov, and M. Antoniou, "Forward scatter RCS estimation for ground targets," in *2007 European Microwave Conference*. IEEE, 2007, pp. 1700–1703.

[35] G. M. Muthu, J. V. Kumar, and R. Jayaraman, "Computation and analysis of RCS for a kinetic energy type anti armour missile at ka band," *International Journal of Applied Electromagnetics and Mechanics*, vol. 47, no. 1, pp. 45–59, 2015.

[36] R. Ashraf, S. T. Tabassum, and M. Hossam E Haider, "Analytical study of bi-static radar cross section with a comparison at S band and X band of F-117 nighthawk stealth aircraft," in *2018 4th International Conference on Electrical Engineering and Information and Communication Technology (ICEEICT)*. IEEE, 2018, pp. 406–410.

[37] R. Ashraf, S. T. Tabassum, R. Tahmid, and M. Hossam-E-Haider, "Study and analysis of bi-static radar cross section of a stealth aircraft," in *2018 3rd International Conference for Convergence in Technology (I2CT)*. IEEE, 2018, pp. 1–5.

[38] J. Ji, J. Jiang, G. Chen, F. Liu, and Y. Ma, "Research on monostatic and bistatic RCS of cloaking based on coordinate transformation," *Optik*, vol. 165, pp. 117–123, 2018.

[39] C. Blaauw, "Recent improvements in asymptotic RCS calculations of large complex targets," in *2018 International Workshop on Computing, Electromagnetics, and Machine Intelligence (CEMI)*. IEEE, 2018, pp. 19–20.

[40] M. A. Alves, R. J. Port, and M. C. Rezende, "Simulations of the radar cross section of a stealth aircraft," in *2007 SBMO/IEEE MTT-S International Microwave and Optoelectronics Conference*. IEEE, 2007, pp. 409–412.

[41] A. A. Mauro, R. J. Port, and M. C. Rezende, "Simulations of the radar cross section of a stealth aircraft," in *Proceedings of the IEEE MTT-S International Microwave and Optoelectronics Conference*, 2007, pp. 409–412.

[42] M. A. Alves and M. C. Rezende, "Teaching radar cross section concepts to undergraduates with a simulation software," 2008.

[43] M. A. Alves, I. M. Martin, A. C. Coelho, L. C. Folguera, and M. C. Rezende, "Measurement and interpretation of radar cross section data in an educational setting: A comparison between simulations and experiments," in *PIERS Proceedings*, 2009, pp. 297–300.

[44] B. Chaudhury and S. Chaturvedi, "Radar cross section reduction using plasma blobs: 3-D finite difference time domain simulations," in *2007 IEEE Applied Electromagnetics Conference (AEMC)*. IEEE, 2007, pp. 1–4.

[45] A. Sefer, M. A. Uslu, and L. Sevgi, "MATLAB-based 3-D MOM and FDTD Codes for the RCS analysis of realistic objects [testing ourselves]," *IEEE Antennas and Propagation Magazine*, vol. 57, no. 4, pp. 122–148, 2015.

[46] G. Cakir, M. Cakir, and L. Sevgi, "An FDTD-based parallel virtual tool for RCS calculations of complex targets," *IEEE Antennas and Propagation Magazine*, vol. 56, no. 5, pp. 74–90, 2014.

[47] S. Hu, Z. Liu, and B. He, "Research on the RCS of complex target using FEKO," in *2011 Second International Conference on Mechanic Automation and Control Engineering*. IEEE, 2011, pp. 4366–4369.

[48] S. Horsmanheimo, A. Hujanen, L. Tuomimäki, and J. Kylmälä, "CAST-RCS tool for modelling versatile size targets," in *MILCOM, IEEE Military Communications Conference*. IEEE, 2015, pp. 1076–1080.

[49] P. Galloway, "A network application interface for RCS calculations," *ARMMS RF and Microwave Society*, pp. 23–24, 2009.

[50] S. Simpson, P. Galloway, and M. Harman, "Applications of epsilon a radar signature prediction and analysis tool," in *International Radar Symposium IRS*, vol. 98, 1998.

[51] M. Harman and S. Simpson, "EPSILON-A radar cross section modeling package," *Proc. UKSCS*, 1990.

[52] V. D. Charris and J. M. G. Torres, "Analysis of radar cross section assessment methods and parameters affecting it for surface ships," *Ciencia y tecnologia de buques*, vol. 6, no. 11, pp. 91–106, 2012.

[53] J. Houssay, N. Pinel, Y. H. Hellouvry, G. Monnier, C. Le Barbu, C. Cochin, and Y. Hurtaud, "A physical radar simulation tool of the sea clutter," in *2014 International Radar Conference*. IEEE, 2014, pp. 1–6.

[54] P. A. Lees and M. R. Davies, "Computer prediction of RCS for military targets," in *IEE Proceedings F (Radar and Signal Processing)*, vol. 137, no. 4. IET, 1990, pp. 229–236.

[55] F. Chatzigeorgiadis, "Development of code for a physical optics radar cross section prediction and analysis application," Naval Postgraduate School Montery CA, Tech. Rep., 2004.

[56] M. Y. M. Mirza, N. M. Khan, A. Jamal, and R. Ramer, "Characterization of spatial reflection co-efficient for ground-to-aircraft and satellite-to-aircraft communication," *Applied Computational Electromagnetics Society Journal*, vol. 33, no. 1, 2018.

[57] A. Jamal, "Characterization of reflection co-efficient for ground-to-aircraft and satellite-to-aircraft communication links," Ph.D. dissertation, Department of Electrical Engineering, Capital University of Science and Technology, Islamabad, 2016.

[58] Airport Operations - AutoCAD 3D view aircraft drawings. [Online]. Available: www.airbus.com/aircraft/support-services/airport-operations-and-technical-data/autocad-3-view-aircraft-drawings.html